Experimental Investigation and Parametric Optimization of Adhesively Joining Composite

Rahel Haile Sahle

A Thesis Submitted to

The Department of Mechanical Engineering

School of Mechanical, Chemical, and Materials Engineering

Presented in Partial Fulfillment of the Requirement for the Degree of Master of Science in Manufacturing Engineering

Office of Graduate Studies

Adama Science and Technology University

Septemper, 2022

Adama, Ethiopia

Experimental Investigation and parametric Optimization of Adhesively Joining Composite

Rahel Haile Sahle

Advisor: Dr. Moera Gutu Jiru (Ph.D)

A Thesis Submitted to

The Department of Mechanical Engineering

School of Mechanical, Chemical and Materials Engineering

Presented in Partial Fulfillment of the Requirement for the Degree of Master's in manufacturing engineering

Office of Graduate Studies

Adama Science and Technology University

September, 2022

Adama, Ethiopia

DECLARATION

I hereby declare that this Master Thesis entitled “Experimental Investigation and Parametric Optimization of Adhesively Joining Composite” is my original work. That is, it has not been submitted for the award of any academic degree, diploma or certificate in any other university. All sources of materials that are used for this thesis have been duly acknowledged through citation.

Rahel Haile Sahle _____ _____

Name of the student Signature Date

RECOMMENDATION

I, the advisor of this thesis, hereby certify that I have read the revised version of the thesis entitled “Experimental Investigation and Parametric Optimization of Adhesively Joining Composite” prepared under my guidance by Rahel Haile Sahle submitted in partial fulfillment of the requirements for the degree of Masters of Science in manufacturing engineering.

Therefore, I recommend the submission of revised version of the thesis to the department following the applicable procedures.

Dr. Moera Gutu Jiru (PhD) _____ _____

Advisor Signature Date

APPROVAL

I, the advisors of this thesis entitled “Experimental Investigation and Parametric Optimization of Adhesively Joining Composite” and developed by Rahel Haile Sahle; hereby certify that the recommendation and suggestions made by the board of examiners are appropriately incorporated into the final version of the thesis.

Dr. Moera Gutu Jiru (PhD)	_____	_____
Advisor	Signature	Date

We, the undersigned, members of the Board of Examiners of the thesis by Rahel Haile Sahle have read and evaluated the thesis entitled “Experimental Investigation and Parametric Optimization of Adhesively Joining of Composite” and examined the candidthe ate during open defense. This is, therefore, to certify that the thesis is accepted for partial fulfillment of the requirement of the degree of Master of Science in manufacturing engineering.

_____	_____	_____
Chairperson	Signature	Date
_____	_____	_____
Internal Examiner	Signature	Date
_____	_____	_____
External Examiner	Signature	Date

Finally, approval and acceptancearef the thareis is contingentthe upon submission of its final copy to the Office of Postgraduate Studies (OPGS) through the Department Graduate Council (DGC) and School Graduate Committee (SGC).

_____	_____	_____
Department Head	Signature	Date
_____	_____	_____
School Dean	Signature	Date
_____	_____	_____
Office of Postgraduate Studies, Dean	Signature	Date

ACKNOWLEDGMENT

Before anything else, I would like to Thank and Praise, God, the Almighty, and Holy Virgin Mery for the things that have been done to me, for the blessing, and the grace that has been given to carry out this thesis work. The Compilation of this thesis work could not have been fulfilled without the assistant of My Advisor Dr. Moera Gutu I would love to reveal my big and deepest gratitude to him for his encouragement, guidance, and understanding. It was a great honor for me to study under his advice. I express my sincere thanks to mechanical engineering department staff, for their outstanding suggestions and continuous inspiration during this thesis. I extend my deep gratitude to Adama Science and Technology University for allowing me to join a master's program with a full scholarship.

I would also like to appreciate and acknowledge My colleagues and classmates for their motivation and counsel. I am supremely delightful to My Family, for their attention, prayers, and sacrifice to make me mature for the future. It might be tough to imagine this success without their favor. And also My last thanks go to those, who had given any kind of contribution to the realization of this thesis work.

TABLE OF CONTENTS

CHAPTER PAGE

DECLARATION ii

RECOMMENDATION iii

APPROVAL iv

ACKNOWLEDGMENT v

LIST OF TABLES x

LIST OF FIGURES xi

NOMENCLATURE xiii

LIST OF ACRONYMS AND ABBREVIATIONS xv

ABSTRACT xvi

CHAPTER ONE 1

INTRODUCTION 1

1.1 Background of the Study 1

1.2 Classification of Composite Joining Techniques 3

1.2.1 Mechanical Joining of Composite 3

1.2.2 Physical (Welding) Joining of Composite 4

1.2.3 Chemical (Adhesive) Joining of Composite 5

1.3 Statement of Problem 7

1.4 Objective 7

1.4.1 General Objective 7

1.4.2 Specific Objective 7

1.5 Scope of the Study 8

1.6 Significance of the Study 8

1.7 Limitation of the study 8

1.8 Organization of the Thesis 9

CHAPTER TWO 10

LITERATURE REVIEW 10

2.1 Introduction 10

2.2 Mechanical joining of composite 10
2.3 Welding type of composite joining 12
2.4 Adhesive joining of composites 13
2.4.1 Stresses of adhesive bonds 14
2.4.2 Surface treatments prior to adhesive bonding 15
2.4.3 Mechanical abrasion 17
2.4.4 Chemical pre-treatment 18
2.4.5 Energetic pre-treatment 18
2.5 Process Parameter that Affect the Strength of Adhesively Joined Composite 20
2.5.1 Joint Configuration of the Adhesive Bond 20
2.5.2 Overlap Length 20
2.5.3 Adhesive Thickness of the Adhesive Bond 21
2.5.4 Environmental Factor (Temprature) 22
2.6 Failure Modes of Adhesively Joined composites 26
2.6.1 Adhesion or Interface Failure 27
2.6.2 Cohesive Failure 27
2.6.3 Substrate or Adherend Failure 27
2.7 Hybrid Taguchi Based Grey Relational Analysis Optimization 29
2.8 Data Analysis of Responses 30
2.9 Phases of Optimization by GRA 31
2.9.1 Normalizing S/N Ratios 31
2.9.2 Calculating the Grey Relational Coefficients 32
2.9.3 Determination of Grey Relational Grade 32
2.9.4 Optimal Parameter Setting 32
2.9.5 Conformation Experiment 32
2.10 Reviewing Related Literature 33
2.11 Research Gap 35
CHAPTER THREE 36
MATERIAL AND METHODOLOGY 36
3.1 Introduction 36
3.2 Materials 36
3.2.1 Banana Fiber 36
3.2.2 Aluminum oxide 37

3.2.3 Sodium Hydroxide 37
3.2.4 Honey Wax 38
3.2.5 Distilled Water 38
3.2.6 Hardener (Catalyst) 38
3.2.7 Adhesives and Matrix Selection 39
3.3 Process Parameters 42
3.3.1 Joint Overlap Length 42
3.3.2 Design Configuration of Joint 42
3.3.3 Environmental Factor (Temprature) 43
3.3.4 Joint Adhesive Thickness 43
3.4 Sample Preparation Method 44
3.4.1 Alkali Treatment of Banana Fiber 44
3.4.2 Cutting of banana fiber 45
3.4.3 Calculating Weight, Mass and Volume Fraction of the Particulate, Fiber and Matrix for Samples 46
3.4.4 Weight Measurements and Mixing of Alumina, Fiber and Polyester 49
3.4.5 Fabrication of Composite (Molding) 49
3.4.6 Cutting the Composite 50
3.4.7 Surface Treatment 50
3.4.8 Mix Liquids and Sample Preparation 51
3.5 Equipment's and Machines Used 51
3.5.1 Analytical (Digital) Balance 51
3.5.2 SEM Microscopy 52
3.5.3 Jig Saw Cutting Machine 52
3.5.4 Universal Testing Machine (UTM) 53
3.5.5 Laboratory Oven 54
3.5.6 Hydraulic Press Machine 54
3.6 Characterization of the Adhesively Joined Composite 55
3.6.1 Tensile Strength 55
3.6.2 Flexural Strength Test 56
3.6.3 Compression Test 57
3.7 Methodology 58
CHAPTER FOUR 59

RESULTS AND DISCUSSION 59
4.1 Introduction 59
4.2 Tensile Test 59
4.2.1 Analysis of Main Effect Plot for S/N Ratio of Tensile Strength 62
4.2.2 Response table for S/N ratios of tensile strength 63
4.2.3 Analysis of variance of tensile strength 63
4.3 Flexural Test 64
4.3.1 Analysis of Main Effect Plot of Flexural Strength 67
4.3.2 Response Table for S/N Ratios of Flexural Strength 67
4.3.3 Analysis of Variance for Flexural Strength 68
4.4 Compression Strength 69
4.4.1 Analysis of Main Effect Plot of Compression Strength 72
4.4.2 Response Table for S/N Ratios of Compression Strength 72
4.4.3 Analysis of Variance for Compression Strength 73
4.5 Grey relational analysis of Mechanical properties 74
4.5.1 Analysis of main effect plot for S/N ratios of GRG 77
4.5.2 Response table for S/N ratios of Grey relational grades 77
4.5.3 Analysis of variance for Grey relational grades 78
4.6 Analysis of Failure Mechanism 78
4.7 Fractography Analysis 79
CHAPTER- FIVE 81
CONCLUSION AND RECOMMENDATIONS 81
5.1. Conclusion 81
5.2. Recommendations 82
5.3. Future work 82
REFERENCE 83
Appendix A xvi
Appendix B xviii
Appendix C xx
Appendix D xxii

LIST OF TABLES

TABLE PAGE

Table 1.1 The advantage and dis advantage of the three joining techniques 6

Table 3.1 List of materials used and quantity..... 36

Table 3.2 Criteria for selection best adhesive (Nurazzi et al., 2017) 40

Table 3.3 Mechanical properties of unsaturated polyester..... 41

Table 3.4 Composition of particulate, fiber and matrix used for sample preparation..... 46

Table 3.5 Tabulated composition of polyester, banana fiber and alumina..... 48

Table 4.1 Tabular description of tensile strength test result..... 59

Table 4.2 Response for S/N ratios of tensile strength 63

Table 4.3 Analysis of variance of tensile strength..... 63

Table 4.4 Tabular description of flexural strength test result..... 64

Table 4.5 Response table for S/N ratio..... 68

Table 4.6 Analysis of variance for flexural strength 68

Table 4.7 Tabular description of compression strength test results 69

Table 4.8 Response Table for S/N Ratios of Compression Strength..... 73

Table 4.9 Analysis of variance for compression strength 74

Table 4.10 Response table..... 74

Table 4.11 S/N ratios table 75

Table 4.12 Tabular description for normalizing sequence 75

Table 4.13 Tabular description of deviation sequence..... 76

Table 4.14 Grey relational coefficients and Grey relational grade..... 76

Table 4.15 Response table for S/N ratios of GRG 78

Table 4.16 Analysis of variance for GRG 78

Table 4.17 Tabular description of failure mechanism..... 79

LIST OF FIGURES

FIGURE PAGE

Figure 1.1 Different types of composite joining techniques (a) mechanical joining, (b) welding joining, (c) adhesive joining (Pulido, 2019) 5
Figure 2.1 Number of bolts V_S load (a) Number of bolts V_S shear stress (b) 11
Figure 2.2 Number of rivets VS load (a) Number of rivets VS shear stress (b)..... 12
Figure 2.3 The five kinds of stresses that an adhesive bond can experience (Ebnesajjad and Landrock, 2015b)..... 15
Figure 2.4 The different types of surface treatments..... 16
Figure 2.5 (a) overlap length vs load (b) overlap length vs shear stress 21
Figure 2.6 Bonding thickness Vs Load (a), Bonding thickness Vs Shear stress (b). 22
Figure 2.7 The three main modes of adhesive bond failure 29
Figure 3.1 Alkali treatment of banana Aluminum Oxide..... 36
Figure 3.2 Nano alumina powder 37
Figure 3.3 Sodium haydroxide (NaOH) flakes..... 37
Figure 3.4 Honey Wax..... 38
Figure 3.5 Distilled water 38
Figure 3.6 Hardener..... 39
Figure 3.7 ABRO epoxy (a) polyester (b) 41
Figure 3.8 Overlap length (a) 40mm, (b) 30mm, (c) 25mm..... 42
Figure 3.9 Selected joint configuration (a) Single lap joint, (b) Scarf, (c) Stepped 43
Figure 3.10 Flow diagram of sample preparation..... 44
Figure 3.11 Alkali treatment of banana fiber 45
Figure 3.12 Chopped banana fiber 45
Figure 3.14 Weight measurements of alumina, fiber and polyester..... 49
Figure 3.15 Mixture of polyester, hardener, alumina and banana fiber (b) Fabricated banana fiber rainforced composite 49
Figure 3.16 Composite cut by jigsaw 50
Figure 3.17 Surface treatment 51
Figure 3.18 Final Samples..... 51
Figure 3.19 Analytical (digital) balance..... 52
Figure 3.20 SEM microscopy..... 52

Figure 3.21 Jig Saw 53
Figure 3.23 Universal testing machine 53
Figure 3.22 Labratory Oven 54
Figure 3.24 Hydraulic press machine 55
Figure 3.25 Flexural testing machine 56
Figure 3.26 Sample under compression test 57
Figure 3.27 Flow chart 58
Figure 4.1 Tensile strength of different samples 60
Figure 4.2 Tensile strength Vs (a) Overlap length (b) Joint configuration (c) temprature .. 61
Figure 4.3 Main effect plot of tensile strength 62
Figure 4.4 Flexural strength Vs experiment number 64
Figure 4.5 Flexural strength Vs (a) Overlap Length (b) Temprature (c) Joint Configuration 66
Figure 4.6 Main effect plot of flexural strength 67
Figure 4.7 Compression strength Vs experiment number 70
Figure 4.8 Compression strength Vs (a) Joint Configuration (b) Overlap Length (c) Temprature 72
Figure 4.9 Main effect plot of flexural strength 73
Figure 4.10 Main effect plots for S/N ratios of GRG 77
Figure 4.11 Fractography of the joint 80

NOMENCLATURE

φ	Distinguishing coefficient
ρ_a	Actual/measured density of composite
ρ_c	Density of composite
ρ_f	Density of fiber
ρ_m	Density of matrix
ρ_p	Density of particulate
ρ_t	Theoretical density
ρ_w	Density of water
b	Width of the sample
d	Athematic mean of two diagonals
D	Indentation surface
F	Applied force for indentation
L	Number of levels
M_C	Mass of composite
M_F	Fiber mass fraction
M_f	Mass of fiber
Mf	Matrix mass fraction
Mm	Mass of matrix
Mp	Mass of particulate
Mp	Mass of polyester
Mt	Total mass
P	Number of factors
S/N	Signal to noise ratio
Vb	Volume of banana fiber
Vf	Fiber volume fraction
Vm	Matrix volume fraction
VP	Volume of Polyester
Vv	Void content
W %	Percentage of water absorption
Wa	Weight of the sample in air
Wf	Final weight of sample after immersed

Wf	Weight of fiber
Wi	Initial weight of sample before immersed
Wm	Weight of matrix
Wp	Weight of particle
Wt. %	Weight percentage
Ww	Weight of the sample in water

LIST OF ACRONYMS AND ABBREVIATIONS

ANOVA:	Analysis of variance
ASTU:	Adama Science and Technology University
BA:	Bidirectional abrasion
CM:	Composite material
CNT:	Carbon Nanotubes
DOE:	Design of Experiment
FRP:	Fiber reinforced polymer
FRPMC:	Fiber Reinforced Polymer matrix composite
GFRPC:	Glass Fiber Reinforced Polymer composite
GRA :	Grey relational analysis
GRC:	Grey relational coefficient
GRG:	Grey relational grade
MWCNT:	Multi-Walled Carbon Nanotubes
NFRPC:	Natural fiber reinforced polymer composite
PMC:	Polymer matrix composites
SEM:	Scanning Electron Microscope
UA:	Unidirectional abrasion
UPR :	Unsaturated Polyester Resin
UTM:	Universal Testing Machine
UTS:	Ultimate tensile strength or peak stress
UR :	Ultraviolet radiation

ABSTRACT

Composites materials are used in aerospace and automotive industries replacing aluminum and titanium alloys. As demands of composites increased in complex applications leads to high research works for joining the parts by adhesive joining techniques. Adhesively bonded joints can solve problems such as joint area cracks, corrosion and wear during welding or screwing methods. Composite joining by this method was advantages due to uniform stress distribution along the bonded areas which improves stiffness than a riveted join. In this research study, a small scale laboratory composite adherends for adhesively purpose was prepared by simple hand layup method using polyester as matrix and nano alumina powder of particle size ≤ 50nm and banana fiber as reinforcing materials. Then adhesively joined composite samples were prepared by binding the adherends using ABRO epoxy adhesive. The performance of bonding schemes was related to multiple factors like, overlap length, joint configuration and environmental factors. Nine samples were made by varying the configuration joint (single lap, stepped and scarf), overlap length of 25 mm, 30 mm and 40mm and temperature (0℃, 20℃ and 60℃). Experimental tests were conducted to evaluate mechanical properties of tensile, flexural, compression and fractography analysis. Taguchi based grey relational analysis was used to develop a statistical model to describe the relationship between mechanical properties of the joint; independent parameters were selected to optimize the process parameters. The maximum tensile, flexural and compression strength were 12.80MPa, 54MPa and 22.8MPa respectively at sample 9, sample 7, and sample 4 respectively. The minimum tensile, flexural and compression strength was 5.12MPa, 18MPa, and 6.24MPa.the failure occure during the mechanical tests were adhesive, cohesive, and adherend failure. Fractography analysis depicted that even though there was small void at the bonding line, the joint of composites showed better bonding between the adherends and adhesive. The optimum combination obtained through Taguchi based grey relational analysis was single lap joint, 30 mm overlap length, and 20℃. The investigation revealed the suitability of overlap length, configuration joint as an effective parameter in adhesively joined composite.

Keywords: *Composite, Matrix, Reinforcement Joint, Adhesive, Aderend, Temprature, Bonding, Taguchi, Grey relation analysis.*

CHAPTER ONE

INTRODUCTION

1.1 Background of the Study

A composite material is a type of material made from one or more constituent materials with different chemical or physical properties that can be combined to create new materials. The properties of composites are a function of the properties of the matrix and reinforcement materials. The matrix material is the continuous material used to bind the reinforcements and determines the quality of the surface. Matrix materials can be metallic, ceramic, or polymeric (Murugan et al., 2020). Reinforcements are added to improve the mechanical properties of the matrix and give quality to the composite. Composite reinforcements are either fibrous or non-fibrous. Fiber composites are either natural fiber reinforced composites or synthetic fiber reinforced composites. Factors affecting the properties of fiber-reinforced polymer composites are fiber parameters (orientation, length, and treatment) and fiber-matrix interfacial (Kumar et al., 2014a).

The development of composite materials represents a step forward in history as it enables the use of whole classes of solid materials and ceramics in many applications. The main advantage of using composite materials in the automotive sector is weight reduction. Composites are up to 35% lighter than aluminum and 60% lighter than steel, and their use in the automotive industry can reduce overall vehicle weight by up to 10% (Kutz & Wiley, 2015).

As the basic building block of all things is the bonding of atoms, the ability to bond artificial structures must become more powerful and versatile to meet future demands. Most, if not all, structures are assemblies of numerous individual components that must be connected to form an integrated load transfer path. These connections are often called joints and can come in many forms, such as screwing, riveting, or other mechanical attachments, welding or soldering to join metal elements, or gluing. Regardless of the form of connections used within the structure, these connections are potentially the weakest areas within the structure and where weight penalties can occur (Bakri et al., 2017).

There are only three ways to create a bond between materials and parts made from them. (1) mechanical forces that can be distinguished at the atomic or molecular level while the

materials remain separated; (2) chemical forces that bind the constituents together. chemical reactions and (3) the physical forces by which atoms, ions, and molecules form joints (Marcella, 2015). Mechanical bonding using mechanical force is accomplished by drilling holes in the two materials to be joined, placing mechanical fasteners in the holes, and locking the fasteners in place. The advantage of using mechanical force is that the structure is simple and the connection is not permanent. Therefore, rebuilding can be performed without problems.

Adhesive bonding, whereby chemical forces are being used, is a material joining process in which an adhesive, placed between the substrates, solidifies to produce an adhesive bond. This method offers lower structural weight, lower fabrication cost, and improved damage tolerance, in addition to design flexibility and ease of fabrication (Sumesh et al., 2020a). Bonded structures are far more fatigue-resistant than equivalent mechanically fastened structures, and when designed correctly, can sustain higher load levels than equivalent mechanically fastened joints (Marcella, 2015). An example of physical force is welding. Welding is done by melting the two materials and adding a filler material to form a pool of molten material that cools to become a strong joint. The welding process does not rely on parts to fit exactly, and there is no extra weight due to nuts or bolts.

The science and technology of adhesion is growing as a method of joining materials due to the rapid development of new adhesive formulations and the improvement of the conditions of use, and has been successfully introduced in applications reserved for other joint systems such as welding or mechanical joints The popularity of adhesive bonds is due to the advantages over other binding systems, an adhesive connection distributes more evenly and homogeneously the stresses than riveted joints and screws, avoiding areas of high-stress concentration, as exhibited in the holes required in such connections (Pulido, 2019).

Currently, there is a tendency to replace all or part of traditional fixing systems such as welding or riveting, by adhesive joints due to the high performance offered by these components. Adhesives permit binding of different materials with different physical, mechanical or electrochemical properties. They result especially useful for composite materials of polymeric matrix, where conventional bonding methods could yield in stress concentrator or are not feasible (Marcella, 2015). They may also act as sealants, obtaining in this way watertight mechanical joints, preventing the presence of corrosive agents such

as moisture in air. Due to these advantages of adhesive over other methods of joining, it becomes the best and desired joining technique for materials especially composites.

Adhesion is defined as the state in which two surfaces are held together by interfacial junctions, and cohesion denotes the state that tends to associate particles of a substance by secondary valence forces. The curing or setting is the process during which an adhesive develops its cohesive strength and therefore, their physical and chemical properties (Subramanya et al., 2020). A bonded joint produces a bi material body and, thus, yields stress discontinuities even in the absence of any geometric discontinuity due to mismatch of the elastic properties of the materials connected. The mechanical test used to characterize adhesive bonds is the tensile shear test, because of its ease of implementation and simplicity, and their use can lead to a reduction of costs, as well as an acceleration of assembly processes and, consequently, an improvement in the production processes for developing countries(Pulido, 2019).

Adhesive joining is commonly used for different applications. However, less research was use this type of joining for composite joining,. Therefore, this work is aimed on experimental investigation and parametric optimization of adhesively joining of composites using Taguchi to improve the strength of joint. The process parameters are joint overlap length, joint configuration, environmental factor (temprature).

1.2 Classification of Composite Joining Techniques

Composite materials can be joined by different techniques. The three most known joining technique shown in Figure 1.1 were explained clearly as follow.

1.2.1 Mechanical Joining of Composite

The approach of producing joints using only mechanical forces is generically known as mechanical joining. Within mechanical joining there are two major subdivisions: (1) mechanical fastening, and (2) mechanical attachment. Both rely exclusively on the use of physical interference or interlocking at a macroscopic or microscopic level, or both, to hold parts together. In mechanical fastening, a supplemental device is used to cause the interference between parts, with well recognized examples being rivets, bolts, screws, nails, and staples, and less well recognized but well-known examples being stitches, laces, lashings, wire-wraps, as well as buttons and zippers (Fong et al., 2020).

In mechanical attachment, no supplemental devices (or fasteners) are needed. Joining is accomplished by interference or interlocking between designed-in or fabricated-in geometric features integral to the parts being joined. Examples include dove-tails, tongues-and-grooves, T-slots, wedges, and integral snap-fit features molded into plastic parts, as well as elastic thermal shrink-fits, elastic or plastic mechanical interference fits, and plastic staking, crimping, folding and hemming all also found in plastic (especially thermoplastic) parts (Lotf et al., 2019).

With the exception of the plastic deformation methods listed above, all mechanical attachments and all mechanical fasteners can be removed at will without damaging parts or materials. As a result, neither mechanical fastening nor mechanical attachment can be considered to be truly permanent. Thus, the two greatest advantages of mechanical joining are that it can be accomplished without changing the composition or structure of material comprising parts and it allows intentional disassembly. Ironically, the greatest disadvantage is that it makes possible accidental disassembly unless very special precautions are taken at the design stage.

1.2.2 Physical (Welding) Joining of Composite

Without question, the most permanent of all joints are made by welding, where welding is the process in which materials of the same type or class (e.g., metals, or ceramics, or polymers) are joined together through the formation of primary (or, occasionally, secondary) chemical bonds under the combined action of heat and pressure (Lokesh et al., 2020). As opposed to adhesive bonding, welding usually does not involve or require any chemical reaction; relying solely on the natural tendency of atoms, ions, or molecules to attract one another and bond.

The types of bonds formed across the joint are the same as the types of bonds found in the materials being joined. The principal advantage of welding is the production of joints of high structural integrity and efficiency and permanence. Shortcomings of the process are alteration of the composition and microstructure of materials (for most methods) and, ironically, the inability to disassemble the joint without severely damaging the parts (Kumar et al., 2014c). Two broad classifications of specific welding methods are: fusion and non-fusion. In fusion welding methods, intentional melting of the base materials, and perhaps a filler material, and intermixing of the resulting molten materials leads to bond and joint formation.

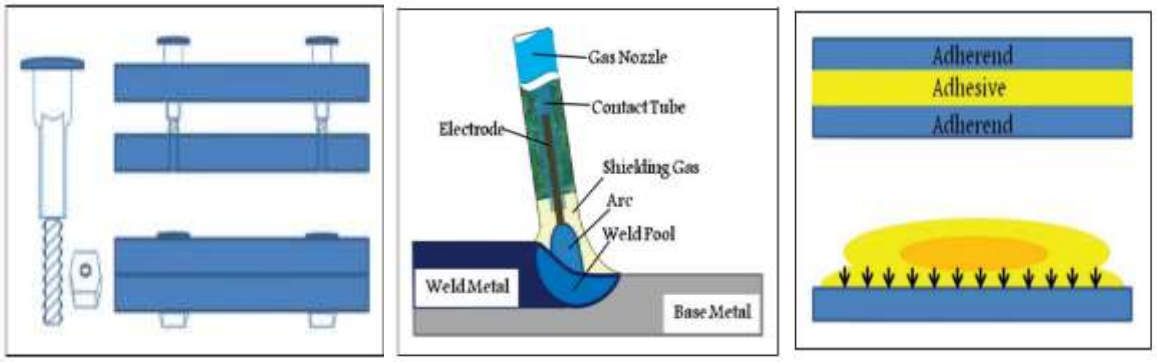

(a) **(b)** **(c)**

Figure 0.1 Different types of composite joining techniques (a) mechanical joining, (b) welding joining, (c) adhesive joining (Pulido, 2019)

In non-fusion methods, bond and joint formation is accomplished without relying on melting and intermixing and re-solidification. Non-fusion methods rely on pressure or friction to cause bonding in the solid state by macroscopic or microscopic plastic deformation. Inter-diffusion in the solid state is also a key to sound bond and joint formation. Welding (commonly referred to as ‘‘thermal bonding’’ by polymer engineers) is commonly used to successfully join thermoplastic PMCs (Pulido, 2019).

1.2.3 Chemical (Adhesive) Joining of Composite

Adhesive bonding is a process of joining materials with the aid of a substance able to hold those materials together by surface attachment. The materials being joined are called adherends, while the bonding substance (or chemical agent) is called the adhesive. The forces that enable the surface attachment are a combination of substantial secondary (and, occasionally, primary) chemical bonding, often the result of some chemical reaction, and, at least for rough-surfaced or porous adherends, some mechanical locking at the microscopic level between the adhesive and the adherends. Thus, the adhesive bonding process is fundamentally a chemical bonding process (Gaurav et al., 2020).

The principal advantages of adhesive bonding are minimal alteration of the chemical composition and microstructure of the adherends, suitability to joining dissimilar materials, ability to produce large load bearing areas, tendency to distribute loading, and capability for sealing, insulating, damping, and resisting fatigue (Pulido, 2019). The greatest shortcoming of adhesive bonding is; susceptibility to degradation by a number of environmental factors, including extremes of temperature and moisture; attack by solvents; difficult inspection except by indirect, nondestructive means; and ; offers the potential for

producing permanent joints that is difficult to repair processing- or service-induced defects (lokesh et al., 2020). Table 1.1 summarizes the relative advantages and disadvantages of mechanical fastening, welding and adhesive bonding for joining composite.

Table 0.1 The advantage and dis advantage of the three joining techniques (Lokesh et al., 2020).

Composite Joining Technique	**Advantage**	**Dis –advantage**
Mechanical Joining Technique	• No special surface preparation needed. • Less critical fit-up requirements. • Disassembly is possible without damage. • Inspection possible by direct observation. • Greater resistance to out-of-plane (peel or cleavage) loading. • Less sensitivity to environmental degradation	• Unavoidable stress concentration from holes for fasteners • Possible leaks at joints or holes • Weight penalty due to fasteners, inserts, or doublers. • Possible galvanic corrosion of fastener by composite
Adhesive Joining Technique	• Little undesirable stress concentration. • Little or no weight penalty. • Smooth external surfaces. • Freedom from galvanic corrosion. • Facility with thin sections. • Lower sensitivity to cycling loading (fatigue)	• Dis-assembly without damage to components. • Susceptibility to environmental degradation. • Need special surface preparation. • Difficult to inspect • Difficult to repair.
Welding Joining Technique	• Freedom from fastener bearing problems. • No extra weight due to nuts or bolts. • The welding process does not rely on parts to fit exactly • production of joints of high structural integrity and efficiency and permanence	• Cause melting of adherends • Use filler material • most permanent of all joints

1.3 Statement of Problem

Metals such as aluminum and titanium alloys in aerospace and automotive industry are replacing by composites. Composites can offer excellent stiffness to weight ratio, corrosion resistance, thermal and electrical properties, and durability. The increasing use of composites in such complex applications leads to the proportional increase of joints. Joining technologies used for metallic elements such as welding, mechanical fastening and riveting are not directly transferable to composite materials joining. Thermoset composites are not thermally weldable, drilling or punching composites with post-manufacture mechanical fasteners or rivets damage the reinforcement, can cause delamination, and initiate cracks in the resin matrix, additional weight of the fasteners, stress concentration. Adhesively bonded joints can solve these problems because they offer more uniform stress distribution along the bonded area, resulting in higher stiffness and coression resistance than a riveted joint. Provide sealing and electrical insulation excellent fatigue strength damping, and shock absorption, manufacturing-friendly process and lower fabrication cost than other joining methods.

1.4 Objective

1.4.1 General Objective

The main objective of this thesis was to study the bond strength of adhesively joined composite materials using experimental investigation and parameteric optimization by Taguchi method.

1.4.2 Specific Objective

1. To investigate the effect of joint configuration on the joint strength of adhesively joined composite.
2. To investigate the effect of joint overlap length of composites (adherends) on the joint strength of adhesively joined composite.
3. To investigate the effect of environmental factors (temperature) on joint strength.
4. Investigation on mechanical properties of the joint (tensile strength, flexural strength, compression strength).
5. Analyze the fractography to characterize the fracture surface of material.
6. To optimize process parameters using Taguchi method.

1.5 Scope of the Study

This thesis was delimited to the study of the effect of joint configuration, joint overlap length, and environmental factors (temprature) on the strength of adhesively bonded composite. This work includes all the necessary steps to the preparation of composite with 15mm chopped banana fiber, 2% nano Al_2O_3 filler, and treated by 5%NaoH at the laboratory scale. At the same time preparation of adhesively joined composite specimens with varying configuration joint, joint overlap length, temprature from the fabricated composites. Then using these samples tests tensile strength, flexural strength, compression strength and fracrography analysis were conducted. Finally experimental results were analyzed and optimized through Taguchi method and the best adhesive joining technique with best joint strength were selected.

1.6 Significance of the Study

Adhesively bonded joints of composite are more beneficial than other methods joining of composite like mechanical joining (rivet) and welding. Some the advantages of adhesive joining are given below.

- ✓ Little undesirable stress concentration but, rather, favorable load spreading.
- ✓ Little or no weight penalty.
- ✓ Smooth external surfaces for aerodynamics and improve visual appearance.
- ✓ Freedom from galvanic corrosion.
- ✓ Facility with thin sections.
- ✓ Lower sensitivity to cycling loading (fatigue) due to lower stress concentration and better strain accommodation.
- ✓ Freedom from fastener bearing problems and noise reduction.
- ✓ Reduce number of production parts and simplify the design.
- ✓ Excellent thermal and electrical insulation.
- ✓ Sufficiently flexible to allow for variation in coefficients of thermal expansion.
- ✓ Improve damage tolerance.
- ✓ Lower fabrication cost and no require special skill.

1.7 Limitation of the study

- ✓ Difficult or impossible disassembly without damage the components
- ✓ Susceptibility to environmental degradation

- ✓ Requirement for special surface preparation to activate for bonding
- ✓ Difficult to inspect except by indirect nondestructive means
- ✓ Difficult to repair processing- or service-induced defects.

1.8 Organization of the Thesis

The organization of the thesis had been done as follows. Chapter one includes introduction in which the background, statement of problem, objectives, scope of the study, significance of the study and limitations were described. Chapter two includes the literature survey, a summary of the literature, and the research gaps. Chapter three covers the material and methods, which include the preparation of adhesively joined composite sample and characterization of mechanical properties of the joint between the adhrends. Whereas chapter four deals with the results and discussion. This implies that the result for every response in addition to this optimization of parameters were included using the Taguchi method and the gray relational analyses. Chapter five comprises the conclusion and recommendation. The interpretations of the obtained results were analyzed and recommendation and future work was directed.

CHAPTER TWO

LITERATURE REVIEW

2.1 Introduction

In this chapter a review of available literature was offered to provide background information on the issues to be focused in this thesis and to highlight the importance of the present study. The review deals with various aspects of the joining of composites with a special reference to adhesively joined composites. This chapter contains review of existing research reports and research gap was identified from the review:

- On mechanical joining of composite.
- On adhesive joining of composites.
- On welding type of composite joining.
- On failure mechanism of adhesively joined composite.
- On fractography analysis of failure.
- On effect of process parameter on strength of adhesively joined composite.
- On Taguchi and Grey analysis method of optimization and finally summery and research gap were presented.

2.2 Mechanical joining of composite

Anna et al., (2020) studied the factors that influence the strength of the bolted joints in composite materials: clamping torque, clearance between the bolt, and the material. It was found out that the increase in clamping pressure by applying the bolt torque has a positive effect on the bolted joint static and fatigue strength, However, only moderate torques improve the situation significantly, however, further increase of torque yields no effect or lead to the decrease of strength. Clearance leads to a decrease in the static bearing strength of the joints. However, a study concerning fatigue strength revealed that the fatigue strength may be improved by the presence of clearance. Drilling holes that are necessary to join composite parts by a bolt is a source of problems. Undesirable damages such as delamination, fiber pull-out, and micro buckling induced by drilling reduce the static and fatigue strength of the joints.

Cezary et al., (2020) studied mechanical methods suitable for connecting fiber-reinforced compostable materials to metal elements, except bolted connections. These techniques were compared to each other and compared to bolting to select the best technique for a particular application. The feasibility of non-destructive degradation of the joint, the damage caused by the joining process, the degree of complexity of the procedure, the feasibility of use for both thermoset and thermoplastic matrix composites, and the development were identified. It was concluded that composite mechanical joining methods have limitations such as stress concentration and unwanted damage.

Josefine et al., (2016) conclude that high joint strength bolts and rivets are often used in highly stressed engine components. In the aerospace industry, composite metal joints are typically joined by titanium rivets inserted through holes in the two materials. The advantage of bolted connections is that the connected components can be separated by removing the connecting elements. This allows for further processing. However, fiber damage, the formation of a polymer matrix in the bolted joint, and loss of bolting force reduce adhesive strength and fatigue life. However, the mechanical strength of the joint can be increased by incorporating high-strength titanium foil into the composite laminate in the fusion zone. The disadvantages are the long production time and the cost of riveting and screwing connections.

The ultimate loads of bolted joints with increasing number of bolt were found to be 5756.8 N, 6609.9 N, and 8434 N and the maximum shear stress are 9.3N/mm^2, 10.5 N/mm^2, and 13.5 N/mm^2. Figure 2.1 shows lowest failure was determined at two bolted joint and highest failure load was determined at four bolted joint. The failure load was increased due to increasing number of bolts (Senguttuvan & Lillymercy, 2015).

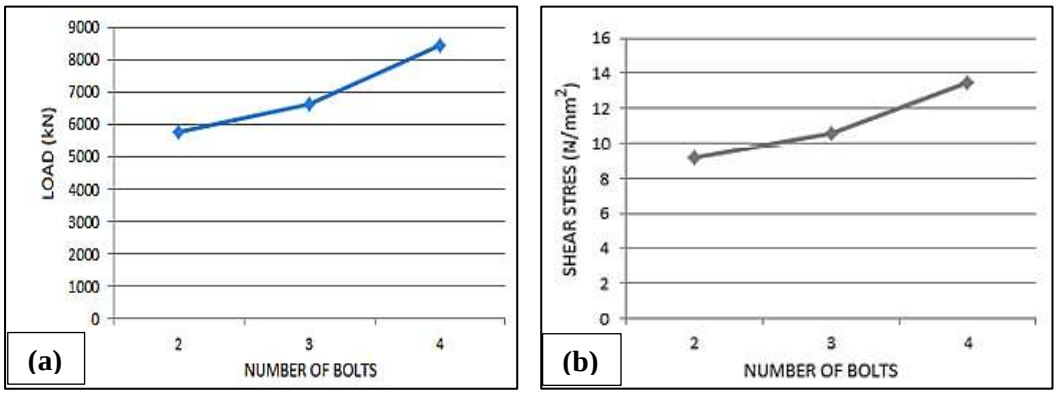

Figure 2.1 Number of bolts V_S load (a) Number of bolts V_S shear stress (b)

The ultimate loads of riveted joints with increasing number of rivets(2,3 & 4 rivets) were found to be 1392.6 N, 2020.2 N, and 2932.3 N, and the maximum shear stress are 2.3N/mm^2, 3.2 N/mm^2 and 4.7 N/mm^2. Figure 3.2 shows lowest failure was determined at two riveted joint and highest failure load was determined at four riveted joint.The failure load was increased due to increasing number of rivets. The strength of the riveted joints increased by increasing the number of rivets (Senguttuvan & Lillymercy, 2015).

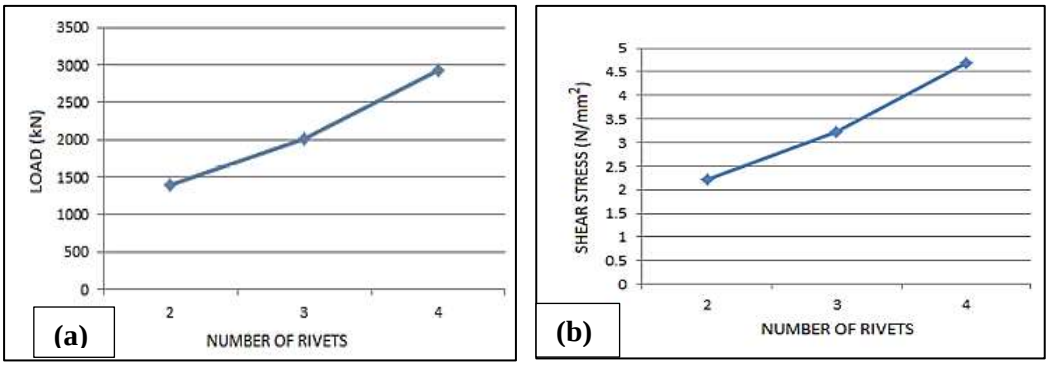

Figure 2.2 Number of rivets VS load (a) Number of rivets VS shear stress (b)

2.3 Welding type of composite joining

One of the advantages of thermoplastic over thermoset composites is that they can be melted and reshaped. As such, they can be joined together by welding, also known as fusion bonding. This joining method is limited to thermoplastic matrix composites. Thermoset composites can be joined using a form of welding, where a thermoplastic interlayer is melted and creates a joint between the thermoset parts, but this process has more in common with adhesive bonding, as there is no comparable molecular diffusion or intermixing at the interface between the thermoset and thermoplastic. Many composite welding techniques have been developed over the past decades. They typically fall into three categories depending on the nature of the energy source used to provide the heat to melt the thermoplastic. Those are electromagnetic heating, mechanical heating and externally heated techniques (Chris et al., 2020)

Conventional joining methods for CFRPs to metals and to CFRPs such as bolting, riveting, adhesive bonding etc. fall under non-thermal process category, whereas welding process is in thermal process category. Therefore, this method is only valid for CFRPs based on thermoplastic matrices. The applications for microwaves, induction heating and friction

heating have been reported to attain localized melting of thermoplastic matrices. The trend of all these thermal processes is the partial melting of matrix material within CFRPs, causing the adhesive bonding and interlocking to metal surfaces(Moller, 2010).

Unlike composites made with a thermoset matrix, thermoplastic composites (TPCs) require neither complex chemical reactions nor lengthy curing processes. Thermoplastic materials require no refrigeration, offering practically infinite shelf life. The polymers used in aerospace offer high damage tolerance in finished parts, as well as moisture and chemical resistance and, thus, do not degrade in hot/wet conditions. And they can be re-melted, promising benefits in repair and end-of-life recyclability. It presents an attractive alternative to the conventional methods mechanical fastening and adhesive bonding used to join thermoset composite (TSC) parts (Gingar, 2018).

2.4 Adhesive joining of composites

Adhesion is described as two surfaces that are held together using interfacial forces. This could be with the help of valence electrons, interlocking actions or both. There are two mechanisms in work for adhesive bonding, which are mechanical interlocking and chemical bonding. Mechanical adhesion makes use of a rough surface and adhesive to secure the parts to each other. Porous materials or materials with cavities are therefore the only types that can make use of mechanical adhesion. Both surface preparation and which adhesive that is used are of equal importance when mechanical adhesion is needed (Çoban et al., 2019).

Adhesive bonds can be divided into two main categories, structural and non-structural adhesives. Structural adhesives are used for applications where the adherends need to withstand large stresses. The bonds are required to deal with the stresses for the entire service life of the part, which could in some cases be several years (Ebnesajjad and Landrock, 2015a). There are no unified rules to determine when an adhesive is thought of as structural. The most common method of determining if an adhesive is structural is if it exceeds 6.9 MPa in tensile shear testing, using the standard ASTM D1002. Nonstructural adhesives do not have to fulfill any of the requirements that structural adhesives are evaluated by. Rather they are used for bonding light-weight materials where the strength of the adhesive bond is less of a factor (Ebnesajjad and Landrock, 2015b).

Adhesive joining of composites components is convincing due to the suitability for joining of any combination of similar or dissimilar materials. Further advantages of adhesive bonding are the flat, uniformly distributed and fiber friendly load introduction and the possibility of bonding components with different thickness. However the material thickness is an important parameter for the overlapping length. Another advantage is the prevention of galvanic corrosion between dissimilar materials (Josefine et al., 2016).

Additionally, adhesive bonding is easier to implement in SME due to the cost efficiency. However the depending of joint durability on adhesive strength must be mentioned, as well as the material degradation over time. The required surface treatments and the long curing time increase the production time and the energy consumption. Further, humidity and temperature requirements necessitate specific attention. To improve the mechanical joint strength sculpted metal components can be used (Çoban et al., 2019).

2.4.1 Stresses of adhesive bonds

Adhesive bonds can experience different kind of stress, which can be divided in five categories. The five types are compression, tension, shear, peel, and cleavage as shown in figure 2.3. It can either be purely one type of stress or a combination of different ones (Ebnesajjad and Landrock, 2015b).

i. **Compression**: An adhesive bond is the strongest when under compression. However, this type of stress is not commonly encountered for applications where adhesive bonds are used.
ii. **Shear**: For this type of stress, the load is evenly distributed across the adhesive bond. Because of this, the bond is fully utilized and therefore failure is less likely to occur.
iii. **Tension**: Stresses in this case is similar to that of shear, as the load is evenly distributed over the bond area. This advantage of even distribution is however lost if any angular offset of the load is present. For these cases cleavage or peel are most likely to occur together with tension.
iv. **Peel**: This type of stress only develops if one or both of the adherends are flexible. Adhesive bonds are typically sensitive towards this type of stress.
v. **Cleavage**: Stress from cleavage is similar to that of peel and appears when a stiff adherend experiences an uneven load. The stress is then larger in one side of the

joint. In order to avoid failure from cleavage, a large joint area needs to be applied which can be expensive.

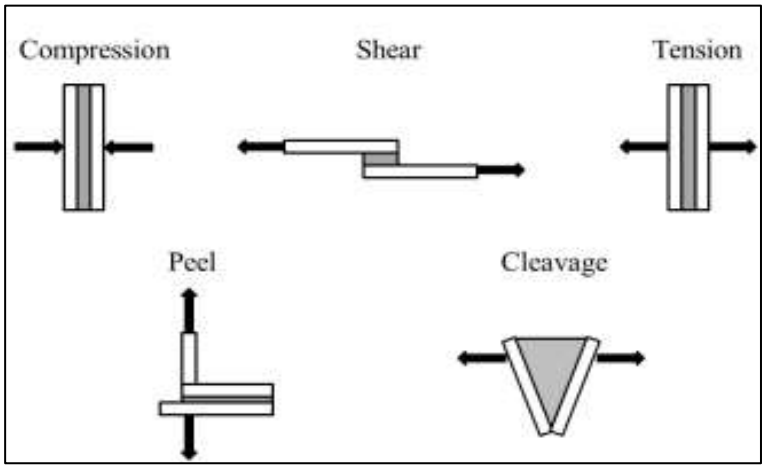

Figure 2.3 The five kinds of stresses that an adhesive bond can experience (Ebnesajjad and Landrock, 2015b).

Just like for the mechanical joining methods the application decides the loads that the joints will undergo but for the sake of simplicity they have been broken down into the same two theoretical load cases as for mechanical joining, transverse- and axial loading. However here, the joints instead rely on adhesion forces to create a bond. Generally adhesively bonded joints are stronger in transverse loading and weak against axial loads, or as they are also called, “peel loads” (Legdin, 2017). However similarly like for mechanical joints, where there were stress concentrations close to the holes, there will be an uneven shear stress distribution in adhesively bonded overlap joints. There will be local peak stresses at the edges of the bond and they decrease as you move towards the middle of the bond.

The reason for the increased use of adhesive joining is that it can provide a number of structural and economic advantages over more traditional methods of joining, of course assuming that the joint is properly designed. One of the most important features to keep in mind during the initial joint design is that adhesive joints are very strong in shear, but unfortunately are very vulnerable to normal stresses (in the context of adhesives commonly referred to as peel stresses) (Çoban et al., 2019).

2.4.2 Surface treatments prior to adhesive bonding

(Española, 2016) studied about the various methods for surface treatment on the adherend surface to create stronger adhesive bonds. Some of these are grit blasting, abrasion, plasma

treatments, acid chemical etching, peel-ply, and laser processing. Blasting and abrasive processes are the most common when it comes to mechanical methods. These methods could cause damage by fracturing the fibers and delamination of the fiber matrix; therefore, it is crucial to perform them with care. Most of the time additional cleaning operations are necessary to remove particles, grease and other contaminants that could occur before and after the surface treatment (Coban et al., 2019).

The type of pre-treatment is often a compromise between the best surface preparation, economics of component manufacture and health and safety issues. The benefits of using appropriate surface pre-treatments are enhanced mechanical performance of joint, improved joint durability in aggressive environments, increased service-life of component and ability to bond difficult adherends like polyolefin and PEEK (Chris, Ewen, & Charlotte, 2020).

It is often necessary to protect the adherend surfaces before bonding as a prepared surface is highly reactive not only towards adhesives but also to atmospheric contaminants. To preserve the integrity of the adherend surface it is usually necessary to bond the surface within a few hours of treatment, or to coat it with a primer which is compatible with the adhesive to be applied later. The full mechanism behind adhesion is complex and can be accounted for via a number of combined mechanisms including mechanical interlocking, Van der Waal's attraction, iffusion theory, adsorption theory (Chris et al., 2020).

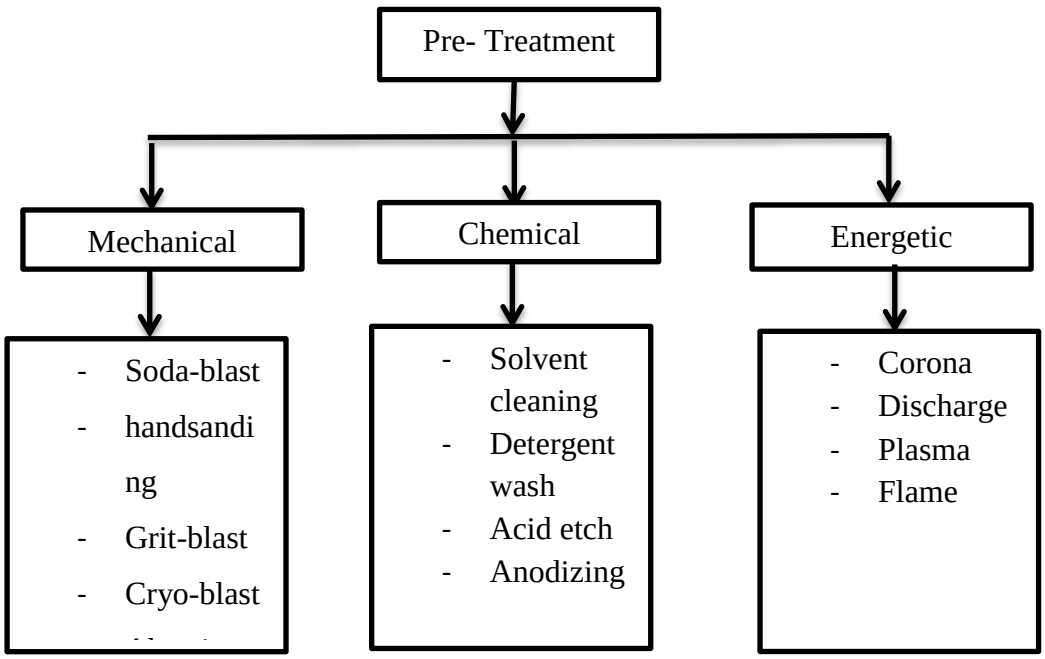

Figure 2.4 The different types of surface treatments (Chris et al., 2020).

Generally there are three main types of surface treatment, whih are mechanical, chemical, and energetict as shown above in Figure 2.4. these types of surface treatments were explained as follow.

2.4.3 Mechanical abrasion

Mechanical abrasion is the most widely applicable surface preparation technique, being suitable for most materials including composites. It include Abrasion, Grit-blast, Cryo-blast, Soda-blast, Peel ply Mechanical abrasion will remove weak boundary layers. It will also change the surface topography of the adherend, increasing the bondable surface area on a micro scale (Moller, 2010). The process will enhance the adhesive's ability to ‘wet’ the surface of the adherend. Mechanical abrasion can lead to better adhesion by providing mechanical interlocking between the adhesive and adherend.

The simplest form of abrasion uses silicon carbide paper to abrade/polish surfaces. This method may be carried out dry or in conjunction with a suitable solvent. The quality of the adherend surface obtained with silicon carbide depends upon the grit size and whether the operation is performed manually or mechanically. It is necessary to monitor carefully the abrasion since, if the process is carried out for too long, surface debris initially removed can be re-deposited. For composites, it is important to note that mechanical abrasion may cause fiber damage and impair performance of the joint (Gingar, 2018).

Blasting is another form of mechanical abrasion and includes alumina grit blasting, cryo-blast and soda-blast. The use of alumina is one of the commonest approaches and can be used effectively on composites if applied carefully. Over-blasting will remove all of the surface resin but can result in fiber damage and potential subsurface cracking if appropriate controls are not in place. Cryo-blast and soda-blast are also used for preparing composite adherends, being less aggressive than alumina grit. Cryo-blast utilizes solid carbon dioxide pellets and relies on thermal shock to remove loosely bound surface material including paints, whereas soda-blast uses sodium bicarbonate particles which are much softer and less likely to cause subsurface damage (charoloth et al., 2020).

For peel-ply surface preparation, a method used almost exclusively for composites, the peel-ply fabric is used as the final layer in the lay-up process. During the cure cycle, the resin matrix flows and penetrates the fabric creating a sacrificial top layer/coating on the composite. When the composite is required for bonding, the fabric is peeled off, fracturing

the resin between the fabric and the first layer of fiber reinforcement, producing a clean, roughened surface to which the adhesive can be applied (Josefine et al., 2019). The surface morphology obtained is dependent on the nature of fabric and type of weave used. However, the peel-ply fabric is often pre-treated with release chemicals to make it easier to peel off. These chemicals then need to be removed from the surface of the composite and this is most commonly done through some type of mechanical process such as abrasion or blast.

2.4.4 Chemical pre-treatment

There are several different chemical methods by which adherends can be cleaned and prepared for bonding including: solvent cleaning, detergent wash, acid etch, anodizing and primers. However, in the case of composite materials, the list is somewhat reduced in that most composite resins have a high surface free energy and little or no change in surface chemistry with regards to the bulk. Solvent cleaning in its simplest form can be performed by using a suitable cloth to apply the solvent to the adherend (Gezary, 2020).

The cloth should be applied so that the surface is wiped in one direction only, to prevent any surface debris from being redeposited. The cloth should also be replaced regularly. Consideration must be given to local or national environmental regulations on the use of organic solvents especially with respect to volatile systems. Many 'tried and tested' systems are being phased out and it is important that the end user is familiar with the replacements e.g. application method, drying times (Anna, 2020).

2.4.5 Energetic pre-treatment

Energetic surface pre-treatments which have been reported in the literature include corona discharge, plasma, and flame and excimer laser. All of these procedures cause a change in the surface texture of the adherend, brought about by the interaction of highly energetic species with the adherend surface. These pre-treatment methods have been applied to metals and in particular composites and plastics (charoloth et al., 2020).

Plasma is an excited gas consisting of atoms, molecules, electrons, ions and free radicals. Applying a high frequency and high voltage between, for example, parallel plate electrodes in a low-pressure chamber, generates plasma. The advantage of this method is that it allows treatment of adherends by different plasmas of argon, ammonia, oxygen or nitrogen. Plasmas created from inert gases are generally used to clean the surfaces of adherends. The

excited species generated can have one or more of the following effects on the adherend: surface clean, degradation and ablation, cross-linking and oxidation: The plasma can lead to introduction of oxygen-containing groups, for example carbonyl, brought about by oxidation of the polymer surface; this can lead to the adherend being readily wetted by the adhesive (Chris et al., 2020).

More recently, laser ablation has been employed to prepare composite surfaces for adhesive bonding. In contrast to plasma processes, lasers deliver a focused beam of energy at the substrate surface which can induce ablation by vaporization of the matrix resin. Depending upon the nature of the laser and associated optics, the beam can be pulsed or continuous enabling the rapid processing of both large areas and discrete regions. The speed of the process enables material to be removed with little or no damage to the surrounding areas and embedded fibers can be exposed intact. In a similar manner to plasma cleaning, the laser can impart additional chemical functionality to the composite surface, thereby enhancing adhesive bonding (Anna, 2020). By varying the power and focus of the beam, the surface topography can be manipulated too. However, in contrast to plasma, lasers can only operate through line of sight, meaning that shadowing can be an issue and internal surfaces cannot be processed. Additionally, laser ablation generates considerable fumes which require careful extraction. The process should therefore be carried out in an isolated cell environment to ensure appropriate health and safety controls (Moller, 2010).

Correct selection of an appropriate pre-treatment is highly dependent upon the adherend composition, structure, properties (mechanical and chemical) and end function. The large majority of the processes described in the previous sections can be applied, at least in part, to most adherends. However, as the process becomes more targeted towards activating the surface chemistry of the adherend. This is particularly relevant to chemical and energetic processes. Additionally, it is not always necessary to select the ‘best’ pre-treatment process when the functional requirements of the final structure do not demand it; cost and pre-treatment time may have a significant impact on the final process selected (Chris et al., 2020).

In the case of composite materials the most significant aspect to consider is the chemistry of the matrix or resin material. For most thermoset systems, the resins employed are either epoxy or polyester in type (Gingar, 2018). Such resins exhibit high surface free energies

once cured and can therefore be pre-treated via some type of abrasive or ablation process in tandem with appropriate removal of loose material/contamination through solvent wiping. In the case of thermoplastic composites, the situation is more complex as the resins employed comprise a number of very different chemistries, most of which have a low surface free energy (Chris et al., 2020).

The commonest resins are PEEK, PEK, PPS, PE and PP, all of which present bonding challenges. In view of this, where possible such materials are therefore preferentially welded rather than bonded, but if bonding is required then the only realistic options are to pre-treat using either energetic technologies (plasma and laser) or possibly some type of chemical etch (Charloth, 2020). It should be stressed that such etches are often complex and hazardous and should only be considered as a last resort. It is for this reason that such approaches are not detailed in this guide.

2.5 Process Parameter that Affect the Strength of Adhesively Joined Composite

The process parametres that affect the bond strength of adhesively joined composite were discussed below.

2.5.1 Joint Configuration of the Adhesive Bond

Joint configuration is one of the main factor that enhance the strength of adhesively joined composites. As the joint configuration changes the bond strength also affect negatively or positively. The area of the adhesive bond must be large enough so that it can endure the maximum force when in use. For a single-lap bond, the stress is the highest at the ends of the lap and the center of the bond carries a relatively low amount of stress. Therefore, if the length of the bond is increased, it will lead to a rather low gain in strength. By increasing the width of the bond it is possible to obtain a higher amount of strength (Ebnesajjad and Landrock, 2015b). The optimum adhesive bond should be stressed in the direction where it has the highest resistance against failure. There are a wide range of different types of adhesive bonds with varying levels of strength (Ebnesajjad and Landrock, 2015a).

2.5.2 Overlap Length

Overlap length is the maximum length in which adhesive placed to join the two adherends. This overlap length has an effect on the bond strength. The ultimate loads of bonded joints

with three adhesive bonding length of 25, 30, and 35 mm were found to be 627.6N, 745.3N, and 902.2N and the maximum shear stress are 1.2 MPa ,0.9 MPa a and 1.1 MPa. Figure 2.5 shows lowest failure load was determined at bonding length of 25mm and highest failure load was determined at bonding length 35 mm.The failure load was increased due to increasing bonding length. The bonding strength of the lap joint increased when increasing the overlap length (Senguttuvan & Lillymercy, 2015)

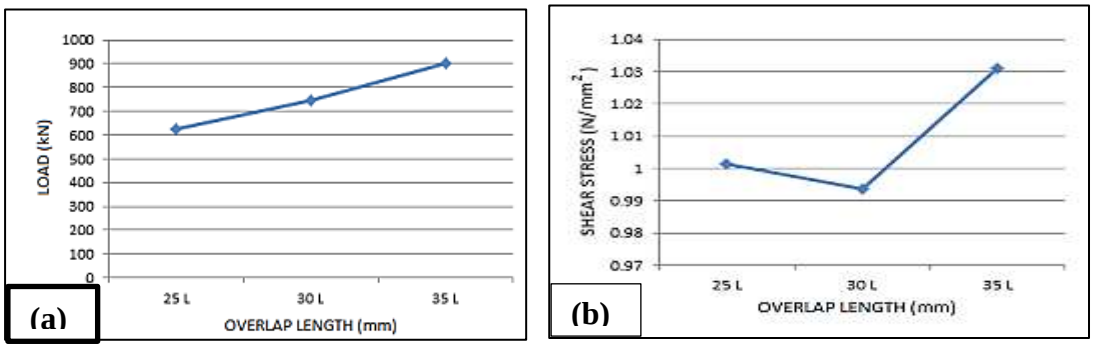

Figure 2.5 (a) overlap length vs load (b) overlap length vs shear stress

2.5.3 Adhesive Thickness of the Adhesive Bond

The thickness of an adhesive bond affects the final strength of an adhesive bond. It has been shown that a thinner bond line increases the strength of a lap joint and the maximum strength was found for bond lines between 0.05-0.5mm. However, this range cannot be applied to all cases as other factors influence the strength, like load type, behavior of the adherend and the type of adhesive. When flexible adhesives are used, for a peel joint,a thicker bond line is sought after because the load can be distributed over a larger area (Silva et al., 2017).

The ultimate loads of bonded joints with three adhesive thickness of 0.2,0.4 and 0.6 mm were found to be 627.6N,460.9Nand 588.4N and the maximum shear stress are 1.00146 N/mm2 ,0.73744 N/mm2 a and 0.94144 N/mm2. Figure 2.6 shows that the lowest failure load was determined at adhesive thickness area 0.4mm and highest failure load was determined at adhesive thickness area 0.2mm.The failure load decreased due to increasing the overlap thickness area. The designers should use minimum adhesive thickness (0.2mm) for maximum bond strength (Senguttuvan & Lillymercy, 2015a).

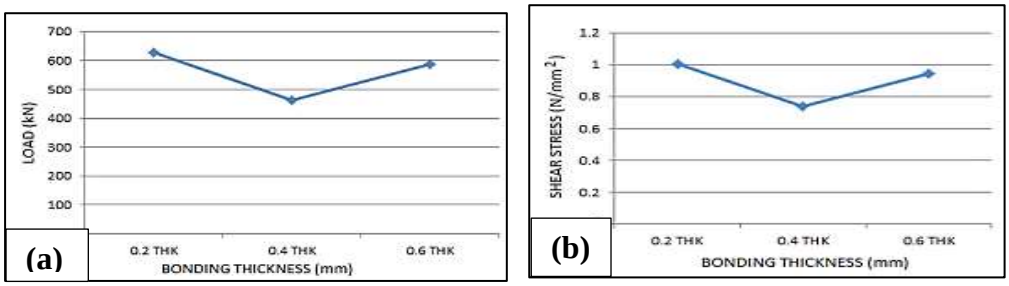

Figure 2.6 Bonding thickness Vs Load (a), Bonding thickness Vs Shear stress (b).

During tensile loading, it was found that as the adherent layer thickness increases, the value of maximum and minimum stress concentration in the joint decreases as the stress was distributed over larger area. Decreasing the adherent layers also increases the level of stress distribution on adhesively bonded lap joints. The loads are transferred from layer to layer on adhesively bonded joints by a shearing mechanism alone and also to reduce or eliminate the shear stress concentration at the ends. Based on the tensile testing, if the adherent lap thickness is increased; the minimum significant stress distributions are developed on adhesively lap joints (Senguttuvan & Lillymercy, 2015b).

2.5.4 Environmental Factor (Temprature)

Pantelakis et al., (2013) Studied the durability of bonded joints was defined and presented for parameters that might influence bonding quality. It was shown that environmental ageing and pre-bond contamination of bonding surfaces may degrade significantly fracture toughness of bonded joints. Durability of two composite adherent-adhesive systems was studied in combination with adhesive thickness by conducting mode I and mode II tests on specimens that have been subjected to accelerated thermal and wet ageing. The experimental results showed a contradictory performance of the two adhesives under the different load conditions and thicknesses. Thermal ageing degraded the performance of the joints. Wet ageing enhanced the fracture toughness of the bonded joints due to plasticization of the adhesive. However, subjection to a humid environment for a larger period is expected to lead to a degradation of fracture toughness of the bonded joints.

The effect of pre-bond contamination on fracture toughness of adhesively bonded CFRP laminates was studied by conducting mode I tests. To this end, five different representative pre-bond contamination scenarios were considered. All considered scenarios were found to affect significantly fracture toughness of adhesive bonds. This finding highlights the criticality of the physicochemical conditions of the bonded surfaces in the quality and

strength of the bond line. Finally, a numerical design optimization methodology for joining profiles was presented. The final geometry has an increased strength compared to the initial one by 4.7%. The methodology is parametric and can be applied for the optimization of any joining profile made of textile composite material (Pantelakis, 2013).

Marcella et al., (2015) Concluded that the most adhesive bond failures could be attributed to poor processes during fabrication, with lack of quality surface preparation was the most significant deficiency. Surface treatment increased the bond strength by altering the substrate surface in a number of ways including increasing the surface tension, increasing surface roughness or changing surface chemistry. Grit blasting, hand sanding and peel ply removal are three common methods used to prepare composite surfaces for adhesive bonding whereby the surface has been roughened.

Budhe et al., (2018) studied the following points: Important concerns were critically expressed here regarding the environmental variants (moisture, temperature, humidity) on mechanical performance of composite repair bonded joints. In this review, several scientific challenges and opportunities have been identified in order to develop more durable and cost-effective composite bonded repair technologies with short repair cycle: There is no generalized trend with respect to the effect of moisture and temperature on the bonded joint as it depends on a number of factors: such as curing temperature, curing method, adhesive and composite laminate material. Hence, urgent needs to assess and evaluate the behavior of advanced composite laminate and adhesive material under high and low temperature as well under different moisture conditions in order to utilize the full capability of the material for bonded repair joints.

Advanced structural adhesives and composite material, could offer opportunities to enhance strength and long-term durability of bonded repairs. Time required to fabricate bonded repair mainly depends on drying of composite before repair bonding and curing the same repair joints, could significantly influence the associated economic aspects. The material system that can cure at low temperature with short cycle but should have higher glass transition temperature could be a good for bonded repairs. A complete drying of composite is in current practice of composite repair, but it is not necessary always as deduced by researchers. So curing at low temperature and not complete drying, both help to reduce the repair time which impact on huge economical aspect (Gezary et al., 2020).

Performance of composite repair can be improved by implementing new methods: such as curing by vacuum method which produce a good quality repair with low bond line void as similar to the autoclave curing method, manufacturing by co-bonded method joints, which absorb less moisture compare to the co-cured bonded joints method (Anonymous, 2019). There is need to work on this aspect and plan for more tests and confirm assurance for the better composite repair bonded joints. The available studies focusing on the effect of moisture and temperature on the mechanical behavior of adhesively bonded joints still have considerable differences in terms of the adherend and adhesive material properties, the material processing methods, adhesive curing temperature and specimen configurations.

Thus it is important to have the pre-knowledge such as curing temperature, glass transition temperature, moisture absorption–desorption limit, swelling, thermal expansion of the adhesive and composite behavior at the specified temperature and moisture level over which structure will expose during service period for the best used of material to obtained a better composite repair joints. Limited studies were carried out on the effect of hydro thermal (moisture and temperature) on the composite bonded joints and it is highly demand for this study as the combined effect is more severe than individual condition. Failure criterion of the composite bonded joints and incorporation of moisture and temperature parameter is the main constraint in scarf and stepped lap joints (Budhe et al., 2018).

Cohesive zone model successfully incorporate the environmental issue on the bonded joints and analysis the joints under the influence of moisture and temperature. Still long term durability is a major concern, as it is difficult to predict accurate environmental behavior of the joints. Open face specimen technique introduced accelerated ageing which help to reduce the exposure time. Open face technique offer opportunities for developing accurate prediction of joint behavior for long term using cohesive zone modeling to any adhesive system that exhibits non uniform degradation (Anonymous, 2019).

Gezary et al., (2020) studied on experimental and numerical (CZM) comparison between several types of adhesive joints (SLJ, DLJ, stepped and scarf joint), and considering three adhesives (Araldite® AV138, Araldite® 2015 and Sikaforce® 7752). From the experimentally obtained results, it is possible to conclude that the performance of the joints is very influenced by the choice of the adhesive. For the Araldite® AV138 and large values of LO, the joint with the best performance was the scarf joint, because this joint takes

advantage of the adhesives' strength, even for brittle adhesives, due to the typically fat stress distributions. However, for shorter L_o, due the area effect in the DLJ, these joints behave better. Higher L_o lead to large peak stresses and the area effect is cancelled because of the adhesive's brittleness. On the other hand, for the Araldite® 2015, since this adhesive is more ductile, the DLJ performs best. Under these conditions, the joints take advantage of the higher bonded area, despite the peak stresses.

The scarf joint approaches the DLJ for higher LO because of taking advantage of the more uniform stress distributions and due the DLJ attaining the adherends' limit strength. The Sikaforce® 7752 also performs best in the DLJ joint type. The other joint types are much below the DLJ, with slight advantage for the scarf joint. However, the fabrication complications may not justify the advantage over the SLJ. The scarf joint showed slightly better strength predictions by CZM modeling (Sadik et al., 2021). Actually, due to the improved stress distributions of this joint type, the cohesive strengths rule the failure process, instead of the failure displacements.

Pulido et al., (2019) from the results obtained through the modeling of the adhesive bond by means of the ANSYS finite element software, it can be concluded that the maximum stress decreases with the increase of the length of overlapping area. Moreover, when modifying the thickness of the adhesive, its behavior shows a reduction of effective stresses along the lap length. The maximum load to be reached is responsible for breakage of adhesion; the greater the thickness of the adhesion, the greater the total displacement, after reaching a maximum load value and anticipating the breakage. In addition, the values in the shear stresses compared to the peeling stresses are lower. From the deformation criterion, it can be affirmed that a greater effect is present in the adhesive joint for the geometrical thickness factor.

Passos et al., (2021) a test was conducted to evaluate the influence of the adhesive type and surface treatment in the strength of composite bonded joints. The mechanical behavior of four adhesives was obtained by tensile tests. Unidirectional abrasion (UA) and bidirectional abrasion (BA) were applied as surface treatment. The roughness was evaluated using a 3D rugosimeter. Tests were carried out in SLJs and the strength and failure mode of the bonded joints were examined. The P 110 adhesive presented a fragile behavior, while the E LTX, E 1500 and E 300 adhesives presented ductile behavior. The

treated samples presented rougher and more homogeneous surface profiles. The increase of the surface roughness was more significant in samples treated using BA.

Tests on the SLJs revealed change in the failure mode with the surface treatment from adhesive to cohesive, indicating an increase in the adhesion quality. In bonded joints with the P 110 adhesive, higher stresses were achieved in the samples treated with UA, while bonded joints with the E LTX adhesive showed higher strength with BA. Both P 110 epoxy adhesive and E LTX polyurethane adhesive presented an increase higher than 150% of the joint strength. The E LTX adhesive showed better improvement than the P 110 adhesive as result of manual surface treatment. It is implied that the ductile behavior of the adhesive together with the higher surface roughness produced by the BA contributed to a more efficient mechanical anchorage of the E LTX polyurethane adhesive (Sadik et al., 2021).

2.6 Failure Modes of Adhesively Joined composites

The different ways in which an adhesively bonded joint may fail are categorized into several different failure modes. These modes of failure are adhesive defects, cohesive defects, substrate defects, adhesive failure, cohesive failure, fiber-tear failure, light fiber-tear failure, stock-break failure, or even mixed failure, which is the combination of one or more failure modes (Anonymous, 2019).

Sadik et al., (2021) concluded that one of the main challenges which face adhesives use in advanced applications was the use of fail-safe features; because it was difficult to detect some critical defects which cause significant or total loss of adhesion. Defects in adhesively bonded joints appear in three categories based on their location: interface, adhesive, and adherends. The uncertainty in these defects was categorized as Epistemic when there are means to control their presence, and Aleatory if their cause was complex and challenging to manage. The investigated defects range from mostly being affected by other defects, to affecting other defects. Hence, to control or quantify the presence of these defects, there is a need to investigate the degree of correlation between them, starting with the higher effect defects and uncertainties as they influence many others.

The performance of a bond cannot be purely based on the mode of failure. For example, adhesive failure could occur for some combinations of adhesives and adherends at higher strengths than a similar bond that fails cohesively with a weaker adhesive. So even though

the failure mode is of interest when looking at adhesive bonds, it is ultimately the maximum strength of a bond that is most important (Messler, 2011). The most common failure modes are shown in Figure 2.7 and explained as follow:

2.6.1 Adhesion or Interface Failure

This failure mode occurs when there is minimal adhesion on one or both sides of the bonding surface; see Figure 2.7a. It is characterized by the absence of the adhesion on one of the surfaces due to hydration of the chemical bond formed. The failure occurs due to the inability to develop a chemically bonded cured adhesive surface due to contamination of the adherent surface during adhesive application. Contamination can be the result of poor surface preparation. It can also occur when the adhesive cures before a bond with the adherent is created. Apart from the direct effects of the manufacturing process, operational and environmental factors can contribute to adhesive failure propagation. Such factors include fatigue, adhesive creep and peel stresses. An adhesive failure can happen if the adhesive bond strength has exceeded overstress loads (Adams & Comyn, 2000).

2.6.2 Cohesive Failure

This failure mode arises when there is breakage along with the adhesive layer; see Figure 2.7b. There should be a clear layer of adhesive material on both the faces of the adherend to characterize the failure as cohesive. Failure occurs due to shear stresses, peel stresses, or a combination of both, which happens due to substandard joint design such as too much peel stress, inadequate overlap area or even excess porosity or voids. Adhesive and cohesive failures are also called bond line failures. Cohesive failure detected in service is usually caused by insufficient overlap length and excessive peel stresses. Excessive porosity due to poor conditions during application of the adhesive (for example, high humidity) and adhesive that has started curing prior to the application could also lead to cohesive failure (Ghorbani, 2018).

2.6.3 Substrate or Adherend Failure

Adherend failure in composite joints occurs when there is an appearance of fiber reinforcement from the composite adherend on the ruptured area; see Figure 2.7c. This failure takes place when the mechanical strength of the substrate is lower than the adhesive bond strength. This type of failure usually happens in brittle and thin adherends. Although it signifies good bond strength, the substrate is unsuitable for the type of adhesive chosen.

Alternatively, adherent failure signifies that an alternative joining method should be considered. Adherend failure usually occurs in dissimilar adherents when one of the adherent is metal weakened by corrosion. When adherend failure occurs on a composite plate, the failure load direction varies according to the stacking angle of the contact (Adams & Comyn, 2000).

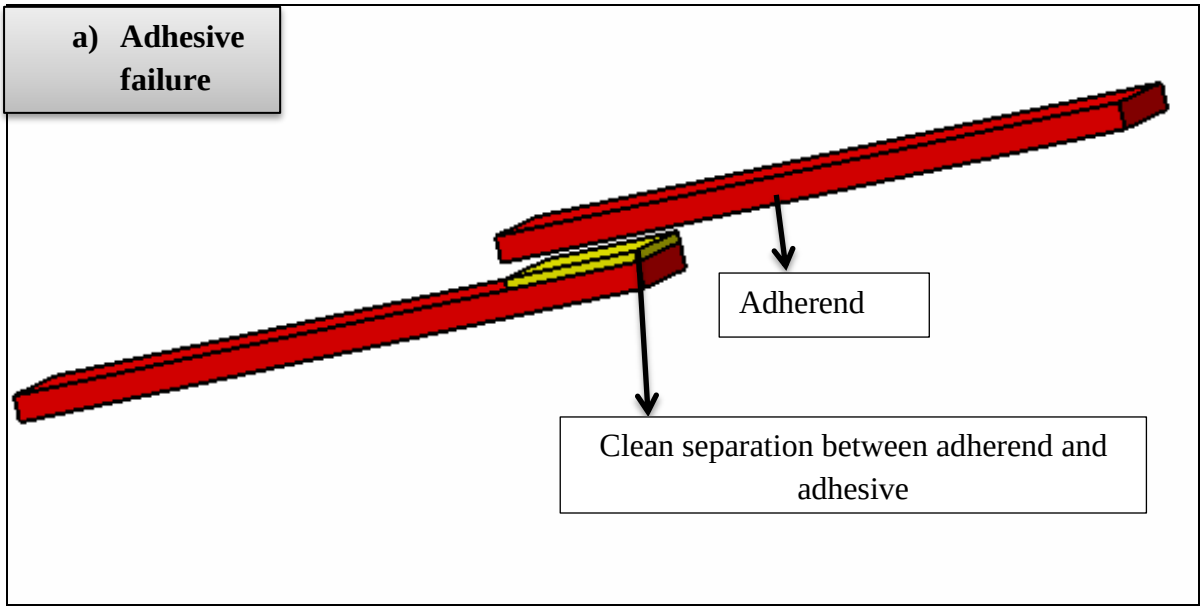

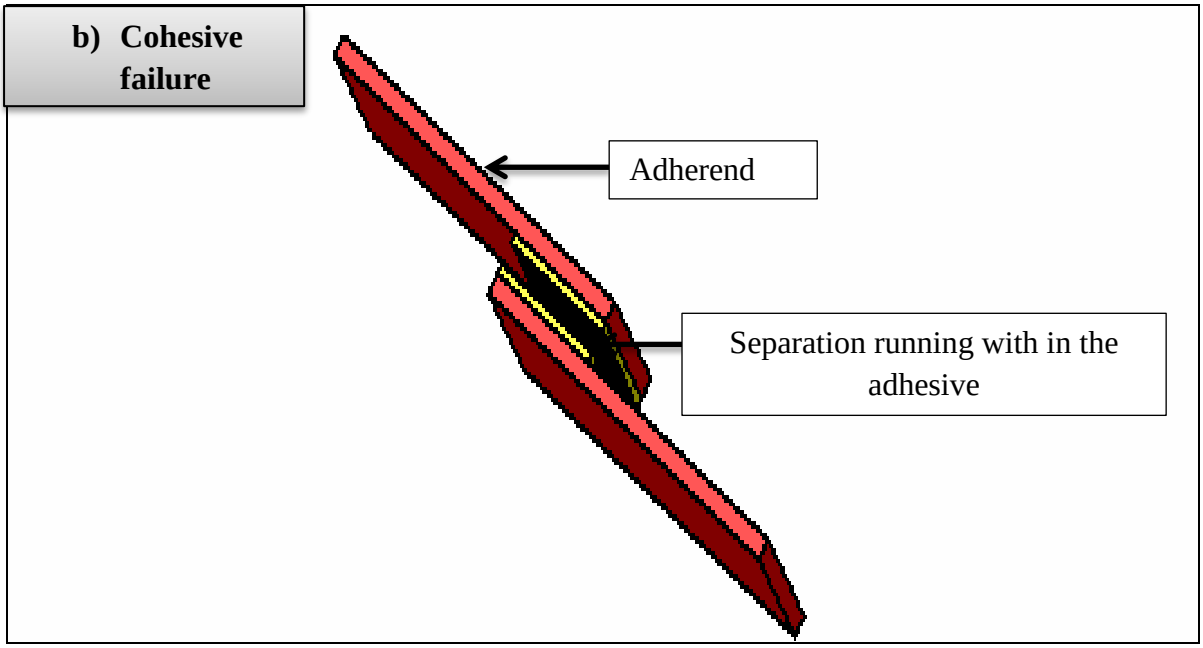

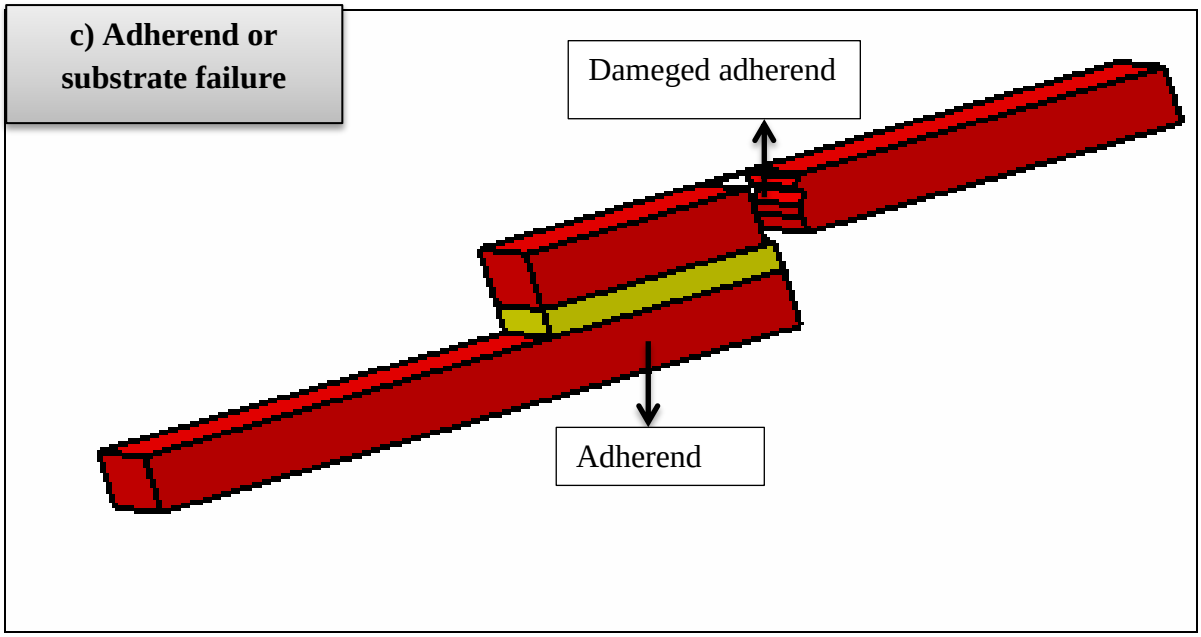

Figure 2.7 The three main modes of adhesive bond failure

2.7 Hybrid Taguchi Based Grey Relational Analysis Optimization

A design of experiment is a systematic, organized method for determining the relationship between factors affecting a process and output of that process. Through various design of experiments, Taguchi method is a statistical approach that is widely used to optimize process parameters and to improve the quality of manufactured products (Singh et al., 2019). The method uses a unique design of orthogonal arrays to provide a reduced variance for the experiment with the optimum setting of process parameters. Orthogonal array is a table (array) whose entries come from a fixed set of symbols arranged in such a way that is an integer n, so that for every section of n columns of the table all ordered-tuples of the symbols formed by taking the entries in each row restricted to those columns, appear the same number of times (Onyekwere et al., 2021).

The advantage of Taguchi's optimization method is that it allows the optimization of the process parameter with a minimum number of experiments. It enables the collection of critical data to discover which elements have the greatest impact on a product's quality with the least amount of trial, saving time and resources. However, the Taguchi method only works effectively for optimization of single performance characteristic (Onyekwere et al., 2021; Sumesh & Kanthavel, 2020a). In this study, multiple performance characteristics are involved.

Taguchi recommends analyzing the mean response for each run in the inner array, and he also suggests analyzing variation using an appropriately chosen signal-to-noise ratio. S/N is a measure used in science and engineering that compares the level of a desired signal to the level of background noise. These S/N ratios are derived from the quadratic loss function and among the three quality exhibition. The optimal setting is the parameter combination that has highest S/N ratio. The statistical analysis of the data is performed by analysis of variance to study the contribution of the factor and interactions and to explore the effects of each process on the observed value (Onyekwere et al., 2021).

Grey system theory developed by Prof. Deng in 1982 has proved to be a useful tool in dealing with poor, incomplete and uncertain information. GRA is a method of calculating grey relational degree and determining the contribution measure of the main behavior of the system or the influence degree between the system factors. The measure of correlation between two factors or between two systems is called grey relational grade. GRA based on the grey system theory can also be used to solve the complicated interrelationships among the multiple performance characteristics effectively. The Taguchi based GRA method was implemented to conduct multi-objective optimization for process parameters (Kopparthi et al., 2021).

The Grey relational analysis procedure is used to combine all the considered performance characteristics into a single value that can be used as the single characteristic in optimization problems (Pandya & Rathod, 2020). The GRG obtained was analyzed by Analysis of Variance (ANOVA), which is a statistical method to analyze variation in a response variable measured under conditions defined by discrete factors. Thus, the study focuses on simplifying optimization of the complicated multiple response of the process using the Taguchi based Grey relation method. All the tabulations were performed using Microsoft excel and Minitab 16 software.

2.8 Data Analysis of Responses

The data from experimentation were hand in to Minitab software and transformed into Signal to Noise ratio (S/N) ratio. Signal to noise ratio is interpreted as the ratio of the mean value of the signal to the standard deviation of noise value. It is used to arbitrate the rank of input process factors or parameters.

In the Taguchi method the response variation was studied using S/N ratio and minimization of variation due to uncontrollable parameter. Taguchi has postulated three objective functions these are (Onyekwere et al., 2021):

- S/N ratio for larger the better which can be calculated using the following formula;

$$S/N = -10\log\frac{1}{n}\sum_{i=1}^{n}\frac{1}{Yi^2} \quad (2.1)$$

Where n and Yi are number of replication on tests and response.

- S/N ration for smaller the better can be also calculated by using the following formula:

$$S/N = -10\log\frac{1}{n}\sum_{i=1}^{n}Y_i^2 \quad (2.2)$$

- S/N ratio for nominal the better calculated using this formula.

$$S/N = -10\,log\frac{Y}{S^2Y} \quad (2.3)$$

2.9 Phases of Optimization by GRA

After obtaining the signal to noise ratio from Taguchi, in order to optimize with GRA we have to proceed with the following steps:

2.9.1 Normalizing S/N Ratios

In the GRA optimization process, the S/N ratio obtained from Taguchi is normalized between 0 and 1. The purpose of this normalization was to remove the variations in the range of responses. In order to normalize the following equation is used (Onyekwere et al., 2021).

$$\text{Larger the better; } Xij = \frac{Y_{ij}-\min Y_{ij}}{\max Y_{ij}-\min Y_{ij}}. \quad (2.4)$$

$$\text{Smaller the better; } Xij = \frac{maxY_{ij}-Y_{ij}}{maxY_{ij}-minY_{ij}} \quad (2.5)$$

Where X_{ij} is normalized S/N ratio, Y_{ij} is signal-to-noise ratio obtained from Taguchi analysis. Min (Y_{ij}) and Max (Y_{ij}) are the minimum and the maximum values of signal-to-noise ratio, respectively.

2.9.2 Calculating the Grey Relational Coefficients

To determine the gray relational grade, first we have to calculate the gray relational coefficient form the normalized S/N value according to the following equation (Onyekwere et al., 2021; Sumesh & Kanthavel, 2020b)

$$GC_{ij} = \frac{\Delta_{min} + \varphi\Delta_{max}}{\Delta_{ij} + \varphi\Delta_{max}} \quad (2.6)$$

Where GCij is the gray relational coefficient, Δmin and Δmax are the minimum and maximum absolute difference, respectively, which is a deviation from the target value. φ is the distinguishing coefficient. The distinguishing coefficient can be used to distinguish the important of each response based on the particular application. φ is a constant value between 0.5 and 1, was assumed as 0.5 for all responses in this study.

2.9.3 Determination of Grey Relational Grade

Grey relational grade were calculated from the relational coefficients. High value of gray relational grade indicates stronger relational degree between ideal sequence and present sequence. The ideal sequence is the best response. Higher gray grade indicates closer to the optimal response in the process. Grey relational grade is obtained from the relational coefficient according to equation (Sumesh & Kanthavel, 2020b).

$$GRG = \frac{1}{m}\sum_{i=1}^{m} GC_{ij} \quad (2.7)$$

Where GRG is the gray relational grade, m is the number of response and GCij is the grey relational coefficient.

2.9.4 Optimal Parameter Setting

Grey Relational Grade was calculated for each experiment data and considered as response for the next analysis. At this stage, the best quality characteristic 'larger the better' was used for further analysis, as it give the best performance characteristics. The GRG obtained was analyzed by ANOVA and the optimal parameter settings was determined (Onyekwere et al., 2021).

2.9.5 Conformation Experiment

Once the optimal levels for each of the factors were determined, a confirming experiment with factors set at the optimal levels should be conducted to validate the earlier results. The

gray relational grade value from the confirmation experiment then compared to the predicted value (Onyekwere et al., 2021).

2.10 Reviewing Related Literature

Banea et al.,(2008) studied adhesive bonding is a viable technique for joining composite materials though the low inter laminar shear and tensile strength limit the joint efficiency. Suitable surface treatments and adhesives for a given application have to be chosen. The choice of which adhesive is best is usually dictated by the type of composite to be bonded, the application, the service environment, and cost. The behavior of specific bonded systems exposed to various environments should be taken into account for durability design. The choice of failure criterion was primarily be dictated by the type of joint considered and is dependent on the joint design philosophy.

An accurate composite bonded joint analysis method must be able to predict failure in the adhesive, at the adhesive adherend interface, and within the surface plies of the laminate itself, and must also account for non-linear material behavior. There was no general agreement about the method that should be used to predict failure since the failure strength and mode are different according to various bonding methods and parameters, but progressive damage models were quite promising since important aspects of the joint behavior can be modeled using this approach. However, a lack of reliable failure criteria still exists, limiting in this way a more widespread application of adhesively bonded joints in principal load-bearing structural applications (Sadik et al., 2021). An accurate strength prediction of the adhesively bonded joints is essential to decrease the amount of expensive testing at the design stage.

Kwon et al., (2011) they studied for both steel–composite and composite– composite adhesive joints that the dispersion of MWCNTs in the adhesive can improve fracture properties. As recent research has exploited the electrical conductivity of CNT networks to monitor crack growth along composite interfaces (while also strengthening these interfaces), adhesive joint strengthening using CNTs may also allow simultaneous damage monitoring. It was shown that nanotube functionalization, concentration, structure, length, and diameter all played a significant role in determining whether nanotube addition strengthened or weakened the adhesive joint. Functionalization of the MWCNTs resulted in better dispersion of the nanotube network, while also shortening the nanotubes. When added to the adhesive, functionalized MWCNTs produced better results than pristine

MWCNTs of similar length for the composite–composite joint. Further research is required to optimize the parameters (concentration, length, side groups, and diameter) for specific bonding cases. Ideally, the specific characteristics of the adhesive of interest would be better known and the functional group could be tailored to chemically react and harden into the adhesive matrix.

Depending on the CNT parameters, adhesive, and loading mode; there exists some optimum concentration of CNTs to produce the best strengthening effect. In general, this optimum was in the neighborhood of 1 wt.% for tests conducted as part of this project. Testing also showed that shorter length nanotubes resulted in weaker bonding in the composite–composite joint tests. Smaller nanotube diameter also produced weaker bonding in the composite– composite tests, all else equal. The key takeaway is that the addition of CNTs is not as straightforward as one might hope in improving fracture characteristics, but rather presents an optimization challenge to get the right length, diameter, concentration, and degree of functionalization to maximize the joint strength (Kwon et al., 2011).

Suwanpakpraek et al., (2019) in this study, the adhesive behavior was found to depend on hydro-static pressure. Drucker-Prager yield criterion with isotropic hardening was used to define the plastic behavior of the adhesive. This criterion was also adapted experimentally as a failure criterion to estimate failure loads of adhesive. The numerical simulation has shown a good agreement of using Drucker-Prager for a yield criterion. For a failure prediction, the Drucker-Prager failure criterion has accurately predicted failure load (0.22% error) when considering all adhesive elements satisfied a failure criterion as a failure of structure (using post-processing method without any degradation rule on elements). However, for a high local stress concentration field, the characteristic length or even characteristic volume were often used to predict a failure of structure rather than all elements failure.

In that case, the single lap shear test can be used to identify a characteristic length and some other test needs to be proceeded in order to validate the identified length. The linear Drucker-Prager yield criterion model proposed in this study significantly differs from the higher order model e.g. hyperbolic Drucker-Prager model at tri-axial state of stress (negative hydrostatic stress) which is a weakest state of stress for adhesive. However, all tests proceeded in this study cannot identify that tri-axial failure, a sophisticated Arcan-Mines test is required in order to justify a suitable failure criterion (Kopparthi et al., 2021)

2.11 Research Gap

A number of researchers had been carried out on the experimental investigation of adhesively joining of composites. However, many of the works were conducted on single process parameter instead of merging different parameters affecting the adhesive bond strength. The use of DOE was rarely done to optimize such kind of work. This work was focused on finding strong joining technique by merging the three process parameters like adhesive overlap length, joint configuration and environmental factors (Temprature). The process parameters were optimized by using one of the DOE technique of optimization called Taguchi.

CHAPTER THREE

MATERIAL AND METHODOLOGY

3.1 Introduction

In this chapter the materials and methods used for the preparation of samples were described. In addition to this the equipment's and machines used to conduct mechanical tests and fractography analysis was also presented.

3.2 Materials

Materials used to prepare composite and adhesively joined composite samples were listed in Table 3.1 and their quantity was shown.

Table 3.1 List of materials used and quantity

Materials	**Banana fiber**	**Polyester resin**	**Nano alumina powder**	**NaOH**	**Distilled water**	**Honey wax**	**Epoxy**
Quantity	2Kg	5 Kg	186g	350g	20L	1	114g

3.2.1 Banana Fiber

Banana fiber was collected from Hawassa city area. The extraction was done by traditional method; the extracted fiber was washed with water and dried by air for one day as shown in Figure 3.1. Combing was carried out to remove dirty and impurities. Then fiber was treated with 5% NaOH to improve physical, chemical and mechanical properties of the fibers. Finally it was washed by distilled water to neutralize the chemicals and dried by air for 3 days. Banana fibere were selected for this thesis work, because it is natural and most available fiber.

Figure 3.1 Alkali treatment of banana fiber

3.2.2 Aluminum oxide

Aluminum oxide has strong ionic inter-atomic bonding and commonly occurs in its crystalline polymorphic phase α-Al_2O_3. Alumina is ceramic material used as the filler in the present investigation were purchased from Mombai, India. These Al_2O_3 powder with particle size of $\leq 50\,nm$ has a density of 0.79 g/cm^3 (Patel & Dhanola, 2016). The packed and measured powder was shown in Figure 3.2. Al_2O_3 was chosen over other ceramics because of it is hard and wear-resistant, has high strength and stiffness and also it serves as filler in plastics (Fathy et al., 2017). It was added to resin and hardener based on the calculated weight percentage by measuring the mass on digital balance.

Figure 3.2 Nano alumina powder

3.2.3 Sodium Hydroxide

Sodium hydroxide has the molecular formula NaOH and is a highly caustic metallic base and alkali salt. Sodium hydroxide is soluble in water, ethanol and methanol. This alkali is readily absorbs moisture and carbon dioxide in air. Sodium hydroxide is used in many industries, mostly as a strong chemical base in the manufacture of pulp and paper, textiles, drinking water, soaps and detergents (Dandesa., 2016). In this work NaOH (5%) in flakes form was used as displayed in Figure 3.3, purchased from local suppliers.

Figure 3.3 sodium haydroxide (NaOH) flakes

3.2.4 Honey Wax

Honey wax allows easy release of fabricated composite from the mold material. Applying a thin coat of wax and wipe off or polish the haze part using a cloth towel is recommended for better surface finish and performance of the material. Figure 3.4 shows the mold release agent, honey wax used in this research work.

Figure 3.4 Honey Wax

3.2.5 Distilled Water

Distilled water is neutral water having a PH of 7, was used for treating and washing the fiber after treatment. Figure 3.5 shows the distilled water used for modifying the fiber surface.

Figure 3.5 Distilled water

3.2.6 Hardener (Catalyst)

The hardener creates a chemical reaction that allows the resin to change from a liquid to a solid state to make polyester resin useful for its intended purpose. This transformation is referred to as "curing" or "polymerization". Topaz-1110 TP; Thixotropic hardener is used as chemical hardener with unsaturated polyester resin. The ratio of catalyst was 2% to the total volume of resin to be used. Generally, it is mixed with polyester resin at normal

atmospheric temperature(Selvam, 2017). it was measured using syringe as shown in Figure 3.6. It was also supplied by World fiber Glass and Water Proofing Engineering PLC.

Figure 3.6 Hardener

3.2.7 Adhesives and Matrix Selection

Since there are many types of adhesives that used for joining of composite, selection of an adhesive for a given situation is necessary. There is a need for selecting the appropriate adhesive because adhesives are versatile and there is frequent overlap of their usage. It requires detailed knowledge of the properties of a particular adhesive and the application in which it is being used. The adhesive selection process is difficult because there is no universal adhesive that works in every application, and the selection of the proper adhesive is often complicated by the variety of available options(Española, 2016; Wahab, 2016).

Adhesive selection includes many factors, such as type and nature of substrates to be bonded, cure and adhesive application method, and the expected environments and stresses that the joint will face in service. Also, the cost of the adhesive may sometimes be an important factor of adhesive selection in a particular production situation. Mechanical actions like impact loads, quasi-static loads, and low and high cycle fatigue loads need to be identified (Nurazzi et al., 2017). The mechanical characteristics of an adhesive vary with factors such as high and low strength, brittle and flexible behavior.

Based on Table 3.2 below the adhesive used for the joint of this study was epoxy. It shows superior mechanical properties compared with polyester and other adhesives. It can be very effectively used for adhesives and laminating resin for most of the engineering applications (Jeyapragash et al 2020). Epoxy imparts improved physical as well as mechanical properties of the composite due to which the composite is needed in high performance

applications such as transportation system, aerospace industries, automobile parts and artificial organ transplantation in biomedical science (Parbin 2019)..

Table 3.2 Criteria for selection best adhesive (Nurazzi et al., 2017)

No	**Adhesive Type**	**Properties of adhesives**	**Temperature Range (℃)**
1.	Epoxy	High strength and temperature resistance, relatively low cure temperatures, easy to use.	−40 to +100
2.	Cyanoacrylates	Fast bonding capability to plastic and rubber but poor resistance to moisture and temperature.	−30 to +80
3	An aerobics	Designed for fastening, in which a tight seal must be formed without light, heat or oxygen, suitable for bonding cylindrical shapes.	−55 to +150
4.	Acrylics	Versatile adhesives with capabilities of fast curing and tolerate dirtier and less prepared surfaces.	−40 to +120
5.	Polyurethanes	Good flexibility at low temperatures and resistant to fatigue, impact resistance, and durability.	−200 to +80
6.	Silicones	Excellent sealant for low stress applications, high degree of flexibility and very high temperature resistance, capability to seal or bond materials of various natures, long cure times, and low strength.	−60 to +300
7.	Polyimides	Thermal stability, dependent on a number of factors, difficult process ability.	40 to 250
8.	Bismaleimids	Very rigid, low peel properties.	50 to +200
9.	Poly ester	Most available in Ethiopia and good for composite joining and preparation.	-20 to +120

From the different type of epoxy; the type of epoxy used for this thesis work was ABRO epoxy with its hardener as shown in Figure 3.7a below. Based on literature and prelimary work the best adhesive for composite joining is abro epoxy than the other to obtain a good bonding strength and it is most available epoxy. Based on the Table 3.2 selection criteria the resin used for this study was unsaturated polyester resin with density 1.29 g/cm^3 for composite preparation and it is shown in Figure 3.7b. UPR is a thermoset, which is capable of being cured from a liquid to solid state when subject to the right condition. Low viscosity for fast wet-out, convenient for hand lay-up applications, low cost, exhibits good mechanical and good chemical resistance, low pressure molding capabilities and capability to cure at room temperature are the advantage of UPR when compared to other thermosetting resins **(**Ouarhim et al., 2018**).** The mechanical properties for the matrix are shown in Table 3.3.

Table 3.3 Mechanical properties of unsaturated polyester (Ouarhim et al., 2018)

Thermoset resin	**Density (g/cm^3)**	**Tensile strength (MPa)**	**Young's modulus (GPa)**	**Elongation (%)**
Polyester	1.09-1.35	50-65	3	2-3

(a) **(b)**

Figure 3.7 ABRO epoxy (a) polyester (b)

It was supplied by World Fiber Glass and Water Proofing Engineering PLC. The weight percentage for each sample resin-hardener mixture was measured on digital mass balance in Chemical Engineering laboratory, ASTU, Ethiopia.

3.3 Process Parameters

The process parameters are the factors that were varying in this process and selected based on literature reviews and preliminary study. Joint overlap length and environmental factor (temprature) were the factors that affect the bond strength of composite materials. Joint design configuration was expected to increase the mechanical property of the composite material. In this experimental investigation all the parameters were utilized to investigate the effect of each parameter on the joint strength of composite and obtain the optimum process parameter from the selected factors.

3.3.1 Joint Overlap Length

Joint overlap length has major influence on strength of adhesively joined composite material. Reviewed literatures revealed that the bonding strength of the lap joint increased when increasing the overlap length but very large overlap length is not recommended. Because this large overlap length leads to increasing production cost. In this research based on review joint overlap length with 25 mm, 30mm, 40mm was selected as shown in Figure 3.9 below.

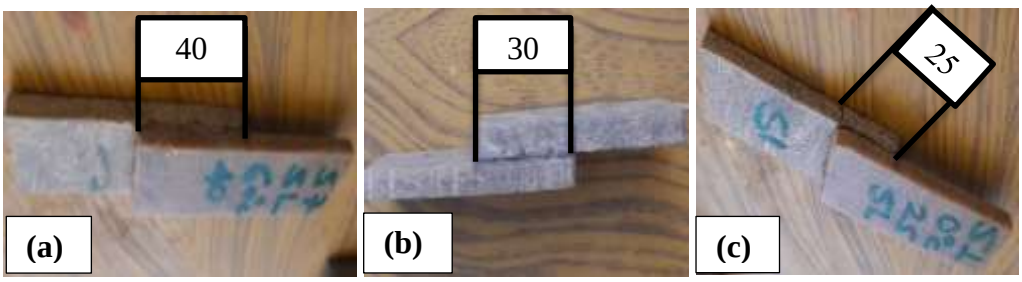

Figure 3.8 Overlap length (a) 40mm, (b) 30mm, (c) 25mm

3.3.2 Design Configuration of Joint

When designing an adhesively bonded structure, one of the first questions that arise is the cross-sectional geometry of the joint. Since the joint geometry greatly affects the stress distribution in the adhesive it must be carefully selected with the expected load case, adherend materials and global structural allowances in mind. Design configuration has gained potential benefits in enhancing the strength of adhesively bonded composites. In this research design configuration of joint was selected in three levels single lap joint (SLJ), scarf joint (SJ), stepped joint (SPJ) as shown in figure 3.9 below.

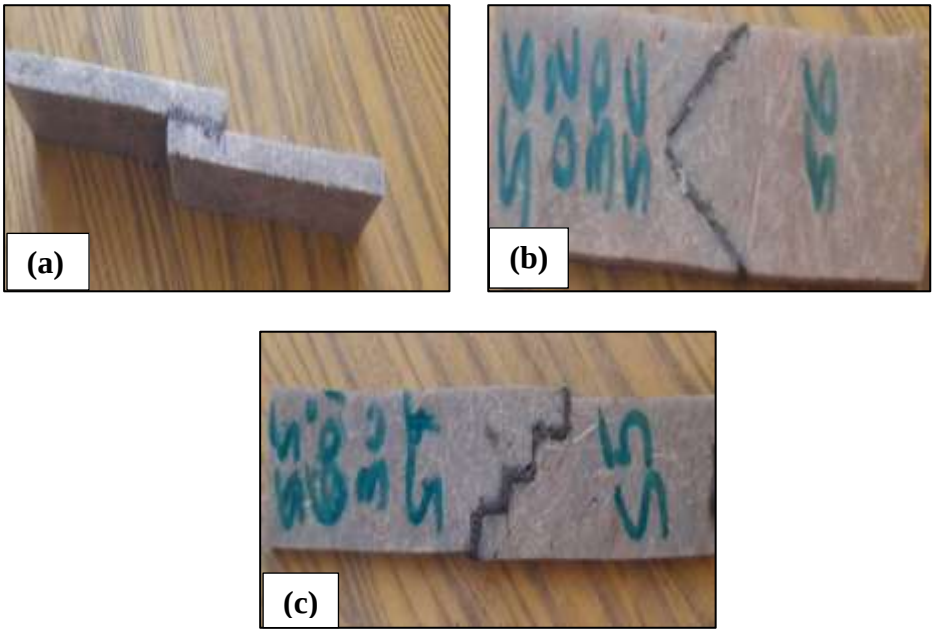

Figure 3.9 Selected joint configuration (a) Single lap joint, (b) Scarf, (c) Stepped

3.3.3 Environmental Factor (Temprature)

Environmental factors (temprature) has major influence on strength of adhesively joined composite material. It was selected in three levels 0℃, 20℃, and 60℃; this selection was based on the Ethiopian environmental temperature condition. The samples was placed in laboratory oven and refrigerator to obtained 60℃ and 0℃ temperature respectively.

3.3.4 Joint Adhesive Thickness

Adhesive thickness has also influence the strength of adhesively joined composite material. Reviewed literatures revealed that very large or small adhesive thickness negatively affect the strength of adhesively bonded composite. Because if the adhesive thickness is very large the strength will decrease and if the thickness become very small the two composite (adhrend) cannot bonded properly. So it is necessary to select the optimum adhesive thickness to get the best joint strength. In this research based on review adhesive thickness of $0.2mm$ was selected, which is the most effective thickness for composite joining to get a good strength (Senguttuvan & Lillymercy, 2015b).

3.4 Sample Preparation Method

The step by step procedure used to prepare adhesively joined composite samples was shown in Figure 3.10.

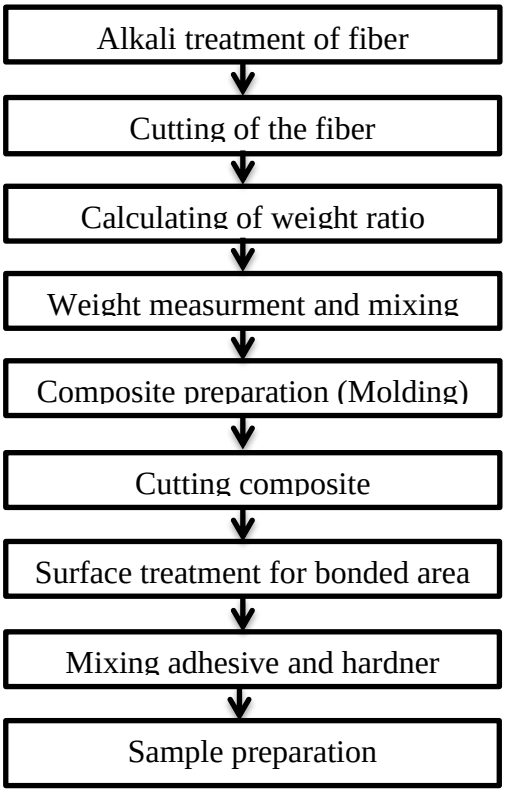

Figure 3.10 Flow diagram of sample preparation

3.4.1 Alkali Treatment of Banana Fiber

The main drawback of natural fibers was their hydrophilic nature resulting in poor adhesion between fiber and matrix. Literatures mentioned that this limitation can be improved by the use of chemical treatment like thermal, alkali, potassium, permanganate and benzoyl chloride on the fiber, which is aimed to remove the impurities like pectin, fats and lignin in the fiber, resulting in improvement in the bond between fiber and matrix (Verma et al., 2013). As a result increased mechanical (tensile, flexural and compression) properties of fabricated composite was obtained.

Alkali treatment also known as mercerization is the oldest and most widely used chemical treatment for natural fibers. In which the natural fibers were immersed in a known concentration of aqueous NaOH for a given temperature and period of time (Faruk et al., 2012a). The concentration of alkali solution that was used to treat the fibers was in the range of 0.5% up to 28%, but most of the researchers used below 10% alkali solution. The

temperature and soaking time to treat fiber in the solution were in the range of 20-180^{0}C and 15 min to 48 hour period of time. The required temperature to dry natural fiber should be below 80^{0}c for 24hr period of time (Naveen & Maheswaran., 2015). The aim of chemical treatment was to improve poor interfacial adhesion between fiber and matrix that lead to poor wetting of fiber with matrix, improve bonding strength, lowers water absorption, increase fiber strength and improve mechanical properties (Faruk et al., 2012a).

In this study alkali treatment of 5% was used to treat the fibers. NaOH flakes were weighted according to the calculation; 50g NaOH was dissolved in 1L distilled water to make 5% NaOH solution (Zin et al., 2018). The fiber was immersed in the alkali solution for 6hr at room temperature. The solution was kept under vacuum condition; once the immersion time ended the fibers were washed thoroughly with distilled water. Finally the fibers were left to dry by air for 2days as we can see from Figure 3.11.

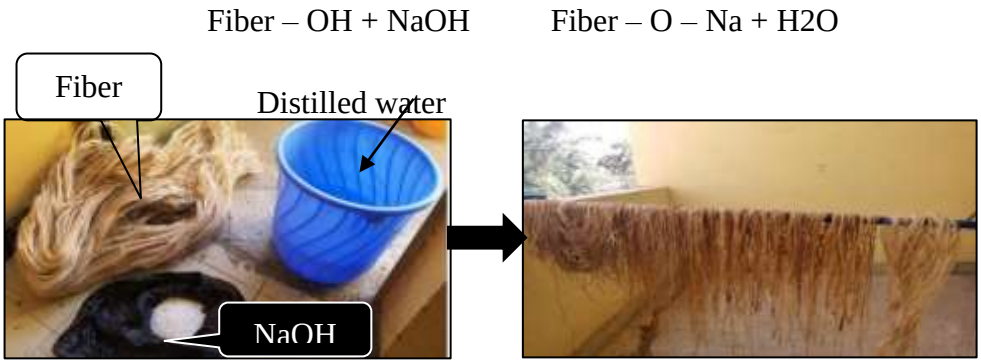

Figure 3.11 Alkali treatment of banana fiber

3.4.2 Cutting of banana fiber

The fiber was chopped to a length of 15mm using scissor and ruler as shown in Figure 3.12.

Figure 3.12 Chopped banana fiber

3.4.3 Calculating Weight, Mass and Volume Fraction of the Particulate, Fiber and Matrix for Samples

Mechanical properties of composite significantly influenced by incorporation of particulate, fiber and matrix materials. These materials can be expressed either as volume fractions or as mass fractions. Based on literature review the composition of each sample was shown in Table 3.4.

Table 3.4 Composition of particulate, fiber and matrix used for sample preparation

	Compositions
Composite	Polyester + Banana fiber (15mm) (15wt.%) + Al_2O_3 (2wt.%)

The mass of composite, matrix and reinforcements were calculated as follow.

$$\text{Mass of composite, } \boldsymbol{mc = \rho c \times Vc} \tag{3.1}$$

Where, mc is mass of composite, ρc is density of composite and Vc is volume of composite.

The mass of Al_2O_3, epoxy resin and banana fiber mass of composite can be multiplied by each weight percentage.

$$\text{Mass of polyester resin} = \text{mass of composite} * 0.83$$

$$\text{Mass of banana fiber} = \text{mass of composite} * 0.15$$

$$\text{Mass of } Al_2O_3 = \text{mass of composite} * 0.02$$

To calculate Mass of Composite, Matrix, Particulate and Fiber ,composite density and volume must calculated first.

The volume of the composite was calculated by multiplying the length, width and breadth of the mold prepared for molding the composite material.

$$\text{Volume of the die} = L \times w \times t \tag{3.2}$$

$$= 300\text{mm} * 300\text{mm} * 5\text{mm}$$

$$= 450\text{cm}^3$$

Where, L is length, W is width and t is thickness of mold.

Since total volume of composite is summation of each volume,the density of composite is given by:-

$$\boldsymbol{Vc = Vm + Vf + Vp} \tag{3.3}$$

$$\text{Volume of fiber} = \frac{\text{mass of fiber}}{\text{density of fiber}} = V_f = \frac{Mf}{\rho f}$$

$$\text{Volume of particulate} = \frac{\text{mass of particulate}}{\text{density of particulate}} = V_p = \frac{Mp}{\rho p}$$

$$\text{Volume of matrix} = \frac{\text{mass of matrix}}{\text{density of matrix}} = Vm = \frac{Mm}{\rho m}$$

Where, Vf is volume of fiber, Mf is mass of fiber, ρf is density of fiber, Vp is volume of particulate, Mp is mass of particulate, ρp is density of particulate, Vm is volume of matrix, Mm is mass of matrix, ρm is density of matrix and Vc is volume fraction of composite.

$$\text{Fiber volume fraction} = \frac{\text{volume of fiber}}{\text{total volume}} = V_F = \frac{Vf}{Vf+Vm+Vp}$$

$$\text{Particulate volume fraction} = \frac{\text{volume of particulate}}{\text{total volume}} = V_P = \frac{Vp}{Vf+Vm+Vp}$$

$$\text{Matrix volume fraction} = \frac{\text{volume of matrix}}{\text{total volume}} = V_M = \frac{Vm}{Vf+Vm+Vp}$$

Where, VF is fiber volume fraction, Vf is volume of fiber, VP is particulate volume fraction, Vp is volume of particle, VM is matrix volume fraction and Vm is volume of matrix.

Total mass of composite = mass of particulate + mass of fiber + mass of matrix

$$\boldsymbol{Mc = Mm + Mf + Mp} \tag{3.4}$$

$$\text{Fiber mass fraction} = \frac{\text{mass of fiber}}{\text{total mass}} = M_F = \frac{Mf}{Mt}$$

$$\text{Particulate mass fraction} = \frac{\text{mass of particulate}}{\text{total mass}} = Mp = \frac{Mp}{Mt}$$

$$\text{Matrix mass fraction} = \frac{\text{mass of matrix}}{\text{total mass}} = Mf = \frac{Mm}{Mt}$$

$$\boldsymbol{Mp + Mf + Mm = 1} \tag{3.5}$$

Where, M_F is fiber mass fraction, Mf is mass of fiber, Mt is total mass, Mp is particulate mass fraction, Mp is mass of particle, Mf is matrix mass fraction and Mm is matrix mass fraction.

$$\frac{mc}{\rho c} = \frac{Mpolyester}{\rho polyester} + \frac{Mbanana}{\rho banana} + \frac{MAl_2O_3}{\rho Al_2O_3} \quad (3.6)$$

Where, Mc is mass of composite, ρc is density of composite, Mpolyester is mass of polyester, Mbanana is mass of banana fiber and MAl_2O_3; ρpolyester is density ofpolyester, ρbanana is density of banana and ρ_{Al2O3} is densitu of alumina. Density of banana fiber, nanoAl_2O_3 powder and polyester resin is 1.32g/cm3, 0.79g/cm^3, 1.15g/cm^3 respectively.

$$\frac{1}{\rho c} = \frac{0.83}{1.15} + \frac{0.15}{1.32} + \frac{0.02}{0.79}$$

$$\rho c = 1.162 g/cm^3$$

Mass of composite, $mc = \rho c \times Vc$

$$= 1.162 g/cm^3 * 450 cm^3 = 522.8 g$$

Mass of polyester resin = mass of composite $*$ 0.83 = 522.8 * 0.83 =433.9g

Mass of banana fiber = mass of composite $*$ 0.15 = 522.8 * 0.15 = 78.43 g

Mass of Al_2O_3 = mass of composite $*$ 0.02 = 522.8 * 0.02=10.45 g

The requied volume of epoxy used to join the two adhrends was calculated as follow. .

$$V = L \times w \times t$$

Where, L is length, W is width and t is thickness of bonded area.

Example for S1; V = 2.5 * 2.5 * 0.2 = 1.25 cm^3

Table 3.5 Tabulated composition of polyester, banana fiber and alumina

Composition (wt.%)			**Mass(g)**			
Polyester	**Banana**	**Al_2O_3**	**Polyester**	**Banana**	**Al_2O_3**	**Total**
83	15	2	433.9	78.43	10.45	522.8

3.4.4 Weight Measurements and Mixing of Alumina, Fiber and Polyester

The masses of the Banana fiber, Al_2O_3 and polyester resin were measured according to the calculated weight fractions as shown in Figure 3.13. The hardener was added 10:2 ratio with polyester resin.

Figure 3.13 Weight measurements of alumina, fiber and polyester

After measurement the polyester resin and hardener were mixed for about 5minute and nano Al_2O_3 was added and mixed well for 5minutes at room temperature continuously and slowly to avoid bubbling during mixing. The mixing was performed in the mixing container made of plastic and the mix was done slowly to avoid oxidation of the powder. Finally as shown in Figure 3.14a chopped banana fiber was added to the mixture and mixed well with the matrix and filler for 10minutes.

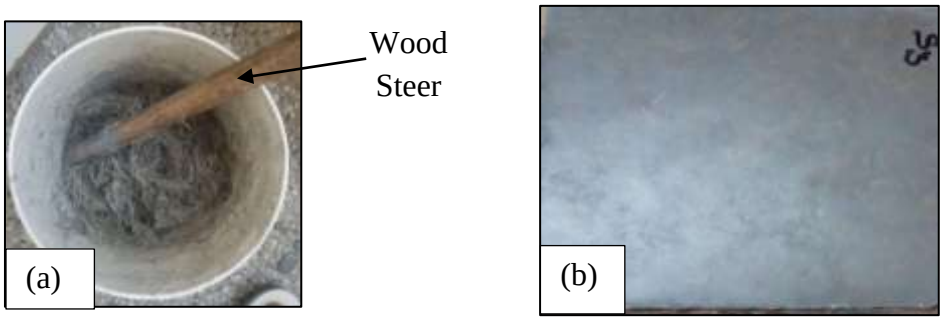

Figure 3.14 Mixture of polyester, hardener, alumina and banana fiber (b) Fabricated banana fiber rainforced composite

3.4.5 Fabrication of Composite (Molding)

The composite was fabricated by hand-layup method. A mold of 300mm*300mm*5mm was prepared from wood and placed the mixture according to the calculated weight. The mold was pressed with C-clamp and sample was then left to be dried. The composite gets dried up in 24 hours in which the Banana fiber and the mixture adheres itself tightly in the presence of hardener. The mechanical properties of this fabricated composite was 21.7,

64.7, and 32.4MPa for tensile, Flexural, and Compression strength respectively. The fabricated samples were shown in Figure 3.14b.

3.4.6 Cutting the Composite

The specimens were cut according to the ISO and ASTM standard cut by jig saw in to required samples base. These samples had different joint design configurations and overlap length as shown in Figure 3.15.

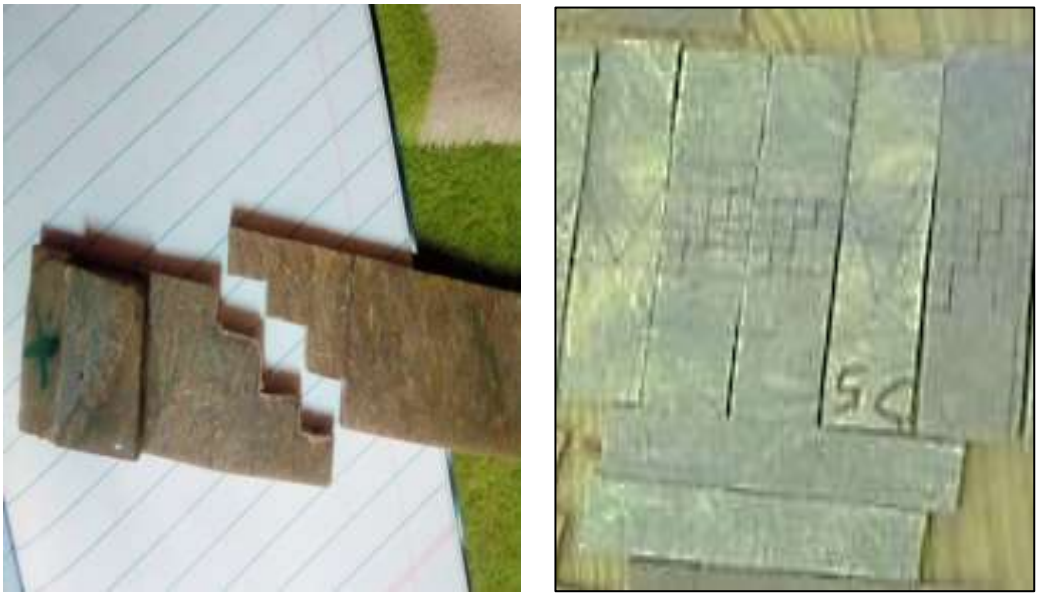

Figure 3.15 composite cut by jigsaw

3.4.7 Surface Treatment

Surface treatment is used to remove dirty on surface of composite, to remove honey wax that used during composite preparation; generally it used to enhance the strength of the joint. There are different types of surface treatment used; this research used hand sanding which is best for composite. Using a hand sanding as a surface treatment is common for composites as a way of removing the gloss from the surface or making it rougher. It is crucial to monitor the process when using the different methods to not make the surface excessively rough. The joint strength could weaken if the surface roughness is too high because of stress concentrations (Rudawska, 2019b).this paper used 80 grit sand paper for surface treatment as shown in Figure 3.16.

Figure 3.16 surface treatment

3.4.8 Mix Liquids and Sample Preparation

the epoxy used for adhesive purpose was ABRO STEEL EPOXY resin. This resin mixed thoroughly with hardener until a uniform color is achieved then apply the mixed resin on the surface required to join by hand layup method. After joining slight compression pressure is required to optain good quality joining.the fianal sample is shown in Figure 3.17 below.

Figure 3.17 Final Samples

3.5 Equipment's and Machines Used

3.5.1 Analytical (Digital) Balance

There are many equipment's used to measure the mass of adhesives. The digital mass balance in the ASTU chemistry labs are very sensitive instruments used to accurately measure mass. Their reliability has a range between 0.1mg to 0.01mg. This device is also important to measure while mixing the composites and to characterization physical properties. Figure 3.18 shows the digital balance

Figure 3.18 Analytical (digital) balance

3.5.2 SEM Microscopy

SEM is the most common method for imaging the microstructure and morphology of material.an electron beam with low energy is radiated to the material and scans the surface of the sample. Several different interactions occur as the beam reaches and inters the material, which leads to the emission of photons and electrons near the sample surface. In order to form imaging the receiving signals produced from the electron-sample interactions are detected with different modes of SEM exist for characterization of material such as X-RAY mapping, secondary electron imaging, back scattered electron imaging, electron channeling and auger electron microscope (Leng, 2008). The Fractography analysis of adhesively joining of composite was studied using scanning electron microscopy at Biology department ASTU, Ethiopia. The instrument used for SEM imaging was shown in Figure 3.19.

Figure 3.19 SEM microscopy

3.5.3 Jig Saw Cutting Machine

This machine was used in this thesis work for cutting the composite in to different desired standard. Figure 3.20 represents jig saw machine used in this research, located at local wood work factory.

Figure 3.20 Jig Saw

3.5.4 Universal Testing Machine (UTM)

The universal testing machines are a computer equipped machines used to measure the material mechanical properties under different load conditions. UTM testing machine is a machine suitable for conducting tests like the tensile, compression, bending and shear test for all kinds of metal and nonmetals by simply changing the jaws and modes of operations. The main components of the UTM are, actuator, attachment kit, safety devices frame, engine, and gear, screws, and crosshead grips extensometer, hardware and software control. The control unit is composed of computer and control system, it process stress, strain and displacement control modes, the test data can be stored at will, and the data and curves can be reanalyzed, part amplified and data re- edition, test conditions (specimen, measurement) are programmable. All the mechanical properties can be obtained automatically and print whole test report and curve(Selvam, 2017). The UTM machine was shown in Figure 3.21 below, located at Bishoftu Defense University college..

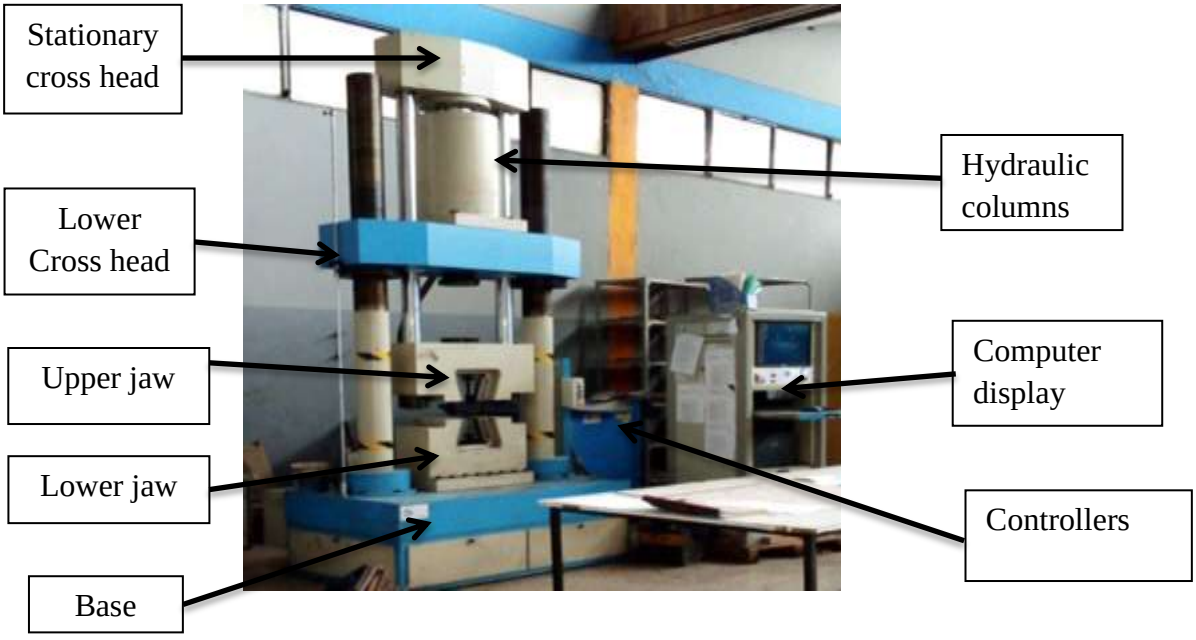

Figure 3.21 Universal testing machine

3.5.5 Laboratory Oven

Laboratory ovens, also referred to as laboratory furnaces, are used to sterilize biohazard waste, dissecting instruments or media/reagents for aseptic assays. The most commonly found laboratory ovens range in temperature from ambient to around 300°C, used in the fields of chemistry, biology, pharmaceuticals, and forensics. Ovens that operate above 300°C are traditionally used for more specialised applications in physics, electronics and materials processing. Fiure 3.22 were the oven used in this thesis work, located at chemical engineering department, ASTU, Ethiopia.

Figure 3.22 Labratory Oven

3.5.6 Hydraulic Press Machine

A hydraulic press is a machine using a hydraulic cylinder to generate a compressive force. Frame, hydraulic cylinder and press table are the main components of the hydraulic press. Hence a hydraulic press is a machine that makes use of the pressure exerted on the fluids to crush, straighten or mold. The concept of the hydraulic press is based on Pascal's theory, which states that when pressure is applied on fluids in an enclosed system, the pressure throughout the system always remains constant. In hydraulic press, the force generation, transmission and amplification are achieved using fluid under pressure. The liquid system exhibits the characteristics of a solid and provides a very positive and rigid medium of power transmission and amplification. In a simple application, a smaller piston transfers fluid under high pressure to a cylinder having a larger piston area, thus amplifying the force. There is easy transmissibility of large amount of energy with practically unlimited force amplification. This machine help to hold the two composites to be joined by applying uniform pressure. Figure 3.23 represents the haydrolic machine used in this thesis work, located at Chemical engineering department, ASTU, Ethiopia.

Figure 3.23 Hydraulic press machine

3.6 Characterization of the Adhesively Joined Composite

Specimen for each test was prepared based on the dimensional requirements of ASTM and ISO standards.

3.6.1 Tensile Strength

Uniaxial tensile tests were performed on the samples using a Universal Testing Machine (UTM). In the tensile test, the samples were pulled until failure occurs to determine the Ultimate Tensile Strength (UTS) and yield strength (σy) of the joint of composites. The amount of load applied to the specimens and their corresponding results were measured throughout the testing process. The output properties of MPM sandwich samples were expressed in terms of stress, which is the ratio of applied force to cross-sectional area and strain, which is the ratio of change in length to original length. Tensile strength is the maximum load that a material can support without fracture when being stretched, divided by the original cross-sectional area of the material. The dimension requirement for tensile strength test on 1000KN UTM of Bshoftu defense university, college of enigneerin based on ISO 6892-1 was 300×30×5mm. Jig saw was used to cut the specimens and then polished by sand paper. During the test the specimens were placed in the grips and axial load was applied through both the ends of the specimen.. Then the samples were left to brake till the ultimate tensile strength occurs. The stress-strain curve was plotted, for the determination of ultimate tensile strength (UTS). It was plotted from the data generated directly from the machine for the tensile test.

$$\textbf{Tensile strength} = \frac{\textbf{Breaking load(KN)}}{\textbf{Original crossectional area } (\mathbf{m^2})} \tag{3.7}$$

3.6.2 Flexural Strength Test

Flexural strength is defined as a materials' ability to resist bending deformation under load. In flexure, the specimen is typically loaded flat on two solid support rods. A third rod is used for loading. This three-point loading setup helps to act the force from the center loading point to two support rods. The flexural Strength of composites was performed according to ASTM-D790 standard using UTM. The loading arrangement was shown in Figure 3.24. The dimension of the specimen was (170 x 25) mm for (4-5) mm specimens and (130 x 25) mm for (3-3.5) mm thickness. The test was conducted in Defense university engineering collage, Bishoftu, Ethiopia.

Figure 3.24 flexural testing machine

Flexural strength of the fabricated composite was calculated using equation 3.8.

$$\sigma_b = \frac{3FL}{2bd^2} \quad (3.8)$$

Where, σ_b is flexural strength, F is applied load, L is span length, b is width of specimen and d is depth of beam.

The maximum bending moment of composite material can be calculated by using equation 3.9.

$$M_{bmax} = \frac{Fmax\ L}{4} \quad (3.9)$$

$$W = \frac{bh^2}{6} \quad (3.10)$$

Where, Fmax is the maximum load applied, h is thickness and b is width of specimen.

3.6.3 Compression Test

Compression test was conducted to determine the materials resistance to a crushing force by applying acompressive pressure to aspeciment as shown in Figure 3.25. The compressive force pushed inward the specimen causing it to shorten in the direction of applied load and expanding in perpendicular direction to the force. ASTM D3410 was followed to prepare the speciement for the compression test. The test was conducted at Defense university engineering college, Bishoftu, Ethiopia.

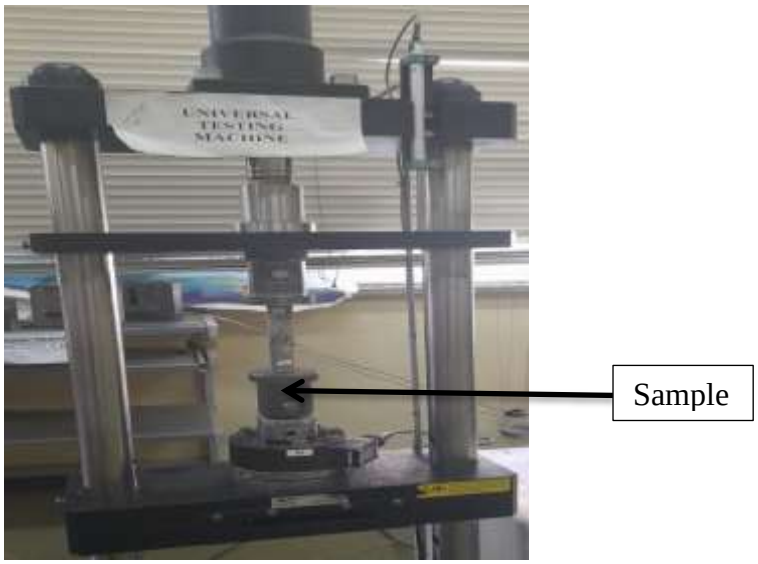

Figure 3.25 Sample under compression test

3.7 Methodology

Experimental investigation and optimization adhesively joined composite material has been proposed in this thesis work. The flow chart for this thesis work was as follow.

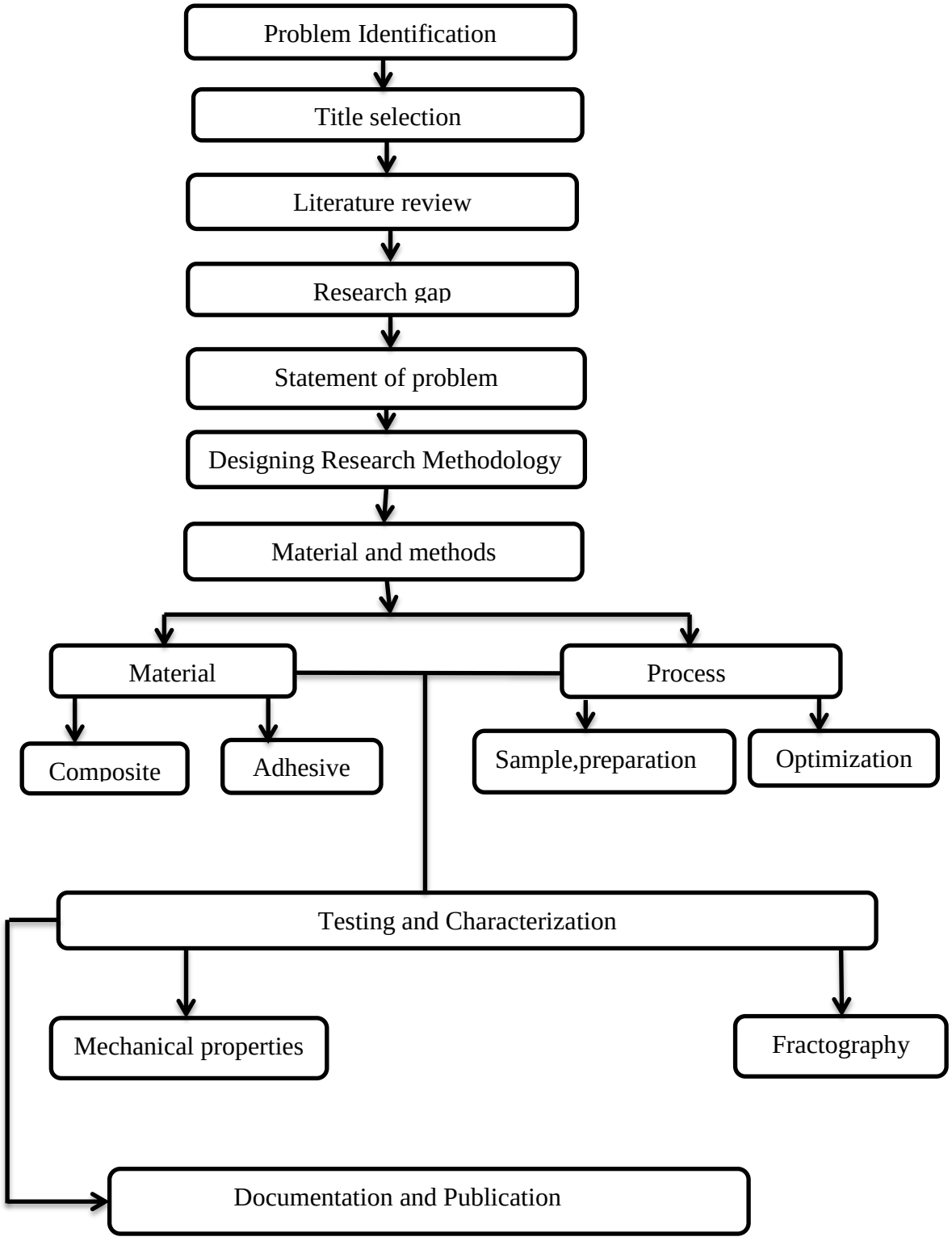

Figure 3.26 flow chart

CHAPTER FOUR

RESULTS AND DISCUSSION

4.1 Introduction

In this chapter, the results of the experimental works were discussed in detail. In different sub sections tensile, flexural, compression and SEM analysis for fractography test results were discussed. Hybrid Taguchi based grey relational analysis method of optimization was discussed for all the results.

4.2 Tensile Test

Adhesively joined composite samples were fabricated by varying the joint overlap length, joint design configuration, and environmental factor (temperature). For tensile strength evaluation nine specimens were tested, one specimen for each sample under UTM. The tensile strength, maximum load and S/N ratios were shown in Table 4.1.

Table 4.1 Tabular description of tensile strength test result

Exp. No	Overlap Length	Environmental Factor (T^0)	Joint Configuration	Tensile strength (MPa)	Maximum load (KN)	S/N ratio
1	25	0	Single Lap	5.12	0.64	14.1854
2	25	20	Stepped	9.44	1.18	14.9638
3	25	60	scarf	9.76	0.70	17.1466
4	30	20	Single Lap	5.60	1.60	19.4994
5	30	60	Stepped	6.00	0.75	15.5630
6	30	0	scarf	9.68	1.21	17.8863
7	40	60	Single Lap	7.20	0.90	19.7890
8	40	0	Stepped	7.84	0.98	19.7175
9	40	20	scarf	12.80	1.22	22.1442

For all single lap joined composites the tensile strength had minimum value, the minimum tensile strength of 5.12 MPa was obtained for S1. At 30 *mm* and 20 ℃ improved strength of 5.60 MPa was obtained for single lap joined composite. At 40 *mm*, 60℃ and scarfly

joinned composites sample showed good tensile strength results than the other single lap joints.

The result of tensile strength for the nine specimens was shown in Figure 4.1. From the graph, it was observed that sample 9 has the maximum tensile strength of 12.8 MPa and 9.76 MPa for scarf joined composite. Sample 1 and sample 4 have lower tensile strength. Sample S4 and S1 had lower elongation; this implies that the material had brittle nature. S2, S8, S6, and S7 have medium elongation this indicates that the materials had less brittle and stiffer. S3 and S5 had more elongation values which means the materials were ductile and stiff.

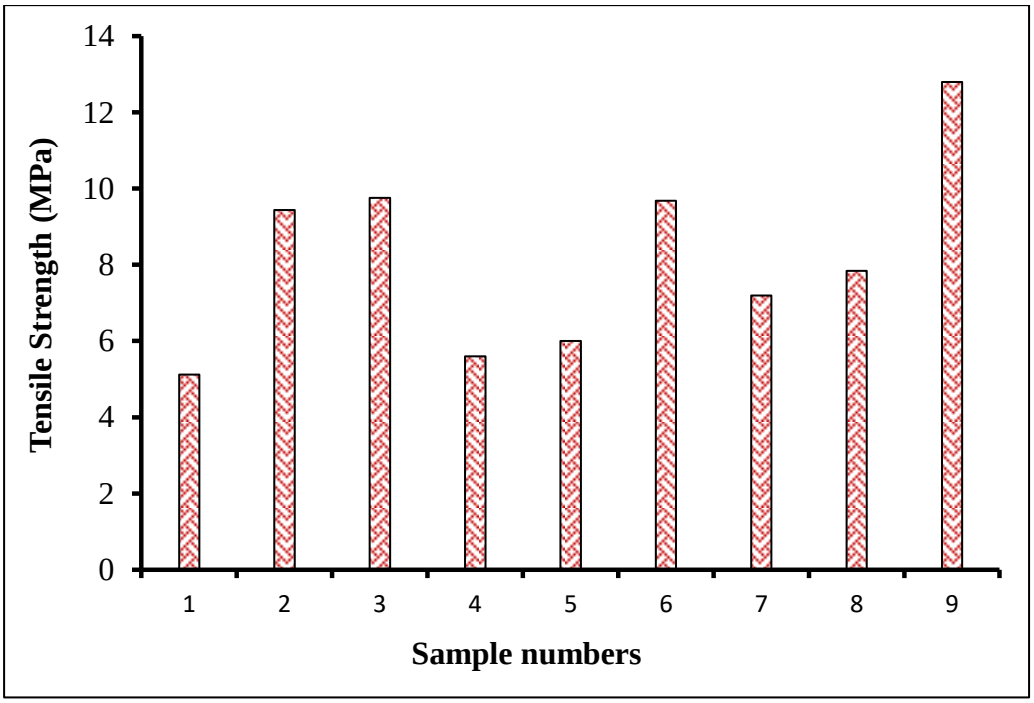

Figure 4.1 Tensile strength of different samples

Figure 4.2 (a) shows that as overlap length increases the average tensile strength decreased from 8.11 MPa to 7.10 MPa. Increasing the overlap length from 30mm to 40mm increased the tensile strength from 7.10 MPa to 9.28 MPa. The increase in tensile strength from 30mm to 40 mm was due to a long overlap length that was sufficient to share the applied load. For this reason, the tensile strength increased with the increase overlap length up to 40mm. The reduction in tensile strength from 25mm to 30mm was because of the epoxy resin was insufficient to share the applied load, thus the adhesion was less. From the results superior tensile strength value of 9.28 MPa at 40mm overlap length. This result was sound (Bakri et al., 2017; Parre et al., 2020; Prasad et al., 2021).

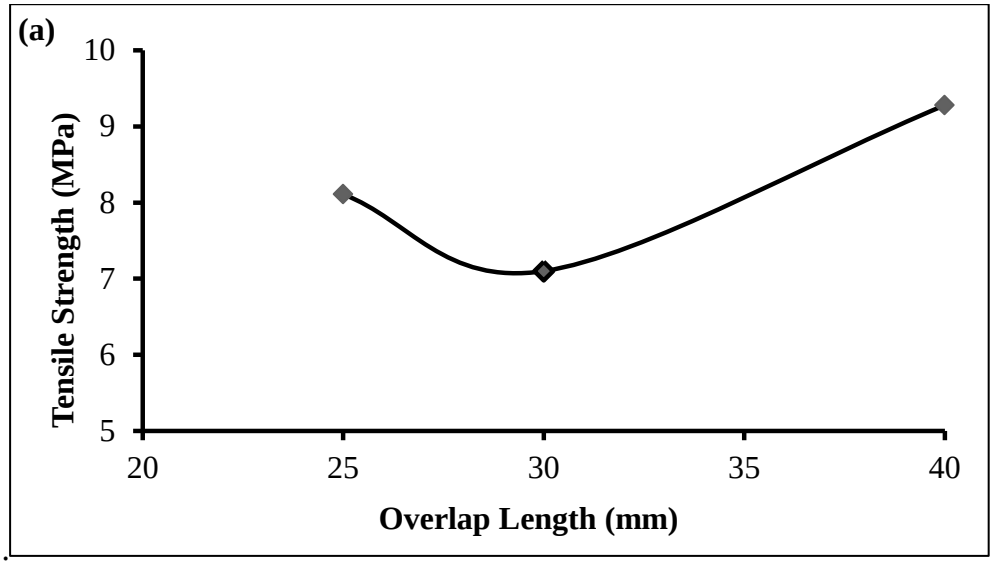

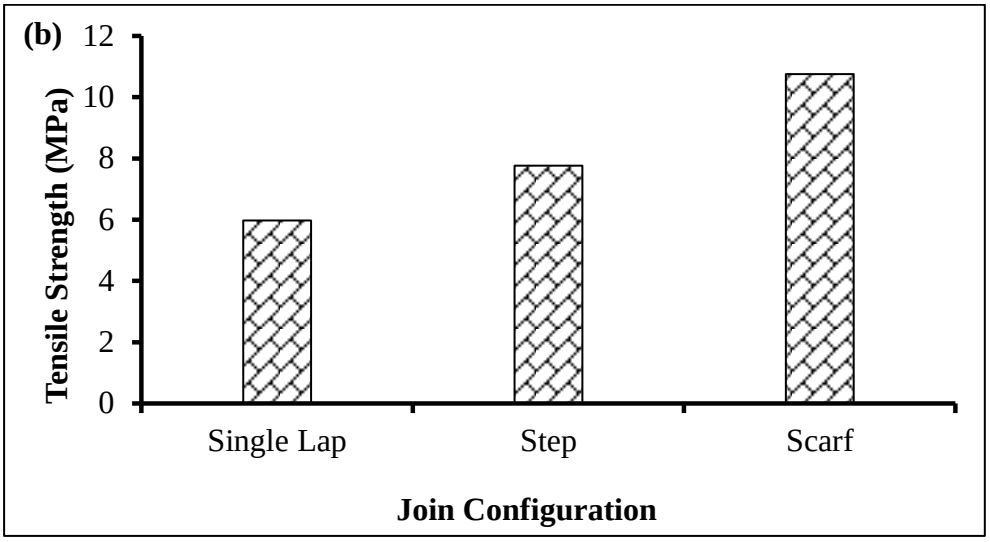

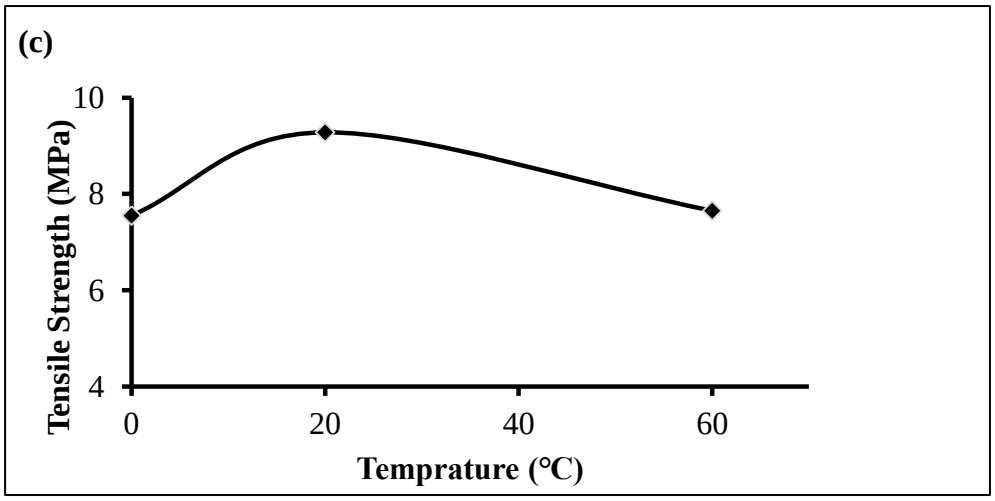

Figure 4.2 Tensile strength Vs (a) Overlap length (b) Joint configuration (c) temprature

The change in joint configuration from single lap joint to stepped joint increased the tensile strength of the composite from 5.97 MPa to 7.76 MPa as shown in Figure 4.2 (b). Tensile strength also increase highly from 7.76 MPa to 10.75MPa as the joint configuration was changed from stepped to scarf joint. This increasing in tensile strength was due to the design modification, the steped joint has more sharp corners than scarf jont, which lead to high stress concentration. The result is in well agreement with (Manjunath et al., 2016; Olayil et al., 2021; Ozsoy et al., 2015).

Regarding temperature effect the tensile strength increase from 5.97 MPa to 9.28 MPa with an increase in temperature from 0℃ to 20℃. At 20℃ it reaches its maximum and further addition temperature reduced the strength in to 7.65MPa. The maximum tensile strength obtained was 9.28 MPa at 20℃ as shown in Figure 4.2 (c). The result was in well agreement with (Karthick et al., 2018).

4.2.1 Analysis of Main Effect Plot for S/N Ratio of Tensile Strength

Figure 4.3 shows the main effect plot for S/N ratios of tensile strength. The graph implies that the best condition (level) for tensile strength was 40 mm overlap length, scarf joint configuration, and 20℃. Using these combination better results can be obtained for tensile strength.

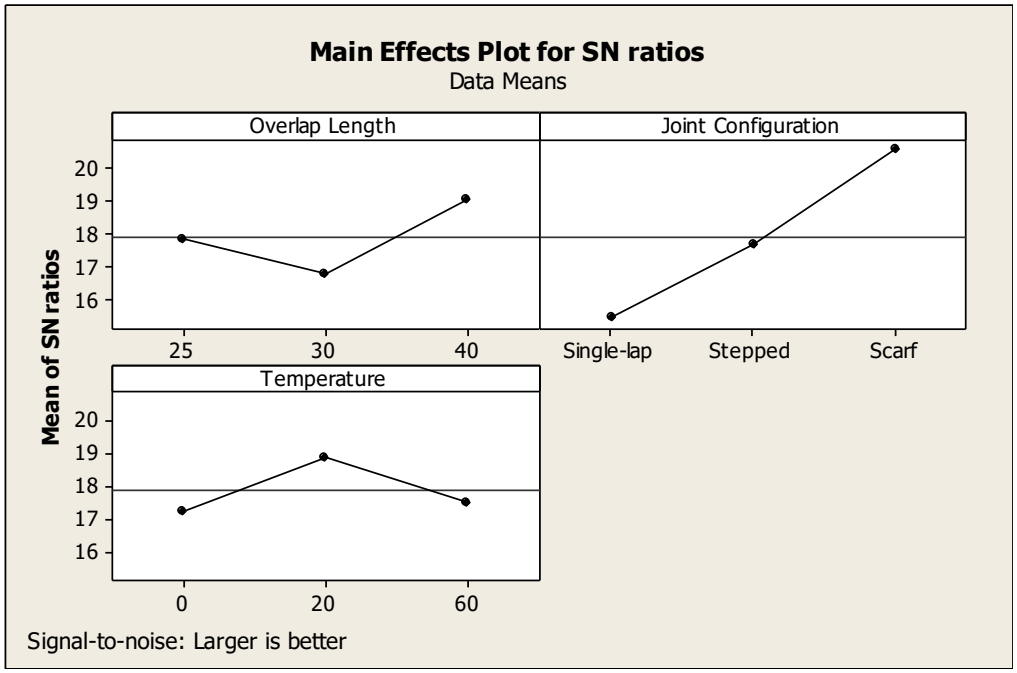

Figure 4.3 Main effect plot of tensile strength

4.2.2 Response table for S/N ratios of tensile strength

Response of tensile strength was displayed in Table 4.2 indicates joint design configuration had the highest effect for the increase in the tensile strength of the composite with delta number of 5.12. Whereas overlap joint legth was the second most contributing factor in increasing the tensile strength with delta value of 2.31. Temprature effect ranked third contributing factor with delta value of 1.61. The optimum combination was A2B1C3.

Table 4.2 Response for S/N ratios of tensile strength

Level	Overlap Length	Joint Configuration	Temperature
1	17.82	15.43	17.26
2	16.75	17.65	18.87
3	19.06	20.55	17.50
Delta	2.31	5.12	1.61
Rank	2	1	3

4.2.3 Analysis of variance of tensile strength

The ANOVA table for tensile strength was shown in Table 4.3 below. It shows that joint configuration had the highest effect for the increase in tensile strength with percentage contribution of 61.0%. The second influencing parameter was overlap length of the joint with percentage contribution of 29.0%. The third contributed factors were temperature effect with percentage contribution of 5.9%. P-value shows that factor A and C are highly significant and factor B is less significant.

Table 4.3 Analysis of variance of tensile strength

Source	DF	Seq SS	Adj SS	Adj MS	F	P	PC
Overlap length	2	20.629	20.629	10.314	2.609	0.000	29.0%
Joint configuration	2	1.216	1.216	0.608	0.153	0.991	61.0%
Temprature	2	5.651	5.651	2.825	0.714	0.000	8.6%
Residual Error	2	3.952					1.4%
Total	8	70.910					100%

4.3 Flexural Test

The results obtained during flexural test of nine specimens with different overlap length, joint configuration, and environmental factor (temprature) were shown in Table 4.4.

Table 4.4 Tabular description of flexural strength test result

Expt. No	Overlap Length (mm)	Environmental Factor (Temprature in ℃)	Joint Configuration	Flexural strength (MPa)	Maximum load (KN)	S/N ratio
1	25	0	Single Lap	36.00	0.10	31.126
2	25	20	Step	18.00	0.05	34.048
3	25	60	scarf	32.40	0.09	34.647
4	30	20	Single Lap	50.40	0.14	25.105
5	30	60	Step	25.20	0.07	27.958
6	30	0	scarf	40.00	0.10	31.865
7	40	60	Single Lap	54.00	0.15	30.103
8	40	0	Step	39.20	0.11	32.041
9	40	20	scarf	43.20	0.12	32.669

The flexural strength and applied maximum load of adhesively joined composite samples shown above were taken directly from the universal testing machine control unit during speciment testing. The data for flexural strength in Table 4.4 above is expressed in graph as shown in Figure 4.4 below.

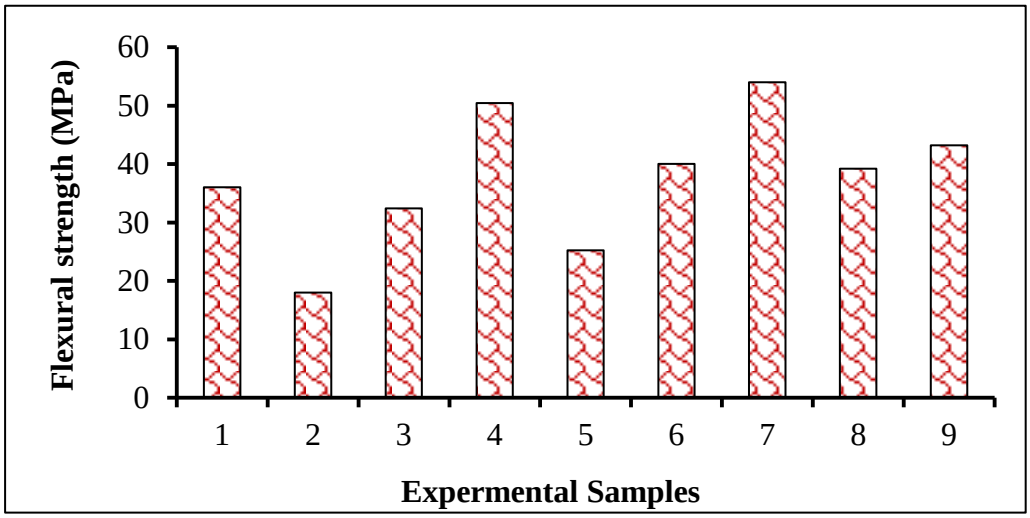

Figure 4.4 Flexural strength Vs experiment number

From Figure 4.4 it was observed that the maximum flexural strength was 54 MPa obtained at S7 with 40 mm overlap length, single lap joint configuration and 0℃. The next two best flexural strength was 50.4 MPa and 43.2 MPa obtained at S4 with 30 mm overlap length, single lap joint configuration, and 0℃ and S9 with 40mm overlap length, scarf joint configuration, and 60℃ respectively. S2 showed the minimum flexural strength 18 MPa, this was due to short overlap length resulted in decreasing in surface contact between the two adherends and adhesive, and the type of joined configuration because stepped joint conifiguration had many sharp corners that leads to high stess concentarion. Even though S1, S4, and S7 had same joint configuration S7 has best flexural strength this was because of increasing overlap length, and at the same time S3, S5, and S7 exposed to the same temperature but S7 had high flexural strength, this is because of the joint configuration and over lap length difference.

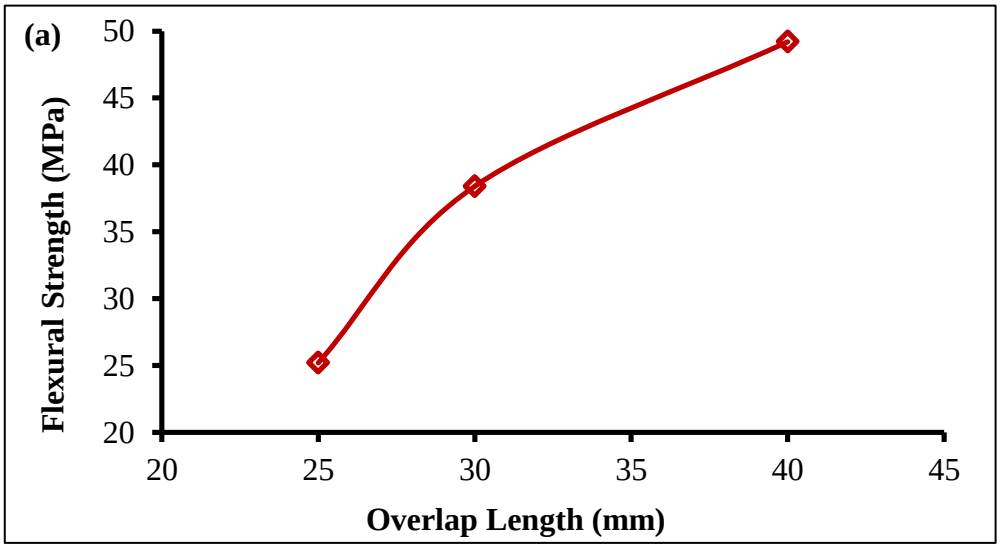

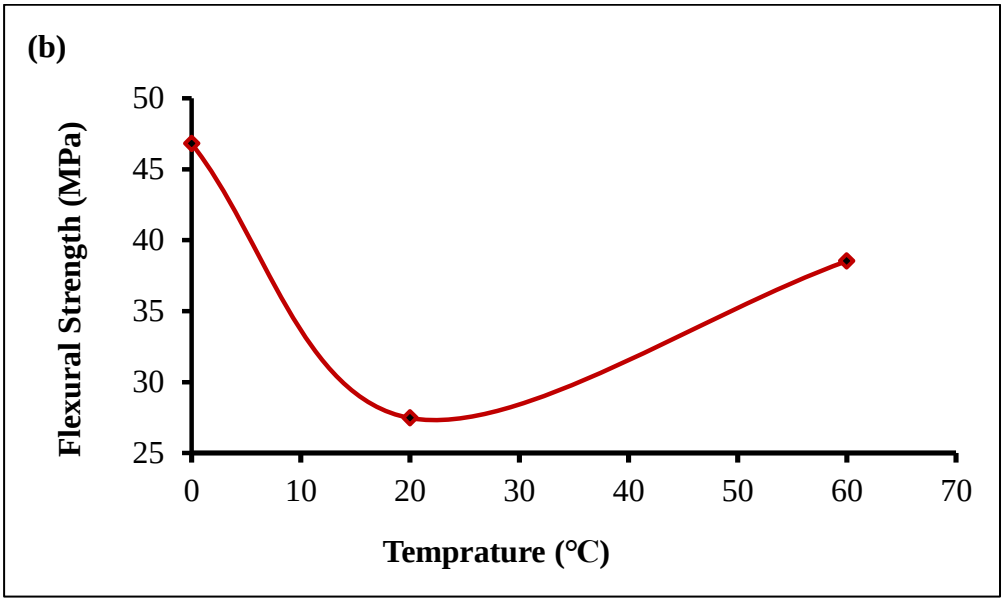

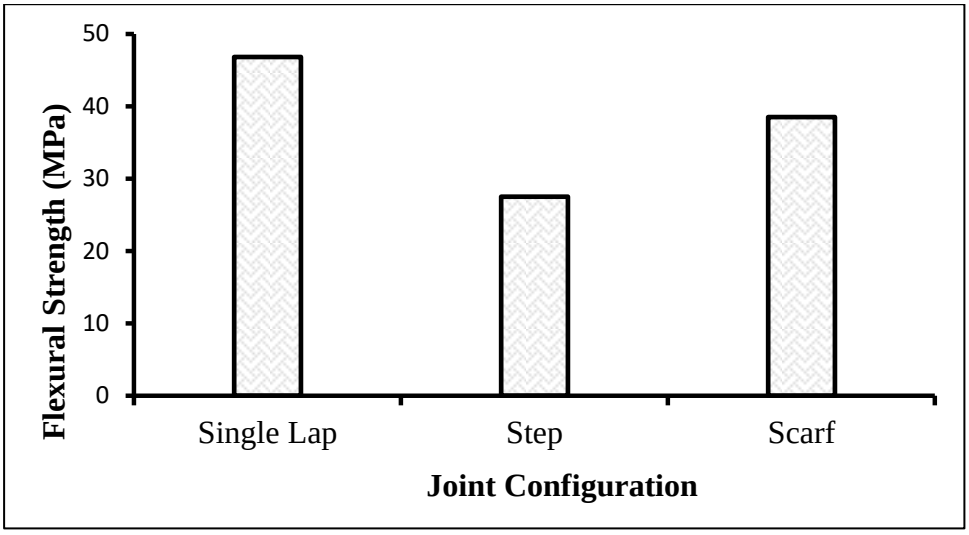

Figure 4.5 Flexural strength Vs (a) Overlap Length (b) Temprature (c) Joint Configuration

The effect of overlap length on flexural strength was shown in Figure 4.5 (a). The result shows that flexural strength increased with an increase in overlap length. This increase of flexural strength with overlap length was due to the increase in the contact area between the two adherends which enables the applied load to be carried by more area of the overlap. Further increase of overlap length enhances the flexural strength but indirectly it affects the production cost because of the more consumption of adhesive, which leads to an increase in production cost. The maximum flexural strength obtained at 25, 30, and 40mm was 36 MPa, 50.4 MPa, and 54 MPa respectively. This result was well agreed with (Senguttuvan & Lillymercy, 2015).

The effect of an environmental factor (temperature) on the flexural strength of the composite was also depicted in Figure 4.5 (b). Results yield that the addition of temperature from 0℃ to 20℃ reduces the flexural strength of the composite. This result was obtained due to the other two factors and the suddenly drop of temprature. Further addition temperature enhanced the flexural strength. This was due to the increasing of ductility with temperature and it might be because of closure of microcracks in the surface. The maximum flexural strength obtained at 20 ℃ was 43.7 MPa. The result was sound with (Ashok et al., 2020; Ozsoy et al., 2015).

Regarding the effect of joint configuration on flexural strength the result was shown in Figure 4.5 (c). The average highest flexural strength was 46.8 MPa and 38.5 MPa at both single lap and scarf joint configuration respectively, but it was decreased with stepped configuration joint which was 27.5 MPa. The single lap joint had better flexural joint

strength than the scarf joint, this was due to the overlapping of the two adhrends over each other which leads to the destruction of bending load over the two adherend rather than the single adherend. The scarf joint was better than step one because the stepped joint has more sharp corners with high-stress concentration leading to initiate propagation and also since the scarf joint was tapered to some angle enabling the joint to carry the more applied load. It was found that the maximum flexural strength was 54 MPa at a single lap joint. Such type of research finding was reported by (Venkateshwaran et al., 2011b).

4.3.1 Analysis of Main Effect Plot of Flexural Strength

The main effect plot for S/N ratios of flexural strength was shown in Figure 4.6. The graph implies that the optimum condition for the flexural strength was 40 mm overlap length, single lap joint configuration, and 0℃ temprature. Using these combination a better adhesively joined composite with best flexural strength could be obtained. This Figure also illustrate flexural strength increase with increasing overlap length, stepped joint configuration was the weakest joining method, and the flexural strength was decrease to some extent but increase with temperature after 20 ℃.

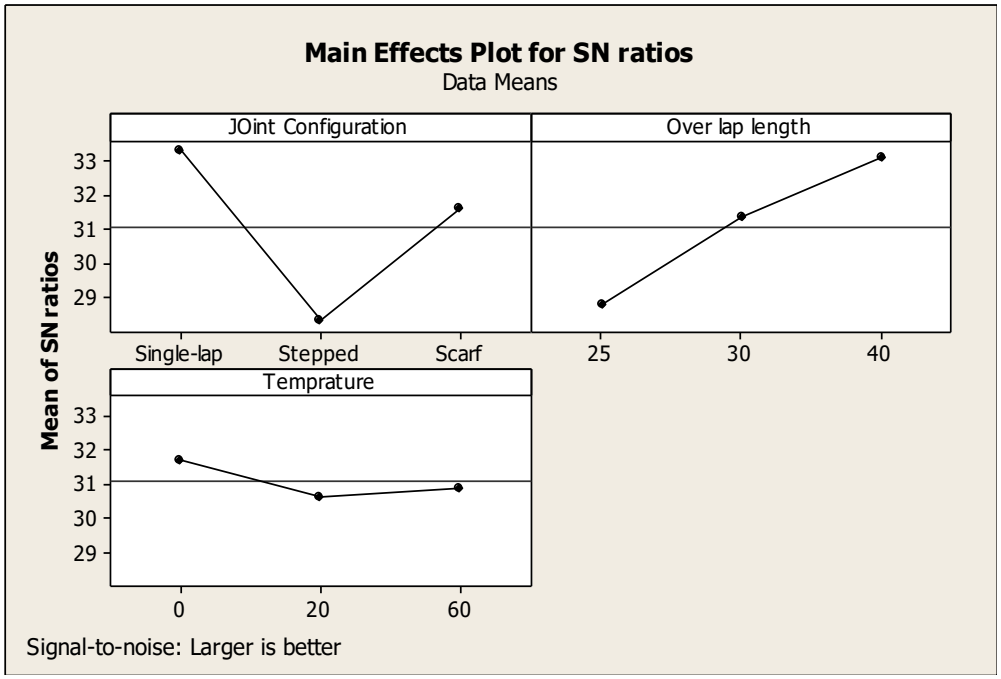

Figure 4.6 Main effect plot of flexural strength

4.3.2 Response Table for S/N Ratios of Flexural Strength

The response Table 4.5 shows that joint configuration had the highest contribution in increasing the flexural strength with delta number of 4.96. While overlap length was the

second contributed factor with delta number of 4.28. The third ranked factor was temperature with delta number of 1.07. It can be concluded that both joint configuration and overlap length highly affect the flexural strength of the adhesively joined composite.

Table 4.5 Response table for S/N ratio

Level	Joint Configuration	Overlap Length	Temrature
1	**33.27**	28.78	**31.68**
2	28.31	31.35	30.61
3	31.60	**33.06**	30.90
Delta	4.96	4.28	1.07
Rank	**1**	**2**	**3**

4.3.3 Analysis of Variance for Flexural Strength

From the ANOVA Table 4.6 it can be discussed that joint configuration contributed 47.28%. The second contributed factor was overlap length with percentage contribution of 31.48%. The third contributed factors were temprature with percentage contribution of 20.22%. Since $F_{0.05,2,2,2}$ at α 0.05 which is 25.56 was less than F of factors, the null hypothesis were rejected, this means the factors were significant. At the same time, since p-value was greater than α the null hypothesis was accepted.

Table 4.6 Analysis of variance for flexural strength

Source	DoF	Seq SS	Adj SS	Adj MS	F	P	PC
Temperature	2	502.90	502.90	251.448	31.185	0.036	20.22%
Overlap length	2	660.70	660.70	330.352	40.966	0.066	31.48%
Joint configuration	2	1225.85	1225.85	612.923	76.011	0.085	47.28%
Residual Error	2	8.064					1.02%
Total	8	2592.45					100%

4.4 Compression Strength

The results obtained during compression test of nine specimens with different overlap length, joint configuration, and environmental factor (temprature) were shown in Table 4.7.

Table 4.7 Tabular description of compression strength test results

Expt. No	Overlap Length (mm)	Environmental Factor (Temprature in ℃)	Joint Configuration	Compression strength (MPa)	S/N ratio
1	25	0	Single Lap	13.68	22.721
2	25	20	Stepped	15.12	23.591
3	25	60	scarf	14.56	23.263
4	30	20	Single Lap	22.64	27.097
5	30	60	Stepped	17.28	24.750
6	30	0	scarf	7.36	17.337
7	40	60	Single Lap	15.92	24.038
8	40	0	Stepped	17.92	25.066
9	40	20	scarf	6.24	15.903

The compression strength and maximum elongation of adhesively joined composite samples shown above were taken directly from the universal testing machine control unit during sample testing. The data for compression strength in Table 4.7 above is expressed in a graph as shown in Figure 4.8 below.

From Figure 4.7 it was observed that the maximum compression strength was 22.6 MPa obtained at S4 with 30mm overlap length, single lap joint configuration, and 20℃ temperature. The next two best compression strength was 18.02 MPa and 17.28 MPa obtained at S8 with 40 mm overlap length, stepped joint configuration, and 0℃; and S5 with 30 mm overlap length, scarf joint configuration, and 60℃ respectively. Sample 9 showed the minimum compression strength of 6.24 MPa, this was due to the V shape of a joint configuration having large pressure and at the same time, large overlap length leading to buckling. Even though S1, S4, and S7 had the same single lap joint configuration S4 has the best compression strength, this was due to the optimum overlap length and temperature difference, and at the same time S2, S4, and S9 were exposed to the same temperature but

S4 had high compression strength, this is because of the joint configuration and overlap length difference.

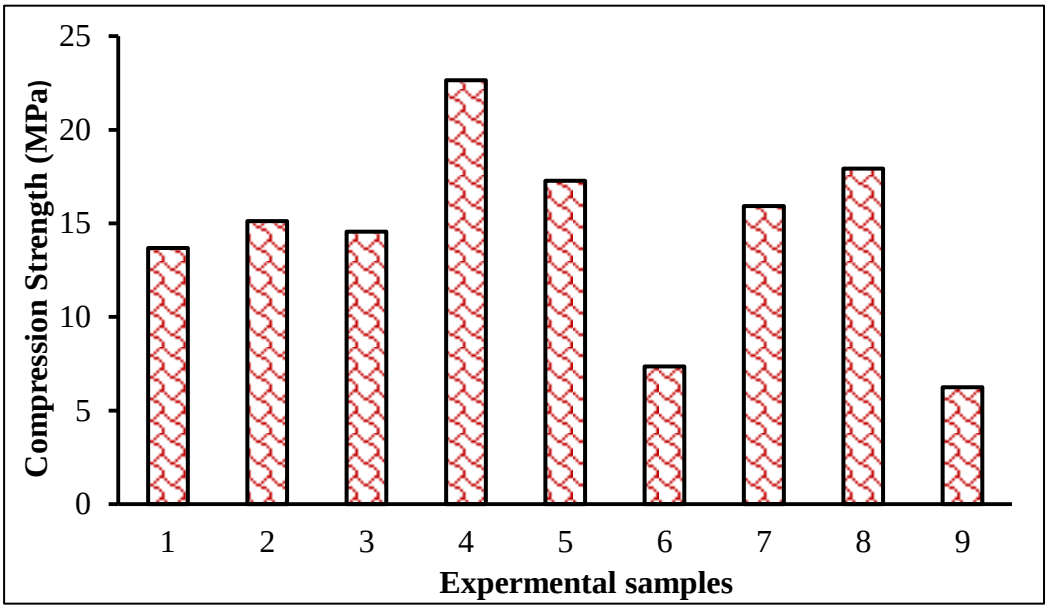

Figure 4.7 Compression strength Vs experiment number

Regarding the effect of joint configuration on compression strength the result was shown in Figure 4.8 (a). The average highest compression strength was 17.41 MPa and 16.77 MPa at both single lap and stepped joint configuration respectively, but it was decreased with scarf configuration joint which was 9.387 MPa. Single lap joint had better compression joint strength than the stepped joint, this was due to the stepped joint has more sharp corners that leads to high stress concentration. The stepped joint was better than the scarf one, because of the high pressure developed as aresult of the V shape of scarf. This lead to initiate propagation after time it become failure. It was found that the maximum compression strength was 22.64 MPa at single lap joint. Such type of research finding was reported by (Venkateshwaran et al., 2011b).

The effect of overlap length on compression strength was shown in Figure 4.8 (b). The results shows that compression strength increased with increase in overlap length up to 30 mm. This increasing of compression strength with overlap length was due to the increasing contact area between the the two adherends which enable the applied load to be carried by more area of the overlap. Further increase of overlap length decrease the compression strength. This decreasing was due to increasing overall length of the sample which leads to develop buckling. The maximum compression strength obtained at 25, 30, and 40mm was

14.45 MPa, 15.76 MPa and 13.36 MPa respectively. This result was well agreed with (Senguttuvan & Lillymercy, 2015).

The effect of environmental factor (temperature) on the compression strength of the joint was also depicted in Figure 4.8 (c). Results yield that the increasing of temperature from 0℃ to 60 ℃ increase the compression strength of the composite. This result was obtained due to the increasing of ductility of the adhesive. The maximum compression strength obtained at 60 ℃ was 15.92 MPa. The result was in sound with (Ashok et al., 2020; Ozsoy et al., 2015).

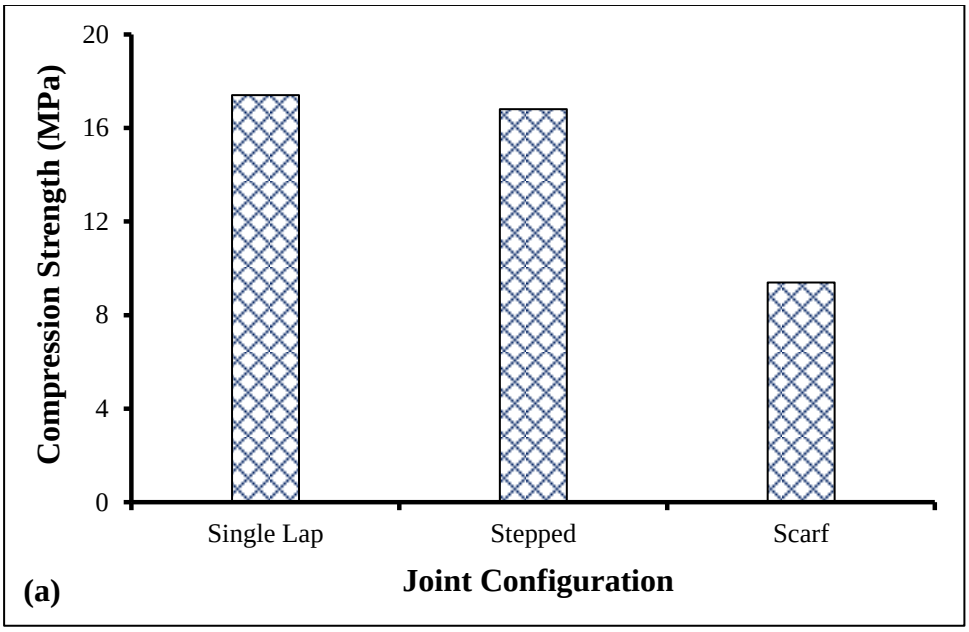

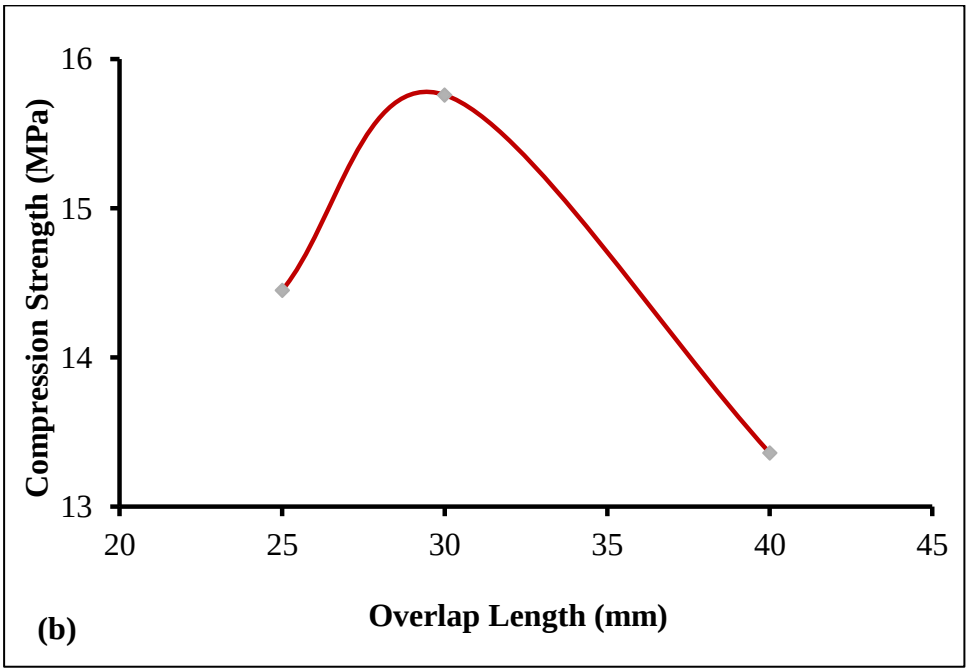

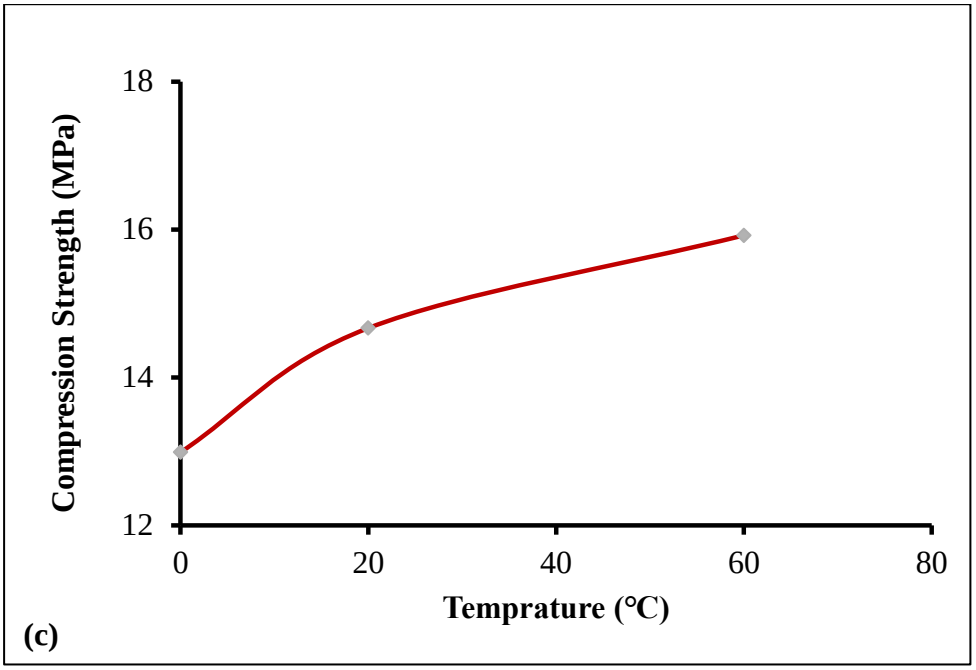

Figure 4.8 Compression strength Vs (a) Joint Configuration (b) Overlap Length (c) Temprature

4.4.1 Analysis of Main Effect Plot of Compression Strength

The main effect plot for S/N ratios of compression strength was shown in Figure 4.9. The graph implies that the optimum condition for the compression strength was 30mm overlap length, single lap joint configuration, and 20℃ temprature. Using these combination a better adhesively joined composite with best compression strength could be obtained. This Figure also illustrate compression strength increase with increasing overlap length to some extent but further increasing negatively affect the compression strength of adhesively joined composite, scarf joint configuration was the weakest joining configuration for compression because failure developed easly at the V- shape of the joint.

4.4.2 Response Table for S/N Ratios of Compression Strength

The response Table 4.8 shows that joint overlap length had the highest contribution in increasing the compression strength with delta number of 5.78 . While temprature was the second contributed factor with delta number of 2.31. The third ranked factor was joint configuration with delta number of 1.52. It can be concluded that compression strength was highly infuleced by overlap length and the joint configuration had little effect on it.

Table 4.8 Response Table for S/N Ratios of Compression Strength

Level	Overlap Length	Configuration	Temperature
1	24.62	23.19	21.71
2	24.47	23.06	22.20
3	18.83	21.67	24.02
Delta	5.78	1.52	2.31
Rank	1	3	2

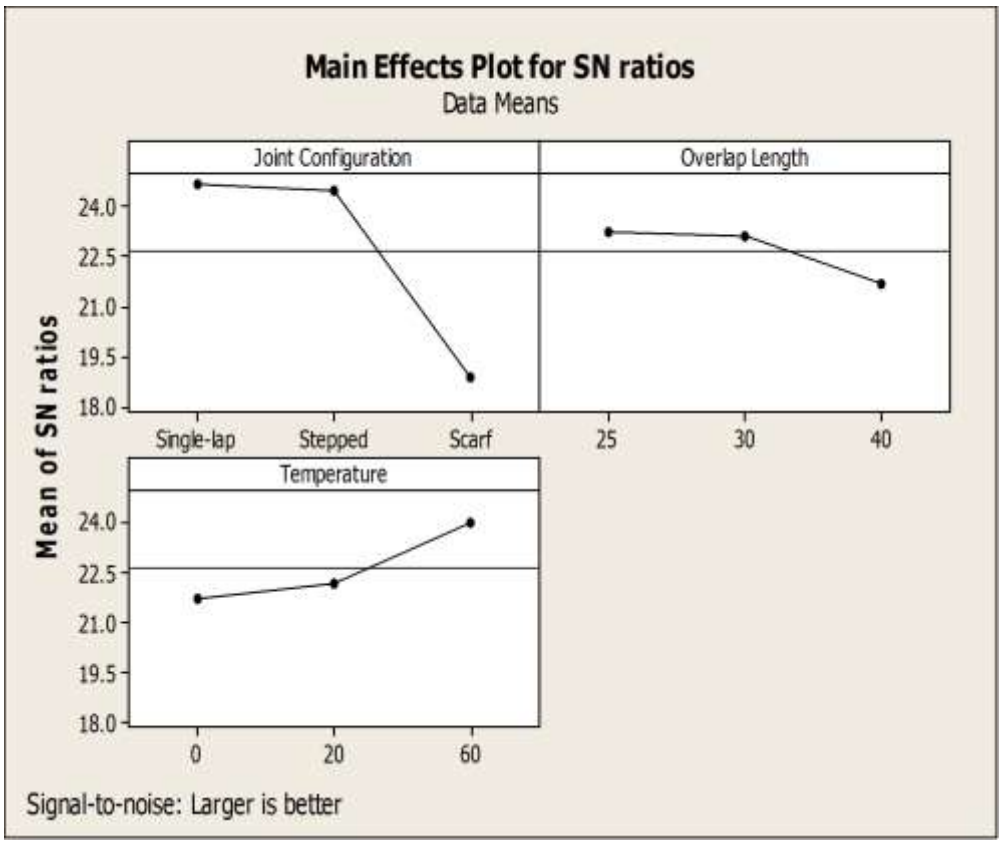

Figure 4.9 Main effect plot of compression strength

4.4.3 Analysis of Variance for Compression Strength

From the ANOVA Table 4.9 it can be discussed that overlap length contributed 47.28%. The second contributed factor was temperature with percentage contribution of 31.48%. The third contributed factors were joint configuration with percentage contribution of 20.22%. Since $F_{0.05,2,2,2}$ at α 0.05 which is 25.56 was less than F of factors, the null

hypothesis were rejected, this means the factors were significant. At the same time, since p-value was greater than α the null hypothesis was accepted.

Table 4.9 Analysis of variance for compression strength

Source	DoF	Seq SS	Adj SS	Adj MS	F	P	PC
Temperature	2	502.90	502.90	251.448	31.185	0.036	20.22%
Overlap length	2	660.70	660.70	330.352	40.966	0.066	31.48%
Joint configuration	2	1225.85	1225.85	612.923	76.011	0.085	47.28%
Residual Error	2	8.064					1.02%
Total	8	2592.45					100%

4.5 Grey relational analysis of Mechanical properties

The experimental results of tensile, flexural and compression shown in Table 4.10 were transformed into Signal to-Noise (S/N) ratio using Taguchi analysis. The normalizing sequence for parameters was calculated from the S/N ratio. Using the normalizing sequence value deviation sequence was calculated. The Gray relational coefficients were calculated using the deviation sequence values. Finally the GRG is calculated from the GRC and the recommended optimum parameter was selected.

Table 4.10 Response table

Expt. no	Tensile (MPa)	Flexural (MPa)	Compression(MPa)
1	5.12	36.00	13.68
2	9.44	18.00	15.12
3	9.76	32.40	14.56
4	5.60	50.40	22.64
5	6.00	25.20	17.28
6	9.68	40.00	7.36
7	7.20	54.00	15.92
8	7.84	39.20	17.92
9	12.80	43.20	6.24

The S/N ratios obtained from Taguchi were shown in Table 4.11 for all experiments except SEM. As discussed in chapter three the next step was normalization of S/N ratios using equation (2.1) for larger the better and equation (2.2) for smaller the better.

Table 4.11 S/N ratios table

Runs	Tensile (MPa)	Flexural (MPa)	Compression (MPa)
1	14.1854	31.126	22.721
2	14.9638	34.048	23.591
3	17.1466	34.647	23.263
4	19.4994	25.105	27.097
5	15.5630	27.958	24.750
6	17.8863	31.865	17.337
7	19.7890	30.103	24.038
8	19.7175	32.041	25.066
9	22.1442	32.669	15.903

The normalization sequence was used to eliminate data repetition and duplicates data from the relation table. The values were normalized between 0 and 1.

Table 4.12 Tabular description for normalizing sequence

Runs	Tensile (MPa)	Flexural (MPa)	Compression (MPa)
1	0.000	0.631	0.609
2	0.098	0.937	0.687
3	0.372	1.000	0.657
4	0.668	0.000	1.000
5	0.424	0.299	0.790
6	0.465	0.708	0.128
7	0.704	0.524	0.727
8	0.695	0.727	0.364
9	1.000	0.793	0.000

The tabulated normalized values were shown in Table 4.12. By using the normalized data the deviation sequence can be calculated as $1 - X_{ij}$. 1 was used because it is the highest value of quality and Xij is the actual value of each experiment.

Table 4.13 Tabular description of deviation sequence

Run	Tensile (MPa)	Flexural (MPa)	Compression(MPa)
1	1.000	0.369	0.391
2	0.020	0.063	0.313
3	0.628	0.000	0.430
4	0.332	1.000	0.000
5	0.576	0.701	0.210
6	0.535	0.292	0.872
7	0.296	0.476	0.283
8	0.395	0.283	0.636
9	0.000	0.207	1.000

The calculated deviation sequence (quality loss) shown in Table 4.13 was used to find the grey relational coefficients. Then the grey relational coefficient was calculated by using equation (2.6). Finally the grey relational grades were calculated by using equation (2.7).

Table 4.14 Grey relational coefficients and Grey relational grade

Runs	Grey relational coefficients			GRG	Rank
	Tensile (MPa)	Flexural (Mpa)	Compression (MPa)		
1	0.333	0.575	0.561	0.489	9
2	0.962	0.888	0.615	0.546	6
3	0.443	1.000	0.538	0.660	3
4	0.601	0.333	1.000	0.822	1
5	0.465	0.416	0.704	0.528	7
6	0.483	0.631	0.364	0.493	8
7	0.628	0.512	0.639	0.593	5
8	0.559	0.638	0.440	0.645	4
9	1.000	0.707	0.333	0.680	2

Ranked of samples were shown in Table 4.14 and according to the GRG experiment number 4 (S4) ranked number 1 at levels of A1B2C3.

4.5.1 Analysis of main effect plot for S/N ratios of GRG

The main effect plot for the S/N ratios depicted in Figure 4.10 shows that the optimum condition for the experiment carried out was single lap joint, 30 mm overlap length,20℃. Best result was achieved by using parameter levels at A1B2C3.

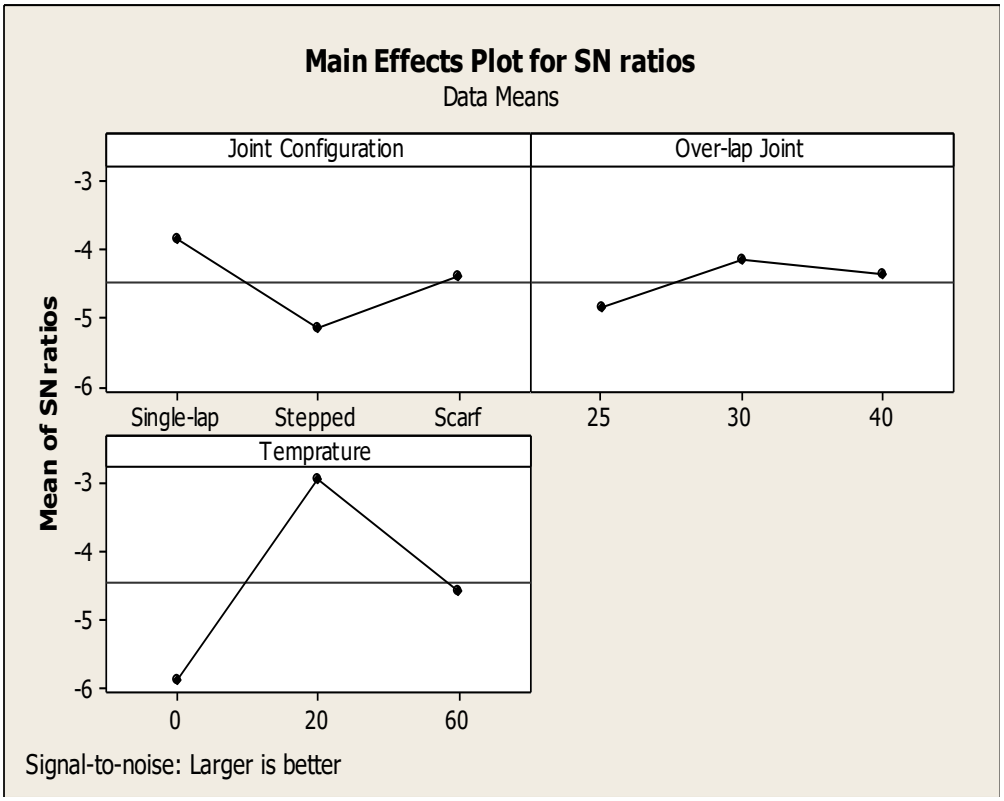

Figure 4.10 Main effect plots for S/N ratios of GRG

4.5.2 Response table for S/N ratios of Grey relational grades

The GRG response Table 4.15 shows that joint configuration had the highest contribution in increasing the tensile, flexural, Compression strength of the composite material with delta number of 0.0563. The second contributed factor was overlap length of the joint with delta number of 0.2063. The third contributed factor was temperature effect with delta number of 0.1017. The obtained result was in well agreement with the literature review mentioned. From Table 4.26 A1B2C3 are the optimum levels, the first ranked experiment has also levels of A1B2C3. The optimal parameter set from the rank and grey relational analysis optimum combinations were similar. Therefore conformation experiment was not required since the experiment was already done.

Table 4.15 Response table for S/N ratios of GRG

Level	Joint Configuration	Overlap Length	Temprature
1	0.5093	0.6570	0.5757
2	0.7157	0.5553	0.6320
3	0.5937	0.6063	0.6110
Delta	0.0563	0.2063	0.1017
Rank	1	2	3

4.5.3 Analysis of variance for Grey relational grades

Analysis of variance for grey relational coefficient shows that joint configuration had the highest contribution of 51.4% for optimized experimental result as shown in Figure 4.16. The second contributed factor was overlap length with percentage contribution of 35.6%. The third contributed factor was temprature with percentage contribution of 12.51%. Depending up on the P-value Factor A and B were more significant factors and factor C was less significant factors.

Table 4.16 Analysis of variance for GRG

Source	DF	Seq SS	Adj MS	F	P	PC
Joint configuration	2	19.520	9.960	55.366	0.092	51.4%
Overlap length	2	3.821	1.760	9.787	0.088	35.6%
Temprature	2	3.615	6.847	10.270	0.017	12.51%
Residual Error	2	0.179				0.49%
Total	8	52.024				100%

4.6 Confirmation Experiment

After obtaining the optimal process parametres and levels the next step was to verify that the predicted result was against experimental results. If the combinztion of optimal process paramertes level coincides with that of any experimental trial in the orthogonal array their will not need of confirmation test. In this studies the optimal process parameter combination for tensile, compression and flexural of the composite concided with sample 4.

4.7 Analysis of Failure Mechanism

The failure developed during tensile, compression, and flexural tests were shown in Table 4.17. The three type of failure developed during this study was adhesive, adherend, and cohesive. From the result obtained in Table 4.9 the mostly occure failure were adherend and cohesive, these failure were not due to the joint problem it was due to the low strength of adherend and adhesive used. There was adhesive failure occure in sample 1 and sample 4 in addition to adherend and cohesive failure, this was as aresult of poor surface treatment applied to these samples.

Table 4.17 Tabular description of failure mechanism

Expt. No	**Failure Mechanism**		
	Tensile Strength	**Compression Strength**	**Flexural Strength**
1	Adhesive and adherend	Adherend	Adhesive, cohesive and adherend
2	Cohesive and adherend	Cohesive and adherend	Cohesive and adherend
3	Adherend	Adherend	Cohesive and adherend
4	Adherend	Cohesive and adhesive	Cohesive, adhesive and adherend
5	Adherend	Cohesive and adhersive	Cohesive and adherend
6	Adherend	Cohesive and adherend	Cohesive and adherend
7	Adhesive and adherend	Adherend	Adherend
8	Cohesive and adherend	Cohesive and adherend	Cohesive and adherend
9	Adherend	Cohesive and adherend	Cohesive and adherend

4.8 Fractography Analysis

The qualitative information on the distribution of particles, fiber matrix adhesion and fractography of adhesively joined composite specimen were shown in Figure 4.11. Different samples were used to conduct this experiment. The result showed that the composite with the absence of voids, well yapped no cohesion and good bonding between adherend and adhesive interface was observed. The particle dispersion was good and aggregates of nano alumina were observed. Voids and micro crack propagation was shown in the area between the adhesive and adherends. The fractography of adhesively joined

composite was affected by fabrication technique, since the scanning electron microscope result indicated that the composite with air bubbles, voids, internal crack and rough surfaces. Due to the reason that it was fabricated by hand layup technique, it was more exposed to formation of air bubbles on the surface, void space which are uncontrollable

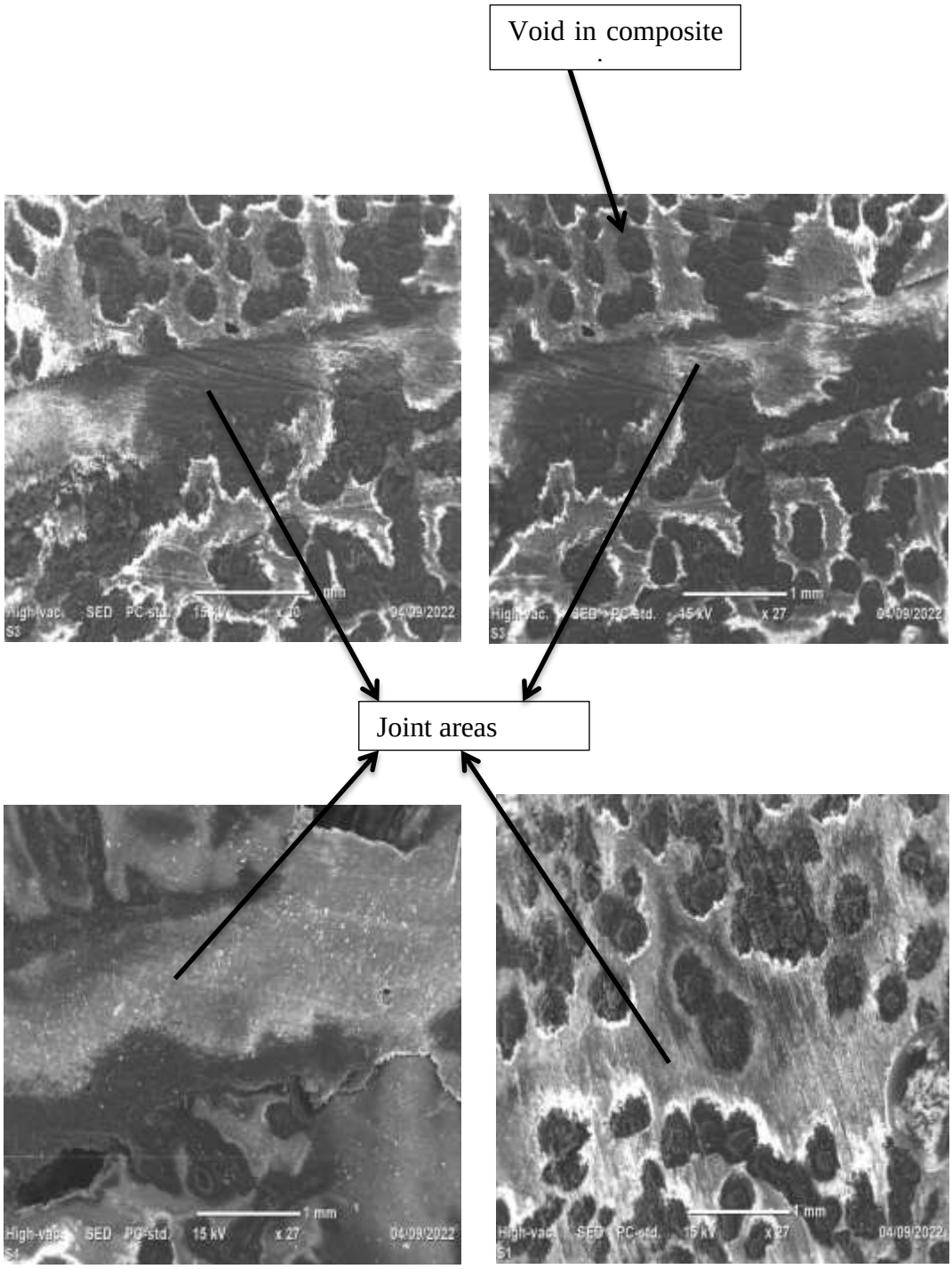

Figure 4.11 Fractography of the joint

CHAPTER- FIVE

CONCLUSION AND RECOMMENDATIONS

5.1. Conclusion

The mechanical properties of different joint configuration of adhesively joined composite were investigated through experimental evaluations. The adherend involved in this study was banana fiber rainforced polyester matrix composites which were joined by epoxy adhesive. The method used to prepare samples was handlay up, and slightly compression force was applied during curing time for better joint strength. Furthermore the effect of overlap length, joint configuration, and environmental (temperature effect) with three levels were investigated and optimized using Taguchi optimization softwre in this thesis study. The conculsion from this investigation are as follows.

- The effect of overlap length used in the different joining techniques were identified in terms of mechanical strength of the adhesively joined composite after static loading. The tensile and flexural strength of the joint increased when increasing the overlap length, but compression strength decreases because of buckling developed as a result of increasing in length of the sample.
- The effect of joint configuration on the bond strength were identified. The maximum flexural and compression strength was obtained at single lap joint. While maximum tesile strength was obtained at scarf joint.
- The effect of environmental factor (temprature) on the bond strength were identified.the bond strength varies with temperature, but as general the bond strength was safe with this temperature range.
- The maximum flexural and compression strength was obtained at S4 (30mm overlap length, 0℃, and single lap configuration joint) 50.40MPa and 22.64 MPa respectively. while for tensile strength the maximum joint strength was 12.8MPa.
- The optimum combination obtained through Taguchi based grey relational analysis was single lap joint, 30 mm overlap length, and 20℃.
- Fractography analysis depicted that even though there was small void at the bonding line, the joint of composites showed better bonding between the adherends and adhesive.

- Most of the failure mechanism appeared was cohesive and adherend failure. This indicaties that the joint strength was stronger than the adherend and adhesive. In sample 1 and sample 4 adhesive failure was obtained, this was because of the weak surface treatment.

5.2. Recommendations

Considering the experimental investigation and results obtained the following recommendation is made:

- During joining of adherends through hand layup method avoiding voids is difficult, therefore it is better to use any other joining method.
- Epoxy resin should be used instead of polyester matrix during composite fabrication to obtain more improved mechanical properties.
- During joining of adherends through hand layup method maintaining the thickness uniformity of adhesive is difficult, therefore it is better to use any other joining method.
- Extraction of fibers should be performed with fiber extraction machine.
- Fiber treatment period has to be investigated and optimize.

5.3. Future work

- Thermal and wear strength of the bond can be studied for potential applications in aerospace and automotive industries.
- The effect of humidity on the strength of adhesively joined composite can be studied.
- Finite element analysis method or ANSYS software have to be conducted to study the stress analysis of automotive body analysis.
- Adhesively joined composite can be further investigated for light weight application

REFERENCE

Amel, B. A., Paridah, M. T., Sudin, R., Anwar, U. M. K., & Hussein, A. S. (2013). Effect of fiber extraction methods on some properties of kenaf bast fiber. *Industrial Crops and Products*, *46*, 117–123. https://doi.org/10.1016/j.indcrop.2012.12.015

Anonymous. (2019). ASTM D5573—99: standard practice for classifying failure modes in fber-reinforced-plastic (FRP) joints. . *ASTM International, West Conshohocken*, 34.

Arpitha, G. R., & Yogesha, B. (2017). An Overview on Mechanical Property Evaluation of Natural Fiber Reinforced Polymers. *Materials Today: Proceedings*, *4*(2), 2755–2760. https://doi.org/10.1016/j.matpr.2017.02.153

Ashok, K. G., Kalaichelvan, K., & Damodaran, A. (2020). Effect of Nano Fillers on Mechanical Properties of Luffa Fiber Epoxy Composites. *Journal of Natural Fibers*, *00*(00), 1–18. https://doi.org/10.1080/15440478.2020.1779898

Banea, S. (2008). Adhesively bonded joints in composite materials. *Materials: Design and Applications*, 8.

Bakri, M. K. Bin, Jayamani, E., & Hamdan, S. (2017). Processing and Characterization of Banana Fiber/Epoxy Composites: Effect of Alkaline Treatment. *Materials Today: Proceedings*, *4*(2), 2871–2878. https://doi.org/10.1016/j.matpr.2017.02.167

Budhe, M. D. (2018). Bonded repair of composite structures in aerospace application: a review . *Applied adhesion science* , 9.

Chandra, S. S. (1999). *"Damping Studies in Fiber-Reinforced Composites - A* (Vols. 41-51). indian: Taylor & Francis, Philadelphia, PA.

Chris, W., Ewen, K., & Charlotte, V. (2020). *Joining of Fibre-Reinforced Polymer Composite.* UK: Composites UK Ltd.

Dandesa, M, (2016). Extraction, characterization and optimization of banana trunk fiber, Unpublished" MSc. Thesis submitted to Addis Ababa University, 69pp

Española, A. (2016). Clasificación de adhesivos termoplásticos para. *UNE-EN 204: (Madrid: Agencia Española de Normalización)*, 6.

Ever, B. (2011). Introduction to Composite Materials Design. *Taylor & Francis,*, 6-12.

Faruk, O., Bledzki, A. K., Fink, H., & Sain, M. (2012b). Progress in Polymer Science Biocomposites reinforced with natural fibers : 2000 – 2010. *Progress in Polymer Science*, *37*(11), 1552–1596. https://doi.org/10.1016/j.progpolymsci.2012.04.003

Fathy, A., Shaker, A., Hamid, M. A., & Megahed, A. A. (2017). The effects of nano-silica/nano-alumina on fatigue behavior of glass fiber-reinforced epoxy composites. *Journal of Composite Materials*, *51*(12), 1667–1679. https://doi.org/10.1177/0021998316661870

Fong, A. L., Khandoker, N. A. N., & Debnath, S. (2018). Development and characterization of sugarcane bagasse fiber and nano-silica reinforced epoxy hybrid composites. *IOP Conference Series: Materials Science and Engineering*, *344*(1). https://doi.org/10.1088/1757-899X/344/1/012029

Ghorbani, A. (2018). Stress analysis of composite adhesive bonded joints under incipient failure conditions. *Proc Struct Integrity,*, 8.

Gingar, G. (2018). Welding thermoplastic composites. *Composites world*, 4-6.

Groover, M. P. (2010). *fundamental of moderen manufacturing, material, processes and system.* United States of America: John Wiley & Sons, Inc., 111 River Street, Hoboken, NJ 07030-5774, (201)748-6011,.

Hasheminia et al. (2019). *Failure mechanism of bonded joints with similar and dissimilar material.* England: Compos Part B.

Karthick, R., Adithya, K., Hariharaprasath, C., & Abhishek, V. (2018). Evaluation of mechanical behavior of banana fibre reinforced hybrid epoxy composites. *Materials Today: Proceedings*, *5*(5), 12814–12820. https://doi.org/10.1016/j.matpr.2018.02.265

Karuppusamy Kanthavel, P. R. (2005). Investigation of the mechanical . *Bioresources 10(2):3749-3756.*, 3-7.

Kumar, S. (2014a). Damping studies in fiber-reinforced composites - a review [National

institute of technology]. In *Composite Structures* (Vol. 46, Issue 1). https://doi.org/10.1016/S0263-8223(99)00041-0

Kumar, S. (2014b). Evaluation of mechanical and thermal properties of banana – flax based natural fibre composite [Elsevier Ltd]. In *JOURNAL OF MATERIALS&DESIGN* (Vol. 60). https://doi.org/10.1016/j.matdes.2014.03.014

Kumar, S. (2014c). Prediction of tensile properties of hybrid-natural fiber composites [Elsevier Ltd]. In *Composites Part B: Engineering* (Vol.43, Issue2). https://doi.org/10.1016/j.compositesb.2011.08.023

Kumar, S. (2014d). Studies on the extraction of naturally-occurring banana fibers. In *The international journal of engineering and Science (IJES)* (Vol. 2, Issue 9). National institute of technology.

Kutz, M., & Wiley, J. (2015). *Mechanical Engineers ' Handbook Third Edition Controls , and MEMS Edited by*.

Kwon, G. L. (2011). Effect of carbon nanotube reinforcement on fracture strength of composite adhesive joints. *J Mater Sci (2011) 46:3370–3377*, 6.

Leng, Y. (2008). material characterization . *Asia john Wiley and Sons introduction to microscope and spectroscope methods. ISBN 978-0-470-82298*, 6-8.

Lotfi, A., Li, H., Dao, D. V., & Prusty, G. (2021). Natural fiber–reinforced composites: A review on material, manufacturing, and machinability. *Journal of Thermoplastic Composite Materials*, *34*(2), 238–284. https://doi.org/10.1177/0892705719844546

Manjunath, M., Renukappa, N. M., & Suresha, B. (2016). Influence of micro and nanofillers on mechanical properties of pultruded unidirectional glass fiber reinforced epoxy composite systems. *Journal of Composite Materials*, *50*(8), 1109–1121. https://doi.org/10.1177/0021998315588623

Marcella, p. v. (2015). effect of material and surface preparationon joining method. *journal of reinforced plastic and composite*, 1-12.

Moller, F. e. (2010). Novel method for joining CFRP to aluminium. *Physics Procedia*, 37-45.

Murugan, K., Venkatesh, S., Thirumalai, R., & Nandhakumar, S. (2020). Fabrication and investigations of kenaf fiber and banana fiber reinforced composite material. *Materials Today: Proceedings*, *37*(Part 2), 110–114. https://doi.org/10.1016/j.matpr.2020.04.540

Naveen.E, V. . and, & Maheswaran.N. (2015). Alkalichemical Treatment on the Surface of. *International Journal of Innovative Research in Science, Engineering and Technology*, *4*(4), 172–178. http://www.ijirset.com/upload/2015/tapsa/25_ME009.pdf

Olayil, R., Arumugaprabu, V., Das, O., & Lenin Anselm, W. A. (2021). A Brief Review on Effect of Nano fillers on Performance of Composites. *IOP Conference Series: Materials Science and Engineering*, *1059*(1). https://doi.org/10.1088/1757-899X/1059/1/012006

Omairey Sadik, N. J. (2021). Defects and uncertainties of adhesively bonded composite joint. *SN Applied Sciences* , 9.

Ouarhim, W., Zari, N., Bouhfid, R., & Qaiss, A. E. K. (2018). Mechanical performance of natural fibers-based thermosetting composites. *Mechanical and Physical Testing of Biocomposites, Fibre-Reinforced Composites and Hybrid Composites*, 43–60. https://doi.org/10.1016/B978-0-08-102292-4.00003-5

Ozsoy, I., Demirkol, A., Mimaroglu, A., Unal, H., & Demir, Z. (2015). The influence of micro- And nano-filler content on the mechanical properties of epoxy composites. *Strojniski Vestnik/Journal of Mechanical Engineering*, *61*(10), 601–609. https://doi.org/10.5545/sv-jme.2015.2632

Pantelakis S, e. a. (2013). Adhesive bonding of composite aircraft structures: Challenges and . *Sci China-Phys Mech Astromy*, 6.

Parre, A., Karthikeyan, B., Balaji, A., & Udhayasankar, R. (2020). Investigation of chemical, thermal and morphological properties of untreated and NaOH treated banana fiber. *Materials Today: Proceedings*, *22*, 347–352.

Prasad, L., Singh, V., Patel, R. V., Yadav, A., Kumar, V., & Winczek, J. (2021). Physical and Mechanical Properties of Rambans (Agave) Fiber Reinforced with Polyester Composite Materials. *Journal of Natural Fibers*. https://doi.org/10.1080/15440478.2021.1904481

Pulido, B. G.-E. (2019). Adhesive joints for composite materials produced by additive. *Journal of Physics: Conference Series*, 2-6.

Rahul Kumar, K. K. (2014). Optimazation of Mechanical Proporties of Epoxy Based Wood Dust Rainforced Green Composite Using Taguchi Mathod. *ELSEVIER Science Direct*, 9.

Ren et al. (2017). aircraft reliability and maintainability analysis and design. *Academic Press, Cambridge*, 37-40.

Selvam, S. R. (2017). Fabrication of SiC particulate reinforced polyester matrix. *IOP Conf. Series: Materials Science and Engineering*, 5-8.

Senguttuvan, N., & Lillymercy, J. (2015). Joint strength analysis of single lap joint in glass fiber composite material. *International Journal of Applied Engineering Research, 10*(7), 16535-16545.

Sumesh, K. R., & Kanthavel, K. (2020a). Grey relational optimization for factors influencing tensile, flexural, and impact properties of hybrid sisal banana fiber epoxy composites. *Journal of Industrial Textiles*. https://doi.org/10.1177/1528083720928501

Sumesh, K. R., & Kanthavel, K. (2020b). Synergy of fiber content, Al2O3 nanopowder, NaOH treatment and compression pressure on free vibration and damping behavior of natural hybrid-based epoxy composites. *Polymer Bulletin*, *77*(3), 1581–1604. https://doi.org/10.1007/s00289-019-02823-x

Suwanpakpraek, B. P. (2019). Study of adhesive bonded joint failure in composite-metal joining. *Materials Science and Engineering 501, 012023*, 7.

Wahab, M. A. (2016). *Joing of composite with addhesive.* USA: DEStCh publication, inc.

Venkateshwaran, N., Elayaperumal, A., & Jagatheeshwaran, M. S. (2011b). *Effect of fiber length and fiber content on mechanical properties of banana fiber / epoxy composite*. https://doi.org/10.1177/0731684411426810

Vignesh, K., Ramasivam, G., Natarajan, U., & Srinivasan, C. (2016). Optimization of process parameters to enhance the mechanical properties of bone powder and coir fiber reinforced polyester composites by taguchi method. *ARPN Journal of Engineering and Applied Sciences*, *11*(2), 1224–1231.

Waghmare, P. M. (2017). Review on Mechanical Properties of Banana Fiber Biocomposite. *International Journal for Research in Applied Science and Engineering Technology*, *V*(X), 847–850. https://doi.org/10.22214/ijraset.2017.10120

Wang, H., Xian, G., & Li, H. (2015). Grafting of nano-TiO2 onto flax fibers and the enhancement of the mechanical properties of the flax fiber and flax fiber/epoxy composite. *Composites Part A: Applied Science and Manufacturing*, *76*, 172–180. https://doi.org/10.1016/j.compositesa.2015.05.027

Woldu, Z., Mohammed, A., Belew, D., Shumeta, Z., & Bekele, A. (2015). Assessment of Banana Production and Marketing in Ethiopia. *International Journal of Sciences: Basic and Applied Research*, *24*, 283–307.

Zin, M. H., Abdan, K., Mazlan, N., Zainudin, E. S., & Liew, K. E. (2018). The effects of alkali treatment on the mechanical and chemical properties of pineapple leaf fibres (PALF) and adhesion to epoxy resin. *IOP Conference Series: Materials Science and Engineering*, *368*(1). https://doi.org/10.1088/1757-899X/368/1/012035

Appendix A

Tensile Test

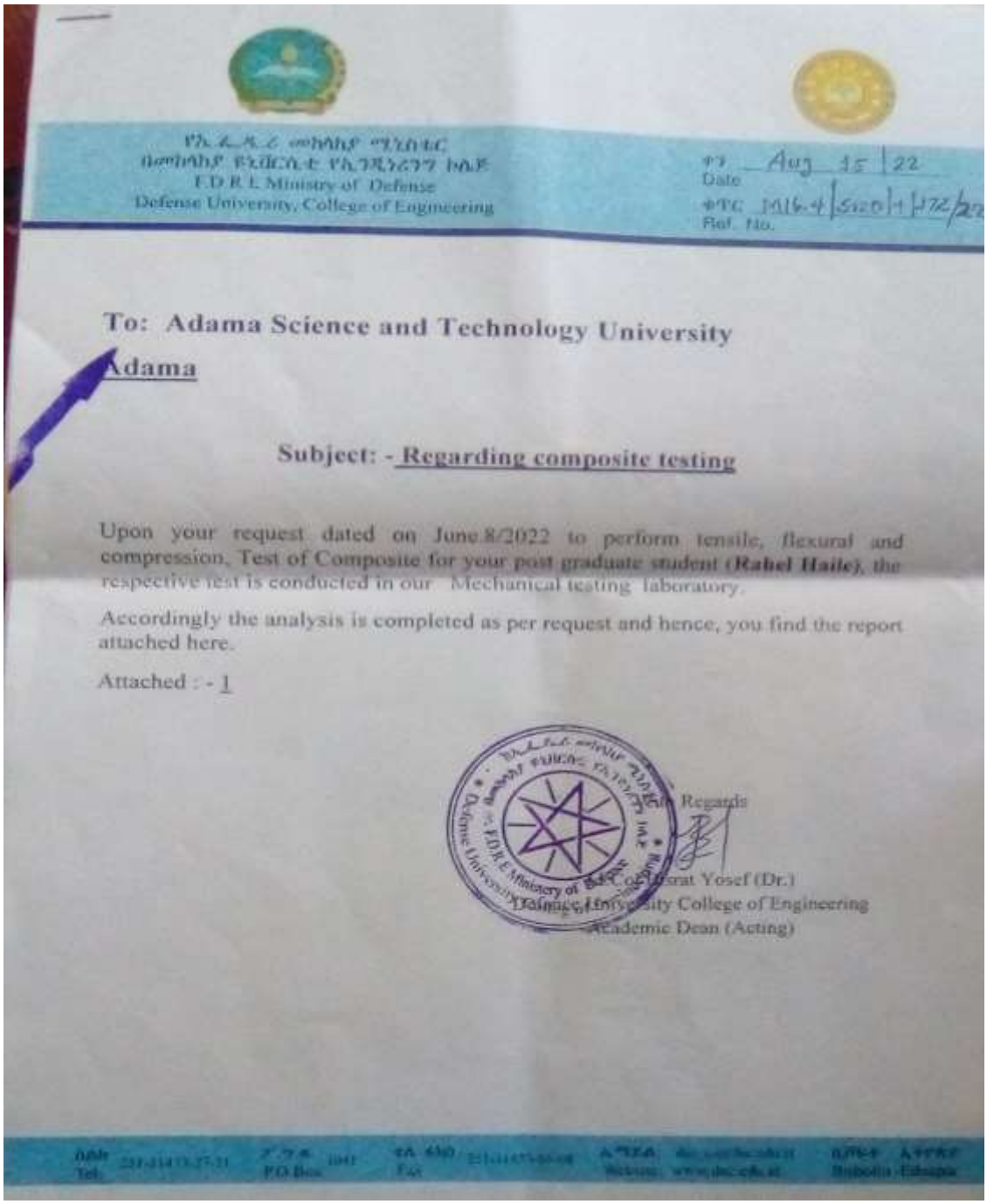

የኢ.ፌ.ዲ.ሪ መከላከያ ሚኒስቴር
በመከላከያ የቴክኒሉ ኮሌጅ ኮሌጅ
F.D.R.E Ministry of Defense
Defense University, College of Engineering

ቀን Date: Aug 15 | 22
ቁጥር Ref. No.

To: Adama Science and Technology University
Adama

Subject: - Regarding composite testing

Upon your request dated on June 8/2022 to perform tensile, flexural and compression, Test of Composite for your post graduate student (**Rahel Haile**), the respective test is conducted in our Mechanical testing laboratory.

Accordingly the analysis is completed as per request and hence, you find the report attached here.

Attached : - 1

Regards

Yasinul Yosef (Dr.)
Defense University College of Engineering
Academic Dean (Acting)

Mechanical properties test result

No	Sample Name	Result in (N/mm^2)		
		Tensile strength	Compression strength	flexural strength
1	S1	5.12	13.68	36.00
2	S2	9.44	15.12	18.00
3	S3	9.76	14.56	32.40
4	S4	5.60	22.64	50.40
5	S5	6.00	17.28	25.20
6	S6	9.68	7.36	36.00
7	S7	7.20	11.92	54.00
8	S8	7.84	-	39.60
9	S9	12.8	6.24	43.20

Name of Tester:-Berhanu Nigatu

Signature:-

With regards,

Capt. Felege Nekatibeb (Ph.D.)
Head, of Metallurgical and Materials Eng. Dep't
Ethiopian Defence University College of Eng.

Appendix B

Flexural Strength

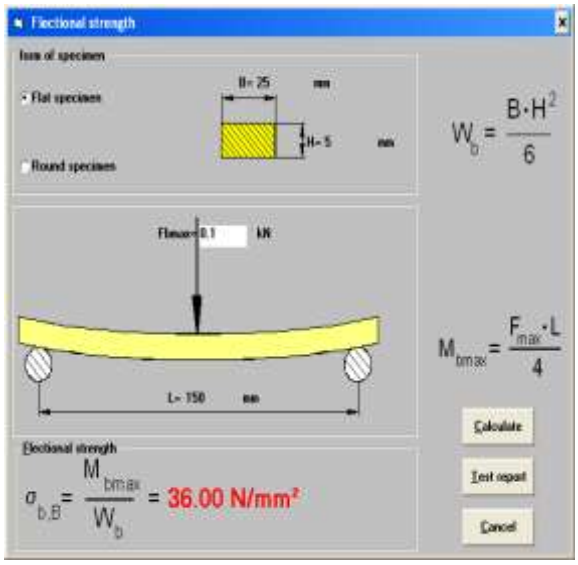

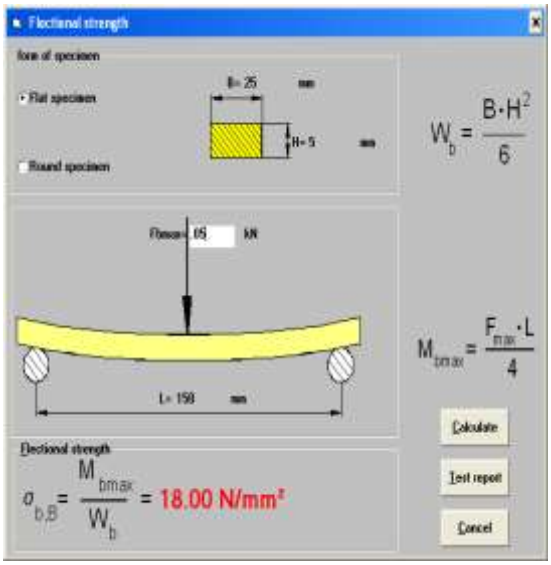

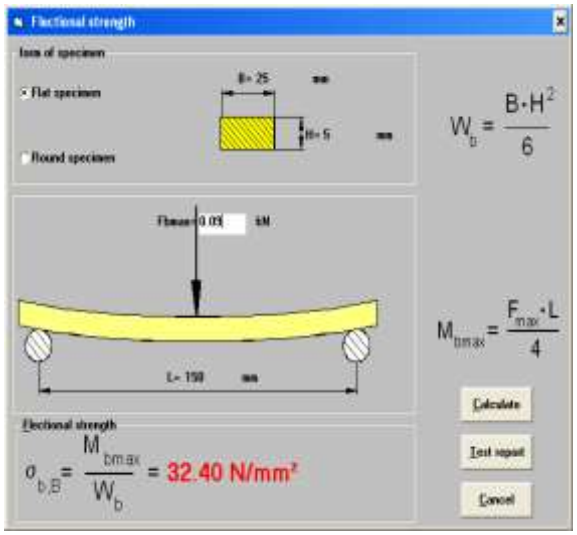

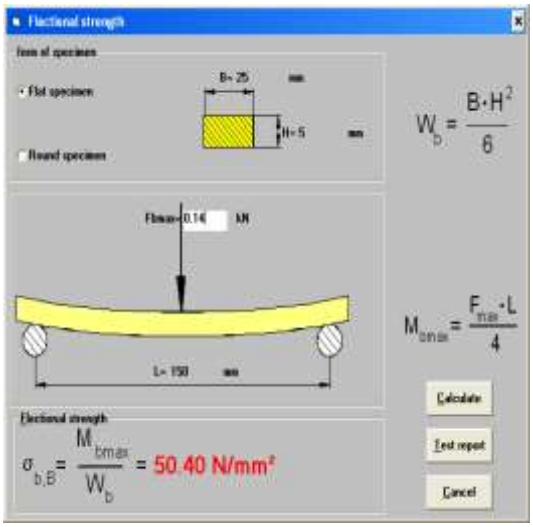

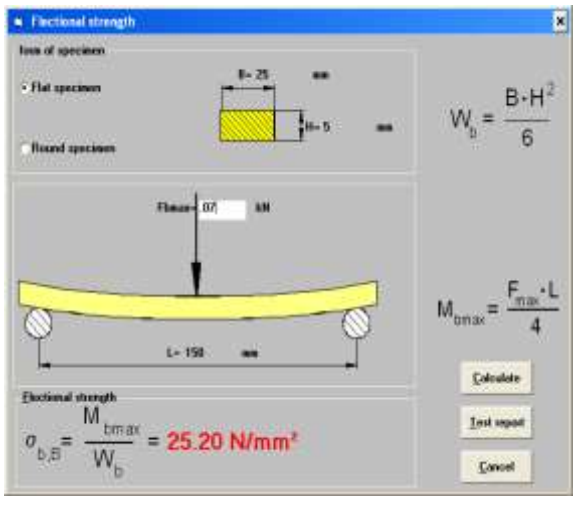

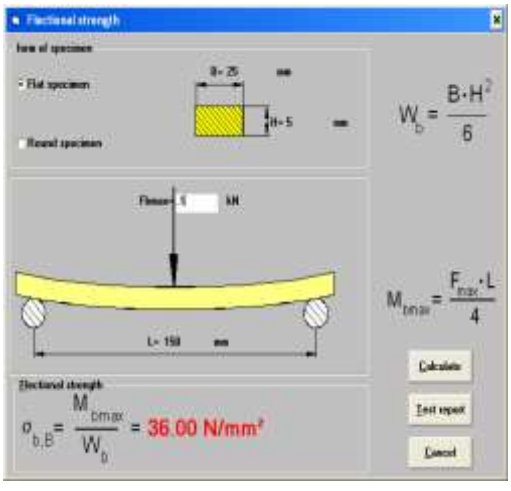

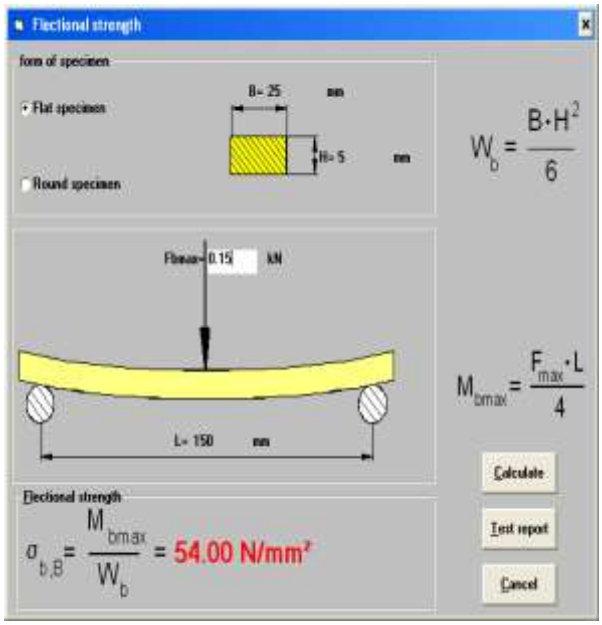
Flectional strength
form of specimen
Flat specimen
Round specimen
B= 25 mm
H= 5 mm
$W_b = \frac{B \cdot H^2}{6}$
Fmax= 0.15 kN
L= 150 mm
$M_{bmax} = \frac{F_{max} \cdot L}{4}$
Calculate
Test report
Cancel
Flectional strength
$\sigma_{b,B} = \frac{M_{bmax}}{W_b}$ = 54.00 N/mm²

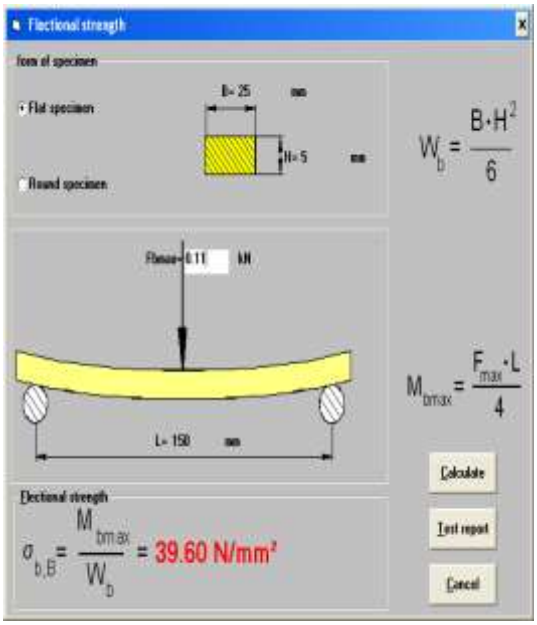
Flectional strength
form of specimen
Flat specimen
Round specimen
B= 25 mm
H= 5 mm
$W_b = \frac{B \cdot H^2}{6}$
Fmax= 0.11 kN
L= 150 mm
$M_{bmax} = \frac{F_{max} \cdot L}{4}$
Calculate
Test report
Cancel
Flectional strength
$\sigma_{b,B} = \frac{M_{bmax}}{W_b}$ = 39.60 N/mm²

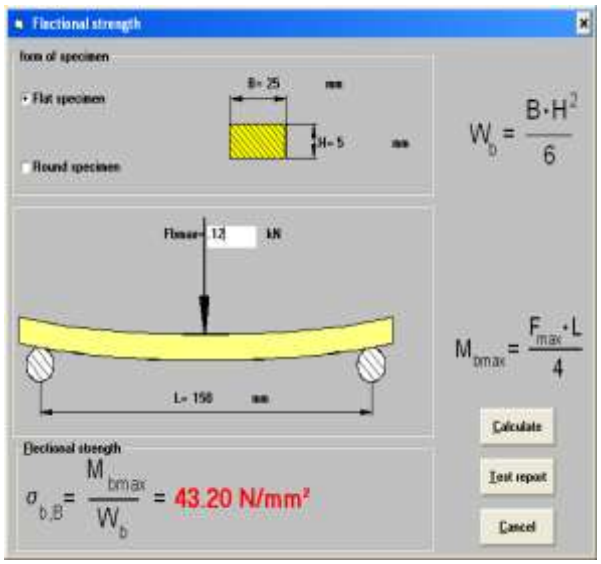
Flectional strength
form of specimen
Flat specimen
Round specimen
B= 25 mm
H= 5 mm
$W_b = \frac{B \cdot H^2}{6}$
Fmax= 1.2 kN
L= 150 mm
$M_{bmax} = \frac{F_{max} \cdot L}{4}$
Calculate
Test report
Cancel
Flectional strength
$\sigma_{b,B} = \frac{M_{bmax}}{W_b}$ = 43.20 N/mm²

Appendix C

Compression Strength

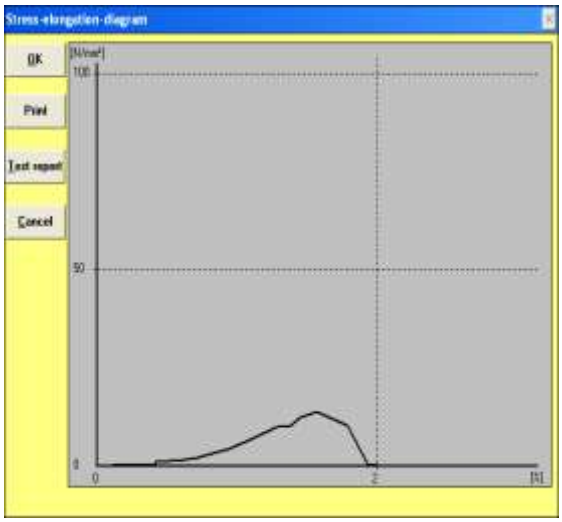

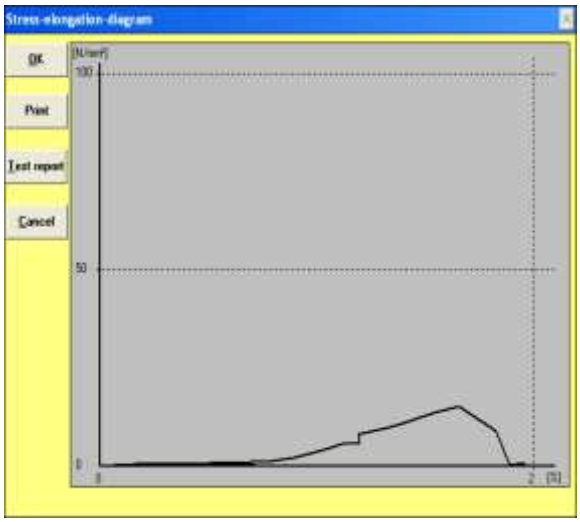

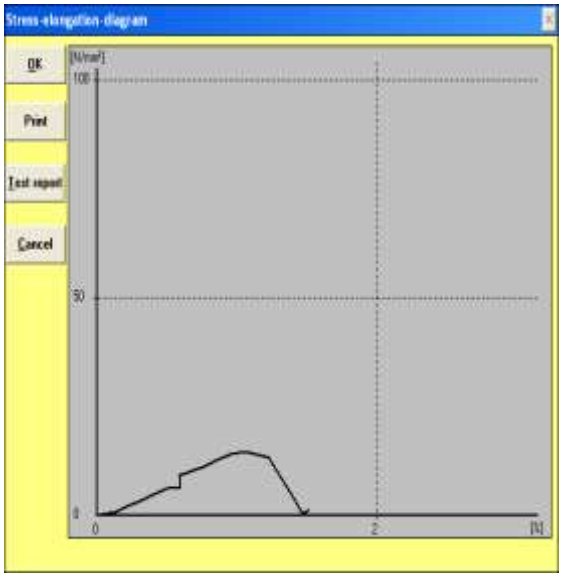

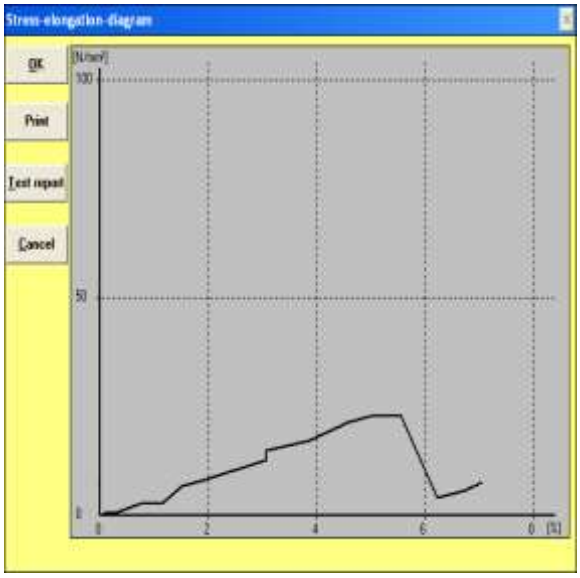

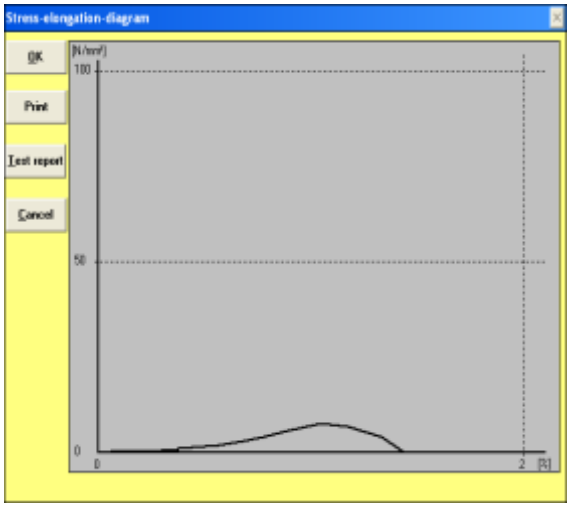

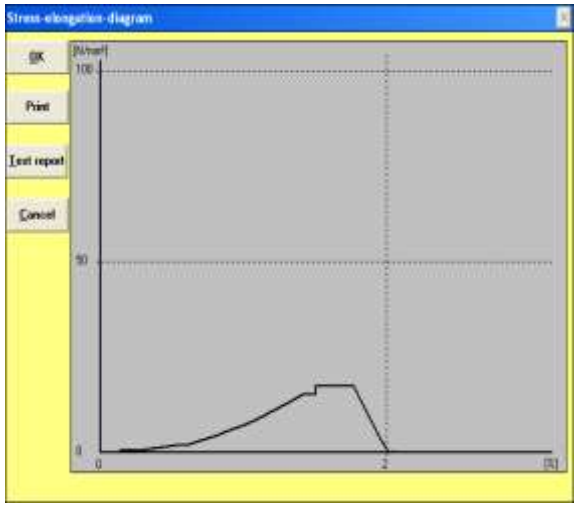

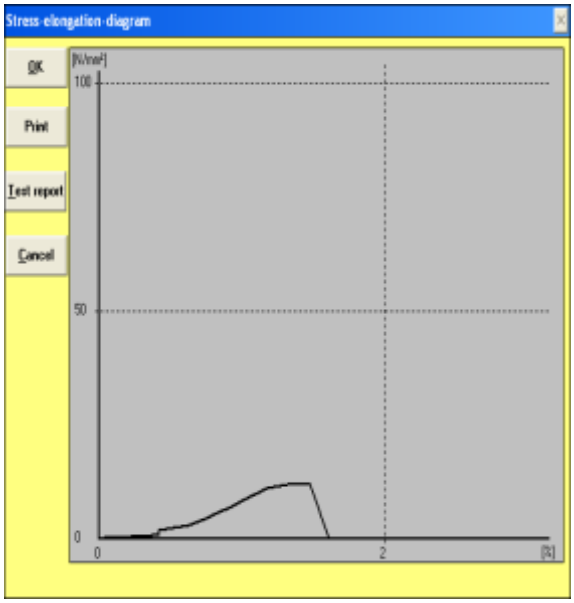
Stress-elongation-diagram
OK
Print
Test report
Cancel
[N/mm²]
100
50
0
0
2
[%]

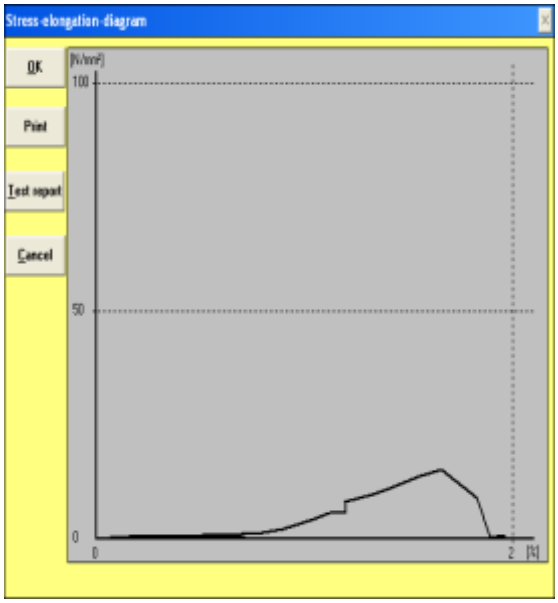
Stress-elongation-diagram
OK
Print
Test report
Cancel
[N/mm²]
100
50
0
0
2
[%]

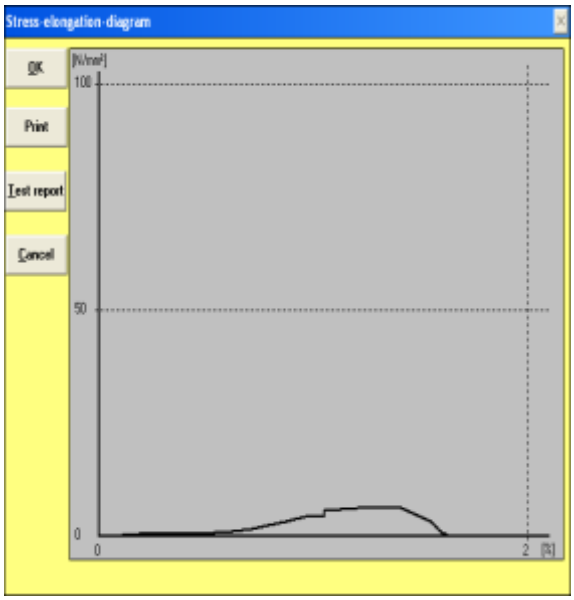
Stress-elongation-diagram
OK
Print
Test report
Cancel
[N/mm²]
100
50
0
0
2
[%]

Appendix D

Fractography

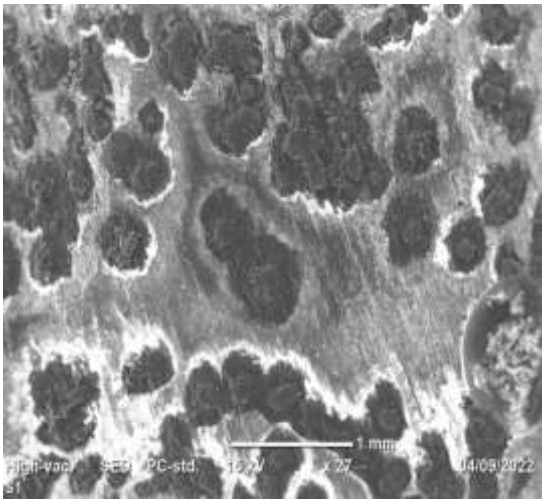

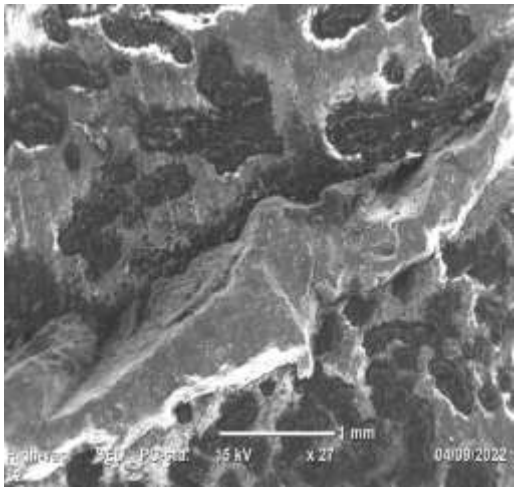

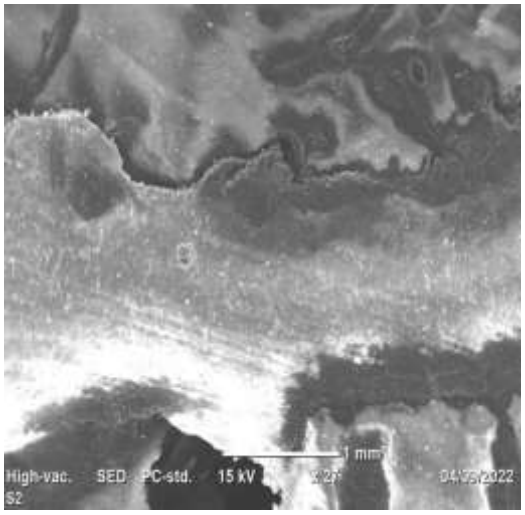

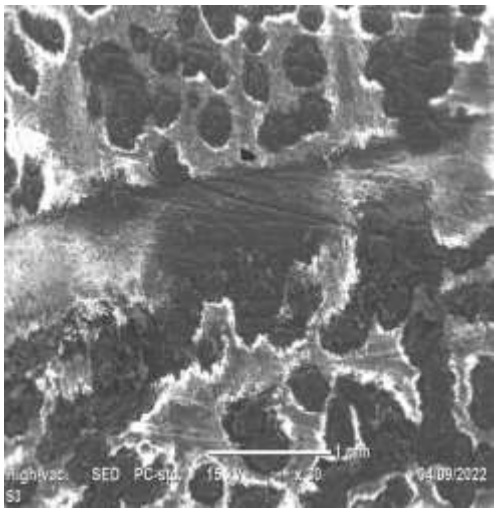

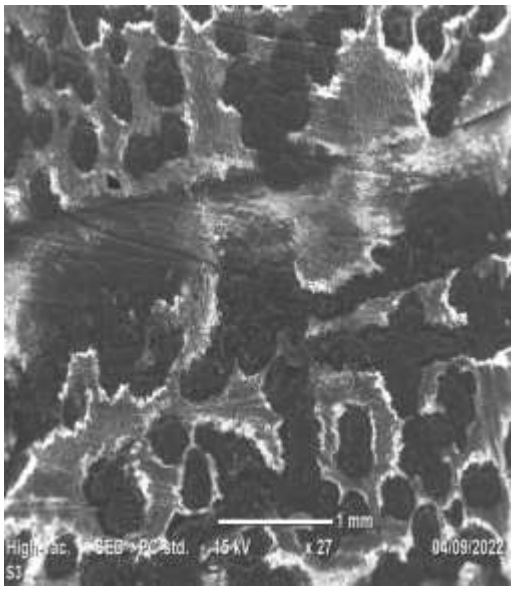

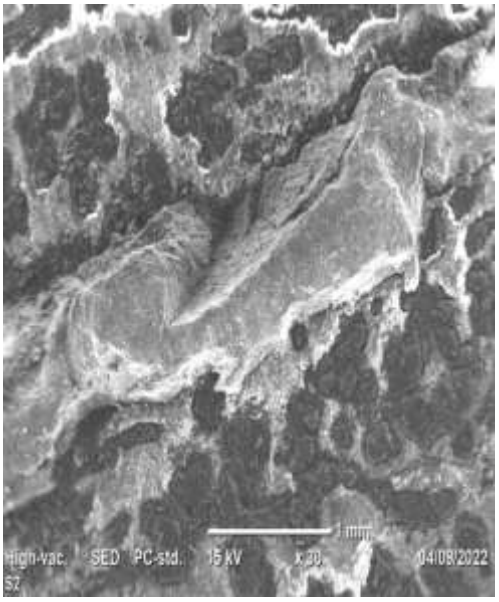

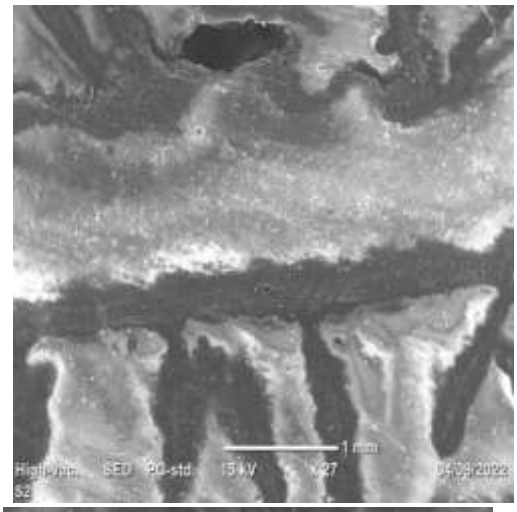
1 mm
High-vac. SED PC-std. 15 kV x 27 04/09/2022
S2

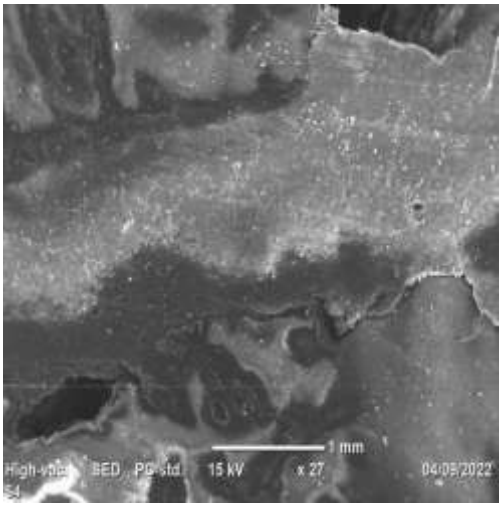
1 mm
High-vac. SED PC-std. 15 kV x 27 04/09/2022
S1

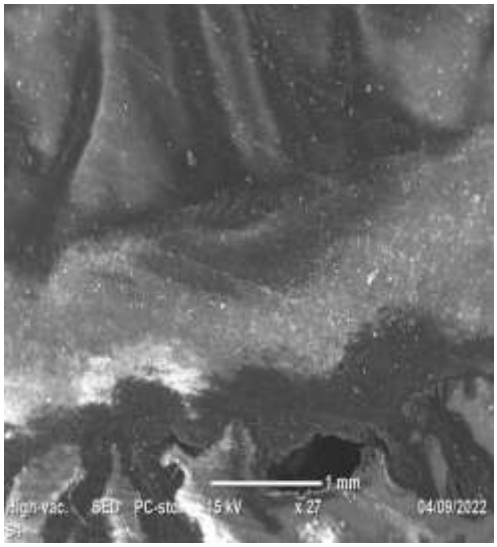
1 mm
High-vac. SED PC-std. 15 kV x 27 04/09/2022
S1

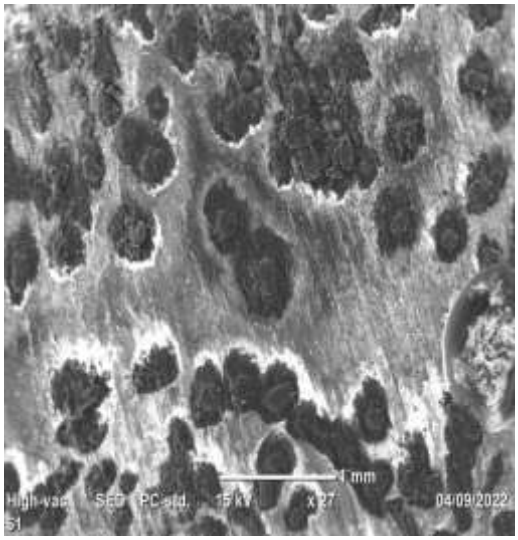
1 mm
High-vac. SED PC-std. 15 kV x 27 04/09/2022
S1